CONFORMATIONAL AND FLUORESCENCE STUDIES OF SMALL PEPTIDES CONTAINING TRYPTOPHAN

by

Gary Samuel Bowitch
'11

* * * * *

Submitted in partial fulfillment
of the requirements for
Honors in the Department of Chemistry

UNION COLLEGE

April, 1980

ABSTRACT

BOWITCH, GARY S. Conformational and Fluorescence Studies of Small Peptides Containing Tryptophan. Department of Chemistry, April, 1980.

Double-exponential decay has been observed for tryptophan and tryptophan-containing dipeptides. The Stern-Volmer mechanism was used to detect such decay. Conformational energy calculations were undertaken to elucidate fluorescence properties of these peptides.

Ionic strength effects were found, for the most part, to be unimportant in Stern-Volmer quenching experiments. $^{2+}LT^{-}$ exhibited non-linear Stern-Volmer plots with cesium quencher. Modified Stern-Volmer plots and theoretical calculations support the existence of double-exponential decay for $^{2+}LT^{-}$.

Efficiency of external quenching is related to peptidyl charge. Electrostatic attraction and repulsion accounts for observed trends with iodide quencher.

Internal peptide quenching has been attributed, by other workers, to exciplex formation. This model is supported by the percentage of indole contacts found for peptides through energy calculations. A low ϕ_R for $^{+}TGG^{-}$ is attributed to increased electrophilicity of amide carbonyl due to interresidue hydrogen bonding.

Weak C_5 intraresidue hydrogen bonding has little affect upon peptide energy stabilization. The N-terminal residue in X-Trp peptides studied has little affect on tryptophan intraresidue hydrogen bonding.

Zimmerman's contention that aromatic residues in Gly-X dipeptides stabilizes the peptide is supported by energy calculations on $^{+}GT^{-}$. Calculations on $^{+}PT^{-}$ agrees well with Zimmerman's findings for Pro-X dipeptides.

ACKNOWLEDGMENTS

I would like to extend my warmest thanks to Professors Janet Anderson and Tom Werner for their advise, guidance, and most of all patience throughout this project.

TABLE OF CONTENTS

INTRODUCTION

Tryptophan, unlike all other naturally occurring amino acids except phenyalanine and tyrosine, exhibits significant fluorescence upon irradiation. Tryptophan fluorescence properties are known to be dependent upon environmental influences. As such, the fluorescence properties of proteins containing one or more tryptophan residues can reveal information about the extent to which these residues are exposed to solvent. In turn, such knowledge can elucidate some of the structural properties of such proteins. One part of this study involved the examination of the fluorescence properties of some short peptides containing one tryptophan residue. This work, it is hoped, will provide information which can later aid in understanding the properties of proteinic tryptophan.

When tryptophan is irradiated, the resulting absorption of light causes certain molecules to be excited from the singlet ground state, S_o to the excited singlet state, S_1. Tryptophan can return to the ground state through either the radiative process of fluorescence or the non-radiative decay pathways of internal conversion and intersystem crossing. Both non-radiative pathways are decay processes which compete with fluorescence decay. The kinetics for such decay is depicted below:

$$^1A^* \longrightarrow {}^1A + h\nu \qquad k_f \qquad \text{(fluorescence)}$$

$$^1A^* \longrightarrow {}^1A \qquad \Sigma k_i \qquad \text{(internal conversion)}$$

$$^1A^* \longrightarrow {}^3A \qquad \text{(intersystem crossing)}$$

where $^1A^*$ represents the excited singlet state, ^1A is the ground singlet state, ^3A is the excited triplet state, k_f is the fluorescence rate constant and Σk_i is the sum of the rate constants for the other decay pathways.

The efficiency of fluorescence for tryptophan, i.e. the percentage of molecules which return to the ground state via fluorescence, is measured by the quantum yield, ϕ_f^o. ϕ_f^o represents the ratio of the rate for fluorescence to the sum of all the rates involved in the decay process and is given by equation (1)

$$\phi_f^o = k_f / (k_f + \Sigma k_i) \qquad (1)$$

An analogous quantity is the relative quantum yield, ϕ_R. ϕ_R, an easily measured quantity, is used in the actual fluorescence studies of tryptophan-containing peptides and is given by equation (2):

$$\phi_R = (F_A / A_{280})_{\text{peptide}} \times (A_{280} / F_{A\ \text{NATA}}) \qquad (2)$$

F_A is the measured area under an uncorrected fluorescence spectrum, and A_{280} is the absorbance at 280 nm. The first ratio refers to these quantities measured for tryptophan, the second refers to those measured for NATA (N-acetyl-L-tryptophanamide), a reference compound. The greater the value of both ϕ_f and ϕ_R, the more efficient is the fluorescence as compared to the other decay processes.

Another very important aspect of the fluorescence studies

of tryptophan-containing compounds is an examination of the fluorescence lifetime, τ_f. This value is given by equation (3)

$$\tau_f = (k_f + \Sigma k_i)^{-1} \qquad (3)$$

and is defined as the time necessary for a given population of excited states to decay to 1/e of its final value.

The fluorescence decay lifetime is related to the fluorescence intensity at time t, I, and the initial fluorescence intensity according to equation (4):

$$I = I_o e^{-t/\tau_f} \qquad (4)$$

Equation (4) applies to tryptophan-containing peptides whose fluorescence decay can be fit to a single-exponential function. Such a compound is said to have a single fluorescence lifetime. Werner and Forster have observed such single-exponential decay for the zwitterion form of some short tryptophan-containing peptides.[1]

Other workers have been able to fit better the fluorescence decays of some compounds to a double exponential decay function of the type given below:

$$I = f_1 e^{-t/\tau_1} + f_2 e^{-t/\tau_2} \qquad (5)$$

where τ_1 and τ_2 are the two lifetime components, f_1 and f_2 are the lifetime weighting factors. A weighted average lifetime, $\langle \tau \rangle$, can be calculated by equation (6):

$$\langle \tau \rangle = f_1 \tau_1 + f_2 \tau_2 \qquad (6)$$

This double-exponential decay has been reported for tryptophan itself by Rayner and Szabo.[2] Werner and Forster have seen that the anionic forms of some short tryptophan-containing peptides as well as larger (20-30 residues) peptides

exhibit double-exponential decay.[1]

Studies using steady-state excitation, it was hoped, would help to verify the existence of double-exponential decay for tryptophan. This work was carried out using the Stern-Volmer mechanism. This type of study examines the effect of external ions, quenchers, upon the fluorescence properties of tryptophan.

Some quenching is believed by some workers to take place at the indole ring of tryptophan by the creation of an excited state charge - transfer complex (exciplex) between the ring and the quenching atom.[3] The Stern-Volmer mechanism provides a means of measuring the stability of this complex and, therefore, the efficiency of quenching by such atoms.

Recall that ϕ_f^o is related to the rates of fluorescence and the other non-radiative decay pathways. When quencher is added to the tryptophan peptide solution, the excited state molecules are allowed another decay pathway. This is seen in the second-order collisional decay as follows:

$$^1A^* + Q \rightarrow {}^1A + Q \qquad k_q [Q] \quad \text{(collisional quenching)}$$

where $k_q [Q]$ is the rate for this process, k_q is the second order rate constant, and $[Q]$ is the concentration of quencher in solution. k_q is a measure of the efficiency of quenching. As its value increases quenching increases.

The quantum yield, ϕ_f in the presence of quencher is given by equation (7):

$$\phi_f = k_f / (k_f + \Sigma k_i + k_q [Q]) \qquad (7)$$

The Stern-Volmer equation is obtained by dividing equations (1) by (7) to obtain (8):

$$\phi_f^o / \phi_f = 1 + K_{sv} [Q] \qquad (8)$$

where $K_{sv} = k_q \tau_f$.

It has been seen that the presence of quencher does not change the position or shape of the fluorescence curves for tryptophan-containing peptides. In this study, we altered the Stern-Volmer equation by substituting the fluorescence intensity at the emission wavelength maximum for the quantum yields. Equation (8) becomes:

$$F_T^o / F_T = 1 + K_{sv} [Q] \qquad (9)$$

where F_T^o and F_T are the total volume-corrected fluorescence intensities in the absence and presence of quencher respectively. A plot of F_T^o / F_T, the Stern-Volmer ratio, versus $[Q]$ should yield a linear plot with a slope equal to K_{sv}. k_q and the efficiency of quenching of external quenchers can subsequently be determined.

Since K_{sv} is proportional to the fluorescence lifetime, it is hoped that Stern-Volmer quenching experiments might reveal exponential decay. Thus, one purpose of this study is to use quenching experiments to find supportive evidence for the double-exponential decay found by other workers.

The external quenchers used in Stern-Volmer experiments were iodide and cesium ion. When charged tryptophan-containing peptides are examined in the Stern-Volmer experiments, one might

expect electrostatic effects to affect the quenching efficiency, k_q, of the quencher ions. Thus another aim of this work is to check for a correlation between charge and quenching efficiency.

Since many of the fluorescence and quenching properties which are observed are dependent upon exciplex formation, electrostatic, and steric interactions between atoms in the peptide (and external quencher ions), conformational analysis of these peptides was believed to be crucial. This analysis, done through the use of computer programs was aimed at first determining those conformations of lowest energy which would most likely be found in nature. Research by Zimmerman and Scheraga has shown that low energy conformations of dipeptides determined by computer analysis correspond fairly well with the conformations observed in x-ray studies.[4,5]

Computer calculations were also thought to be useful in structural (contact with the tryptophan indole ring) and hydrogen bonding interactions among atoms in these low energy conformations of peptides. Zimmerman and Scheraga's work has provided a great deal of information about such interactions in proline- and glycine-containing dipeptides.[4,5]

In our work we wanted to examine these properties in some tryptophan-containing di- and tri-peptides which were also examined through Stern-Volmer quenching experiments. We chose to examine tryptophan-containing peptides with adjacent residues with varied structural properties. These adjacent residues

were glycine, proline, and lysine. Proline was chosen because of the structural restrictions imposed on the residue by the presence of the pyrrolidine ring. Glycine is unique because it lacks a β-carbon. Lysine's properties are of interest because its long side chain can rotate into many possible conformations.

A third major goal of this work, therefore, is to use information regarding the conformational character of tryptophan dipeptides in order to help clarify their observed fluorescence and quenching properties.

EXPERIMENTAL

A. Chemicals:

See reference 6.

B. Instrumentation:

All pH measurements were obtained on a Beckman Century SS pH meter and on an Orion Research 701 digital pH meter.

Absorbtion measurements were obtained on a Beckman DU spectrophotometer and on a Cary 118 spectrophotometer. The excitation wavelength used was 280 nm on both instruments. Slitwidths of 0.7 nm and 0.1 nm were used on the Beckman DU and the Cary 118 respectively.

C. Procedure:

1. Preparation of Solutions:

a. Buffers:

The buffers used were phosphate (pH 5.8-6.4) and carbonate (pH 9.8-10.4). Stock solutions of Na_2HPO_4 and Na_2CO_3 were prepared with distilled, deionized water to a concentration of 0.05M. These solutions were then diluted 1:10 with distilled, deionized water to a concentration of 0.005M. The appropriate buffer systems were produced by adding hydrochloric acid and then adjusting the solutions to the desired pH. The pH of each buffer system was readjusted to the desired pH before each quenching experiment. For

quenching experiments with KI quencher, 1 ml of a 10^{-4}M solution of $NaS_2O_3^{2-}$ was added to 100 ml of buffer solution. This was done to prevent the conversion of iodide to iodine.

b. Sample Solutions for Quantum Yield Measurements:

See reference 6.

c. Sample Solutions for Quenching Measurements:

See reference 6.

d. Quenchers:

See reference 6.

2. Fluorescence Quantum Yields:

See reference 6.

All quantum yield studies of the anion forms of the peptides were carried out in 0.005M carbonate buffer.

Quantum Yield studies of some anion and zwitterion species were carried out in buffer solutions consisting of 10% D_2O and 90% H_2O. A ratio of $\phi_{10\%D_2O}$ to $\phi_{100\%H_2O}$ was constructed for each species. This ratio was then divided by .9 in order to produce a ratio of $\phi_{100\%D_2O}$ to $\phi_{100\%H_2O}$.

3. Stern-Volmer Quenching Experiment:

The Stern-Volmer mechanism was used to examine the quenching efficiency of two external quenchers, cesium ion and iodide ion. Seven 30 μl aliquots of quencher were added to a buffered solution containing the fluorescing peptide at a concentration of about 10^{-5}M. The fluorescence intensity of the fluorescer at

its wavelength maximum was measured after each addition of quencher. An excitation slit of 6 nm and an emission slit of 10 nm were used. The initial volume of fluorescer used with iodide quencher was 3.0 ml. This resulte. in concentration range for iodide in solution of 0.060M to 0.340M. The initial volume of fluorescer used with cesium quencher was 2.0 ml. This resulted in a concentration range for cesium in solution from 0.089M to 0.570M. This greater cesium ion concentration range was used in order to compensate for the low quenching efficiency of cesium as compared to that of iodide.

The fluorescence intensities were corrected for volume changes (due to addition of aliquots of quencher) according to equation (9):

$$F_M(V_T/V_O) = F_T \qquad (9)$$

where F_M is the measured fluorescence intensity at the wavelength maximum, V_T is the total solution volume, V_O is the initial volume of fluorescer in the absence of quencher, and F_T is the 'total' fluorescence corrected for dilution.

The absorbtion wavelength maximum for tryptophan-containing peptides is 280 nm. Since the quenchers, particularly iodide ion, are known to exhibit background absorbtion at this wavelength, the excitation wavelength for fluorescence studies was shifted to 290 nm throughout the duration of the experiment.

4. Ionic Strength Experiment:

a. Method One:

To determine the effect of increasing ionic strength, due

to the addition of quencher ion to the fluorescing solution. on the results of the Stern-Volmer quenching experiment, an ionic strength experiment was devised. All initial conditions for this experiment were identical to those used in the Stern-Volmer quenching experiments. After the fluorescence intensity of the fluorescer at its wavelength maximum was measured in the absence of quencher, one 30 μl aliquot of quencher was added, and the fluorescence intensity was again recorded. Subsequently, ten 30 μl aliquots of 5.0M sodium chloride were added to the fluorescer solution and the fluorescence was recorded after each addition.

The ionic strength, μ, is given by equation (10):

$$\mu = \tfrac{1}{2}(m_1 z_1^{\,2} + m_2 z_2^{\,2} + m_3 z_3^{\,2} + \ldots) \qquad (10)$$

where m_1, m_2, m_3, m_n represents the molar concentrations of the ions in solution, and z_1, z_2, z_3, z_n are their respective ionic charges. Since the ionic charge of all the species in this experiment was one, the ionic strength was simply the sum of the quencher concentration and the sodium chloride concentration. The contribution of the buffer to the ionic strength of the solution was neglected because its concentration, 0.005M, was considered negligible in comparison to that of the quencher.

The measured fluorescence intensities were again corrected for volume changes as in the Stern-Volmer quenching experiments. A plot of F_T^o/F_T vs. μ was constructed where F_T^o is the fluorescence intensity in the absence of quencher. In order to examine at zero ionic strength, a correction factor was to be

determined from a plot of $\left[(F_T^o/F_T)\ \mu = n / (F_T^o/F_T)\ \mu = o\right]$ vs. μ where $(F_T^o/F_T)\ \mu = n$ is the Stern-Volmer ratio at a given ionic strength and $(F_T^o/F_T)\ \mu = o$ is the ratio at zero ionic strength. The value of $\left[(F_T^o/F_T)\ \mu = n / (F_T^o/F_T)\ \mu = o\right]$ at $\mu = n$ can be multiplied by a value of (F_T^o/F_T) at $\mu = n$ determined in the corresponding Stern-Volmer experiment to find $(F_T^o/F_T)\ \mu = o$ for the Stern-Volmer results.

Careful examination of this method revealed that it did not produce a simple way of determining a correction factor. The fluorescence intensity is dependent upon both ionic strength and quencher concentration. The addition of aliquots of sodium chloride to the fluorescer solution caused a change in both μ and the concentration of quencher. There was no simple mathematical method to correct for this effect. A second method for determining ionic strength effects was subsequently devised.

b. Method Two:

In this method, a constant quencher concentration was maintained throughout the experiment resulting in measured fluorescence intensities which were dependent solely on changes in ionic strength.

Seven 10 ml solutions were prepared, each containing 1 ml of fluorescer. One solution contained only fluorescer and buffer. Another was prepared with fluorescer, buffer and 1 ml of quencher. The remaining five solutions contained equal concentrations of quencher and increasing concentrations of sodium chloride.

The quencher concentration used was 0.13M for iodide quencher and 0.19M for cesium quencher. These concentrations were chosen because they represent the concentration at 1/3 the quencher concentration range used in the original Stern-Volmer quenching experiments. The concentration of sodium chloride ranged from 0.0M to 0.380M with cesium quencher and from 0.0M to 0.370M with iodide quencher and was designed to duplicate the range in ionic strength found in the original Stern-Volmer experiments.

5. Conformational Analysis via Computer:

All conformational energy calculations for short tryptophan-containing peptides were carried out on a Burroughs B-6805 computer. Five fortran programs entitled SETVAR, ECEPP, ECEPEMIN, HYGBOND, and INDOLE were utilized for all computations. The five programs are interrelated according to the input-output scheme presented in Appendix A.

a. SETVAR:

SETVAR is used to define all the possible permutations of sets of single residue minimum dihedral angles. The sets of single residue minimum dihedral angles were obtained from work by Zimmerman, et. al.[7] For all residues except lysine, the lowest energy minima within 3Kcal of the global minimum listed in reference 7 were used. For lysine, each conformation used in SETVAR was one representative minimum from each conformational group of minima found for the residue. The SETVAR output file of combined set of angles provides the input values for the

dihedral angles to be utilized by ECEPP in its energy calculations.

b. ECEPP:

ECEPP (Empirical Conformational Energy Program for Peptides) calculates conformational energies of peptides using parameters obtained from x-ray crystal structures of small organic molecules.[8] These parameters are combined with variable geometry to produce four energy terms: electrostatic, nonbonded, hydrogen bonding, and tortional energy. The final energy function is the sum of these four energy terms.

Excluding backbone and side chain dihedral angles, all bond lengths and bond angles remain constant throughout the energy calculations. Geometry data were obtained through x-ray and neutron diffraction studies. Treating bond lengths and bond angles as constants simplifies the calculations considerably by reducing the number of variables to be considered; for example, bending and stretching constants need not be introduced.

ECEPP must utilize values of partial atomic charges in order to calculate the electrostatic energy term. These charges are determined using the CNDO (Complete Neglect of Differential Overlap) molecular orbital method and handle only valence electrons. The resulting reproduction of actual dipole moments is only fair.

The electrostatic energy term utilizes atom-centered monopole charges in order to represent a continuous charge distri-

bution. This energy term is determined using equation (11):

$$U_{el}(r_{ij}) = 332.0 q_i q_j / D r_{ij} \qquad (11)$$

where q is the partial charge using criteria outlined above, 332.0 is a conversion factor to give a final value in Kcal/mole, r_{ij} is the distance between atoms i and j and D is the effective dielectric constant (taken to be 2 in all calculations).

Nonbonded interactions (long-range attractions due to dispersion forces and short-range repulsions) are modeled using a Lennard-Jones "6-12" potential. This energy expression is given by equation (12):

$$U_{NB}(r_{ij}) = F A^{kl} / r_{ij}^{12} - C^{kl} / r_{ij}^{6} \qquad (12)$$

where F is a weighting factor equal to .5 for 1-4 type interactions and equal to 1.0 otherwise, A^{kl} is the repulsive coefficient calibrated by crystal calculations, C^{kl} is the attractive coefficient calculated from the Slater-Kirkwood formalism, and r_{ij} is the inter-atomic distance.

The hydrogen bond energy term is determined by expression (13) and is calibrated with crystal data.

$$U_{HB}(r_{H--X}) = A'_{H--X} / r_{H--X}^{12} - B_{H--X} / r_{H--X}^{10} \qquad (13)$$

where r_{H--X} is the interatomic hydrogen bond distance, A'_{H--X} and B_{H--X} are specific coefficients for particular pairs of atoms undergoing hydrogen bonding.

The final energy term, torsional energy, has an energy contribution of the type given by expression (14):

$$U_{TOR}(\theta) = (U_O/2)(1 + \cos n\theta) \qquad (14)$$

where U_O is the height of an n-fold tortional energy barrier.

A single cosine term was used to obtain a good fit with experimental data.

ECEPP locates each atom in the residue on a X,Y,Z coordinate system. This information can be obtained in a computer printout through the use of a certain print option (refer to Appendix A).

The reader is referred to reference 9 for more specific criteria for ECEPP energy calculations.

c. ECEPEMIN:

ECEPEMIN, an energy minimization program, is identical to ECEPP except for an additional subroutine called MINOP. Subroutine MINOP varies selected dihedral angles in such a way as to minimize the conformational energy. One provides the subroutine with a step size (size of a progression along a potential well function), energy criterion for convergence, and the maximim number of function calls. The lowest determined energy (and the corresponding geometry) was chosen as the minimized total energy of the peptide. The reader is referred to reference 10 for further information on the algorithm used in MINOP.

d. HYGBOND:

HYGBOND is a program designed to identify the presence of hydrogen bonds in a peptide. This program is identical to ECEPP except for three additional subroutines. The peptide's dihedral angles are obtained from ECEPEMIN (refer to Appendix A). The program examines the distance between hydrogen atoms bound to nitrogen or oxygen and other nitrogen or oxygen atoms. If this distance is 2.3 angstroms or less, a hydrogen bond is

assumed to be present. This distance criteria was chosen because it is two times the radius of a water molecule. The output designates the atoms between which this bonding takes place. It will also specify whether there is a back-bone-back-bone bond, back-bone-side-chain bond, or a side-chain-side-chain bond.

e. INDOLE:

INDOLE is a program identical to ECEPP except for one additional subroutine, subroutine Indole. INDOLE is designed to determine the interatomic distances between the indole ring of tryptophan and other atoms in the peptide which may quench indole fluorescence. The distances between two carbons (atom #'s 14 and 16 in Figure 9) and the nitrogen in the five-membered ring of indole and the amino nitrogen, carbonyl oxygen and carboxyl oxygen in the backbone were determined. One selects the range of distances which one wishes to examine. For our work, when the atoms of interest are within 1.50 and 3.35 angstroms of one another, an indole contact is believed to exist. This minimum distance of 1.5Å was chosen so as to allow for solvent water molecules to partially surround the atoms in the peptide (as would be expected in nature). The maximum distance of 3.35Å was chosen because is was believed that any greater distance would be too large to allow for exciplex formation.

INDOLE is a very powerful program because with only a few changes in the subroutine, one can determine the interatomic

distance between any two atoms in the peptide. Additionally, INDOLE could allow one to determine whether the ionic radius of an external quencher is too large to allow for unhindered contact with the quenching sites on the indole ring.

6. Conformational Letter Codes:

A conformational letter coding system developed by Zimmerman and Scheraga was used in order to classify the low energy conformations found for peptides. Letter codes were assigned to each residue in the peptide according to its location on a $\phi - \psi$ map. (See reference 4). The map is divided into 16 regions (A-H, A*-H*). Letter A denotes the region which contains the right-handed α-helix, B is the bridge region, C is the region in which C_7 hydrogen bonding occurs, E contains the extended conformations, H is the high energy region. D, F, and G were assigned to the remaining regions to indicate contiguity. Starred regions indicate left-handed conformations. This system was used to aid in the qualitative comparison of low energy conformations. Side chain dihedral angles were not used for classification.

RESULTS

Table 1 contains a summary of the k_q values for the iodide quenching of the zwitterionic forms of several tryptophan-containing peptides, NATA (N-acetyl-L-tryptophanamide, and NATE (N-acetyl-L-tryptophyl ethyl ester). The lifetime values for all the peptides except $^{2+}LT^-$ (L-lysyl-L-tryptophan) are from the single exponential decay lifetime function proposed by Werner and Forster in reference 1. Table 1 reveals that there is a correlation between the k_q values and the location of charges in the fluorescing species. The following results are seen in Table 1:

(1) The k_q values, within experimental error, are the same for $^+GTG^-$ (glycyl-L-tryptophyl-glycine), $^+T^-$ (tryptophan), NATA and NATE.

(2) k_q values are highest for peptides containing a positively charged tryptophan residue (see $^+TG^-$ (L-tryptophyl-glycine) and $^+TGG^-$ (L-tryptophan-glycyl-glycine)). k_q increases as the tryptophan residue moves farther away from the negatively charged residue.

(3) k_q values are lowest when the tryptophan residue is negatively charged. It increases as the positively charged residue moves closer to tryptophan (compare $^+GGT^-$ (glycyl-glycyl-L-tryptophan) to $^+GT^-$ (glycyl-L-tryptophan)).

Table 2 summarizes the results of iodide quenching of the anionic forms of tryptophan containing peptides. The following information is obtained:

(1) k_q and $\langle k_q \rangle$ values are greatest for GTG^-, $GTGG^-$ (glycyl-L-tryptophan-glycyl-glycine) and TG^-, where tryptophan is uncharged. The k_q value calculated with a single lifetime increases as the negative charge is moved farther away from the tryptophan residue (compare TG^-, GTG^- to $GTGG^-$).

TABLE 1

Results from Iodide Quenching of Zwitterion Forms of Small Peptides, NATA and NATE

Peptide	K_{sv}[a] (M^{-1})	τ_f[b] (ns) (±10%)	$k_q \times 10^9$ ($M^{-1}sec^{-1}$)
NATA	13.2±0.5	2.8	4.7±0.6
NATE	6.3±0.4	1.3	4.8±0.8
$^{+}GGT^{-}$	2.7±0.1	1.2	1.7±0.2
$^{+}GT^{-}$	2.7±0.1	0.90	3.0±0.4
$^{+}GTG^{-}$	4.3±0.2	0.85	5.1±0.5
$^{+}GTGG^{-}$	5.4±0.1	0.88	6.1±0.7
$^{+}T^{-}$	14.0±0.4	2.8	5.0±0.6
$^{+}TG^{-}$	11.5±0.4	1.6	7.2±1.0
$^{+}TGG^{-}$	9.5±0.1	1.1	9.0±1.0
$^{2+}LT^{-}$	7.6±0.3	1.3[c]	5.7±0.8

a. Includes some data from reference 6.

b. Single-exponential decay lifetime τ_f obtained from reference 1.

c. Represents the weighted average lifetime, $\langle\tau\rangle = f_1 \tau_1 + f_2 \tau_2$ obtained from reference 1.

TABLE 2

Results from Iodide Quenching of Anion Forms of Small Peptides

Peptide	$K_{sv}(M^{-1})$	τ_f(ns)[a] (±10%)	$k_q \times 10^9 (M^{-1} sec^{-1})$[b]	$\langle\tau\rangle$(ns)[c] (±10%)	$\langle k_q \rangle \times 10^9 (M^{-1} sec^{-1})$[d]
GT^-	3.8±0.1	1.9	2.0±0.2	1.6	2.3±0.3
GGT^-	3.3±0.2	1.6	2.1±0.3	1.2	2.8±0.4
GTG^-	5.0±0.5	1.7	2.9±0.6	1.1	4.7±0.9
GTG^-	4.8±0.1	1.2	4.0±0.5	---	---
$^+LT^-$	7.5±0.2	3.2	2.3±0.3	2.7	2.8±0.6
PT^-	8.2±0.3	4.9	1.7±0.2	3.2	2.5±0.3
TG^-	19.3±0.1	6.9	2.8±0.3	---	---

a. Single-exponential decay lifetime, τ_f, obtained from reference 1.

b. Calculated using single-exponential lifetime, τ_f.

c. Weighted average lifetime, $\langle\tau\rangle$, obtained from reference 1.

d. Calculated with weighted average lifetime, $\langle\tau\rangle$.

(2) The k_q and $\langle k_q \rangle$ values are lowe . for those peptides in which tryptophan is negatively charged, i.e. GT^-, GGT^-, PT^- (L-prolyl-L-tryptophan), $^+LT^-$. The k_q values (for both single and weighted average lifetimes) are, within experimental error, the same for these peptides.

(3) Comparison of Table 1 to Table 2 reveals that the single lifetime k_q value for all the peptides studied, except GGT^-, are smaller for the anion species.

Table 3 summarizes the results of the cesium quenching of the zwitterionic forms of several tryptophan-containing peptides, NATA, and NATE. The following information can be obtained:

(1) There is no correlation between the location of the charges in the peptide and the quenching efficiency of cesium ion.

(2) The k_q values for NATA, NATE, and $^+T^-$ are the same within experimental error.

(3) The Stern-Volmer plot for the cesium quenching of $^{2+}LT^-$ is non-linear (See Figures 1 and 2).

(4) The k_q values for cesium quenching the peptides in Table 3 are smaller than those for the iodide quenching of the same peptides (compare Table 1 to Table 2). This supports the findings of other workers who have shown that iodide ion is a more efficient quencher than cesium ion.[11]

Table 4 summarizes the Stern-Volmer data for the cesium quenching of the anionic forms of some tryptophan-containing peptides. The following results are observed:

(1) The k_q values calculated with the weighted average lifetime value are greater for all of the peptides studied, except TG^-, than those calculated with a single lifetime value.

(2) There is no simple correlation between the k_q, $\langle k_q \rangle$ values and the location of the negative charge in the peptide (compare GT^- to GTG^- to TG^-).

TABLE 3

Results from Cesium Quenching of Zwitterion Forms of Small Peptides, NATA and NATE

Peptide	$K_{sv}(M^{-1})$	τ_f(ns)[a](±10%)	$k_q \times 10^9 (M^{-1}sec^{-1})$[b]
NATA	1.8 ±0.02	2.8	0.65±0.07
NATE	0.81±0.04	1.3	0.62±0.09
$^{+}TG^{-}$	1.4 ±0.04	1.6	0.87±0.11
$^{+}T^{-}$	1.9 ±0.01	2.8	0.69±0.07
$^{2+}LT^{-}$	*	1.7	---

a. Single-exponential decay lifetime, τ_f, obtained from reference 1.

b. Calculated with single-exponential lifetime.

* Non-linear Stern-Volmer plot.

FIGURE 1

Stern-Volmer Plot

$^{2+}_{LT^-}$ Trial 1

F_T°/F_T vs $[Cs^+]$

λ_{ex} = 290 nm

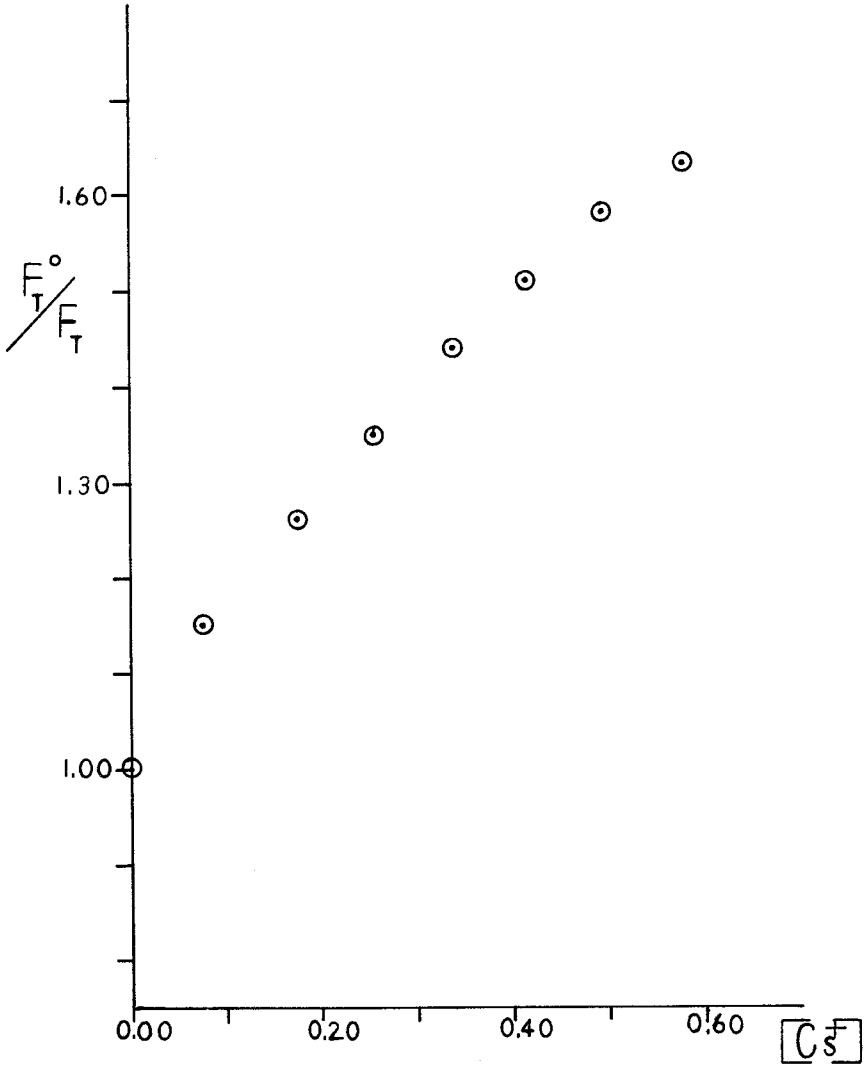
1.60
1.30
1.00
$\frac{F_T^\circ}{F_T}$
0.00
0.20
0.40
0.60
C_S^F

FIGURE 2

Stern-Volmer Plot

$^{2+}LT^{-}$ Trial 2

$F_T°/F_T$ vs $[Cs^+]$

λ_{ex} = 290 nm

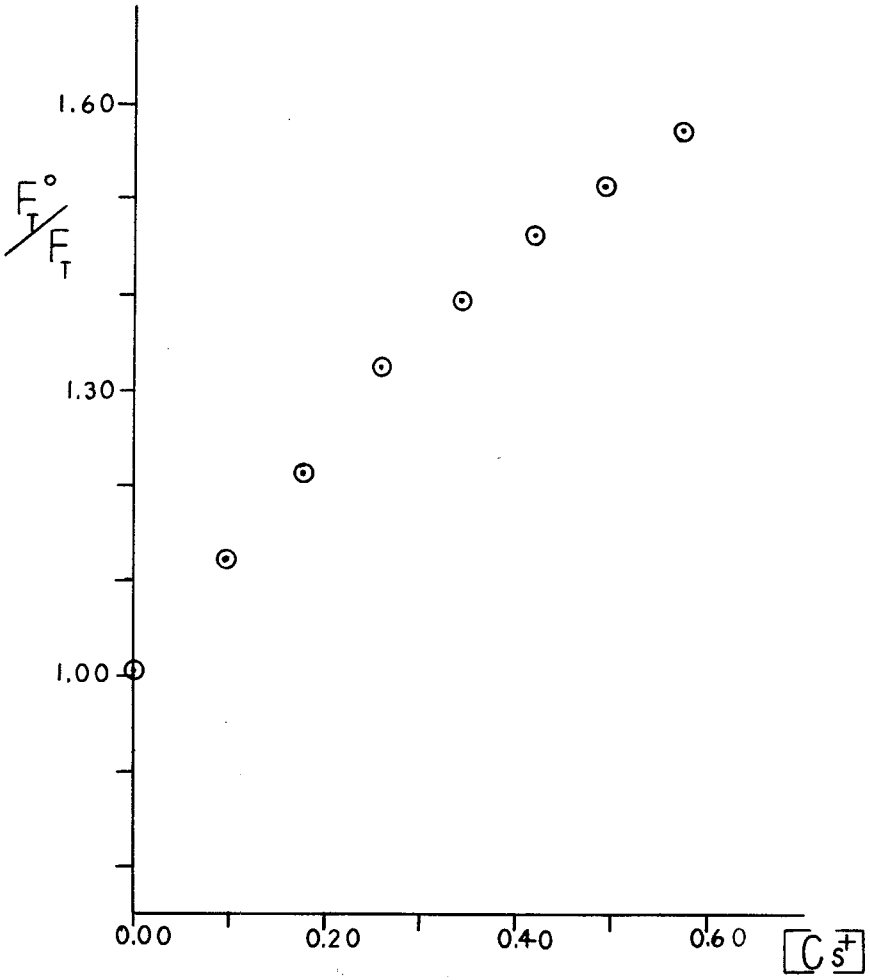
1.60
1.30
1.00
F_T° / F_T
0.00
0.20
0.40
0.60
$[Cs^+]$

TABLE 4

Results from Cesium Quenching of
Anion Forms of Small Peptides

Peptide	$K_{sv}(M^{-1})$	τ_f(ns)[a](±10%)	$k_q \times 10^9 (M^{-1}sec^{-1})$[b]	$\langle\tau\rangle$(ns)[c](±10%)	$\langle k_q \rangle \times 10^9 (M^{-1}sec^{-1})$[d]
GT^-	1.1±0.04	1.9	0.56±0.08	1.6	0.65±0.09
GTG^-	1.2±0.04	1.7	0.73±0.1	1.1	1.2 ±0.2
GGT^-	1.2±0.1	1.6	0.72±0.1	1.2	0.97±0.2
TG^-	4.1±0.2	6.9	0.59±0.09	---	---
$^+LT^-$	1.7±0.05	3.2	0.52±0.07	2.7	0.62±0.08
PT^-	3.5±0.5	4.9	0.71±0.2	3.2	1.1 ±0.3

a. Single-exponential decay, τ_f, obtained from reference 1.

b. Calculated with single-exponential lifetime.

c. Weighted average lifetime, $\langle\tau\rangle$, obtained from reference 1.

d. Calculated with weighted average lifetime.

(3) The k_q and $\langle k_q \rangle$ values for the cesium quenching of the anion species are much smaller than those obtained for the iodide quenching of the same compounds (compare Table 2 to Table 4). This again supports the contention that iodide ion is a more efficient quencher than cesium.

Table 5 shows the results of quantum yield studies of the zwitterionic and anionic forms of T, TG and TGG. The following results are obtained:

(1) ϕ_R values for the zwitterion species are lower than ϕ_R values for the anion species of all the peptides studied.

(2) ϕ_R for TG^- and T^- are identical.

(3) When an additional glycine residue is added to TG, ϕ_R decreases for both the zwitterionic and anionic species (compare TG to TGG).

Table 6 lists $\phi_{R_{100\%D_2O}} / \phi_{R_{100\%H_2O}}$ for the zwitterionic and anionic forms of T, TG and TGG. It is seen that except for $^+T^-$, this ratio is the same for all the peptides studied.

Table 7 shows the position of the fluorescence wavelength maximum for the zwitterionic and anionic forms of TG, TGG, GGT (and the tryptophan zwitterion). The range of variation in λ_{max} is only 10 nm. It is seen, however, that λ_{max} increases by 10 nm when the positive charge is removed from the tryptophan residue.

Table 8 shows the K_{sv} values and correlation coefficients for various mixtures of NATA and $^+GT^-$. The mixtures were created in order to simulate a solution with double-exponential decay. The correlation coefficients reveal that all the Stern-Volmer plots studied were linear.

TABLE 5

Results from Quantum Yield Studies of Zwitterion and Anion Forms of Small Peptides, NATA and NATE

Peptide	ϕ_R
NATA	1.00*
NATE	0.46*
$^{+}T^{-}$	1.00*
T^{-}	2.50*
$^{+}TG^{-}$	0.62*
TG^{-}	2.50*
$^{+}TGG^{-}$	0.37 ± 0.07
TGG^{-}	1.04 ± 0.06

* Data obtained from reference 1.

TABLE 6

Results from Deuterium Isotope Quantum Yield Experiment

Peptide	$\phi_{R_{100\%D_2O}} / \phi_{R_{100\%H_2O}}$
$^{+}T^{-}$	2.0
T^{-}	1.5
$^{+}TG^{-}$	1.6
TG^{-}	1.4
$^{+}TGG^{-}$	1.5
TGG^{-}	1.5

TABLE 7

Fluorescence Wavelength Maximum for Zwitterion and Anion Forms of Small Peptides

Peptide	λ_{max} (nm)
$^{+}T^{-}$	350
$^{+}TG^{-}$	346
TG	356
$^{+}TGG^{-}$	345
TGG^{-}	355
$^{+}GGT^{-}$	355
GGT^{-}	355

TABLE 8

Results from Cesium Quenching of Mixtures of NATA and $^{+}GT^{-}$

Peptide Mixture	$K_{sv}(M^{-1})$	r[a]
NATA:$^{+}GT^{-}$	1.3±0.04	0.9976
2NATA:$^{+}GT^{-}$	1.5±0.04	0.9972
NATA:2$^{+}GT^{-}$	1.1±0.005	0.9962

a. Correlation Coefficient: r = 1 means exact linearity.

Table 9 summarizes the results of Stern-Volmer quenching experiments of the tryptophan zwitterion at fluorescence emission wavelengths of 330 nm and 370 nm (about 20 nm above and below the fluorescence wavelength maximum for tryptophan). It is seen from the correlation coefficients that the Stern-Volmer plots at both wavelengths have linear slopes. There is little variation between the K_{sv} and k_q values found at 330 nm and those found at 370 nm.

Table 10 summarizes the data obtained from the modified Stern-Volmer plots constructed using either experimentally obtained or theoretically derived values for the fluorescence intensities at given quencher concentrations. The correlation coefficients reveal that both plots are linear. It is also seen that the K_{sv} value obtained using experimentally measured fluorescence values in the plot is almost identical to that obtained when theoretically derived values for the quantum yields are used. The fractional maximum accesible protein fluorescence value, f_a, found through experiment is comparable to that obtained with theoretical calculations.

Table 11 presents data on the variation of the Stern-Volmer ratio, F_T^o/F_T, for zwitterion and anion forms of some tryptophan-containing peptides undergoing iodide quenching as a function of ionic strength. Table 12 shows the results of the ionic strength experiments with cesium quencher. The following information can be obtained from these tables:

TABLE 9

Results from Cesium Quenching of Tryptophan Zwitterion Monitored at Emission Wavelengths of 330 nm and 370 nm

λ_{em} (nm)	K_{sv} (M^{-1})	$k_q \times 10^9$ ($M^{-1}sec^{-1}$)	r[a]
330	1.9±0.04	0.68±0.08	.9995
370	1.7±0.04	0.60±0.07	.9995

a. Correlation Coefficient

TABLE 10

Results from Experimental and Theoretical Modified Stern-Volmer Plots for $^{2+}LT^{-}$

Method	$K_{sv}(M^{-1})$	f_a	r^a
Experimental	3.0±0.03	0.59±0.04	.9969
Theoretical	2.9	0.65	.9999

a. Correlation Coefficient

TABLE 11

Results from Ionic Strength Experiment with Iodide Quencher on Zwitterion and Anion Forms of Small Peptides

Peptide	μ	F_T^o/F_T (Trial 1)	F_T^o/F_T (Trial 2)
$^+GT^-$	0.00	1.00	1.00
	0.192	1.36	1.36
	0.253	1.32	1.28
	0.315	1.29	1.36
	0.377	1.29	1.42
	0.438	1.26	1.32
	0.500	1.24	1.29
$^+GTG^-$	0.00	1.00	1.00
	0.192	1.54	1.63
	0.253	1.59	1.57
	0.315	1.49	1.53
	0.377	1.51	1.38
	0.438	1.51	1.33
	0.500	1.42	---
$^+PT^-$	0.00	1.00	1.00
	0.130	1.77	1.21
	0.161	1.77	1.38
	0.192	1.77	1.29
	0.253	1.57	1.37
	0.315	1.10	1.41
	0.377	1.66	1.32
	0.438	1.66	1.09
$^+TG^-$	0.00	1.00	1.00
	0.130	2.23	2.22
	0.161	2.23	2.41
	0.192	2.23	2.25
	0.253	2.23	2.29
	0.315	2.68	2.29
	0.377	2.23	2.29
	0.438	---	2.28
TG^-	0.00	1.00	1.00
	0.130	3.13	3.16
	0.161	3.38	3.08
	0.192	3.44	3.24
	0.253	3.44	3.52
	0.315	4.12	3.43
	0.377	3.59	3.24
	0.438	3.52	3.52

TABLE 11 (Cont.)

Peptide	μ	F_T^o/F_T (Trial 1)	F_T^o/F_T (Trial 2)
$^{+}LT^{-}$	0.00	1.00	1.00
	0.131	1.86	1.99
	0.169	1.80	1.93
	0.192	1.60	1.84
	0.253	1.64	1.91
	0.315	1.64	1.93
	0.377	1.65	1.93
	0.438	1.64	1.91
GTG^{-}	0.00	1.00	1.00
	0.131	1.48	1.50
	0.169	1.60	1.49
	0.192	1.63	1.43
	0.253	1.53	1.49
	0.315	1.58	1.33
	0.377	1.53	1.49
	0.438	1.51	1.46

TABLE 12

Results from Ionic Strength Experiment with Cesium Quencher on Zwitterion and Anion Forms of Small Peptides

Peptide	μ	F_T^o / F_T (Trial 1)	F_T^o / F_T (Trial 2)
$^{+}GT^{-}$	0.00	1.00	1.00
	0.190	---	1.08
	0.221	---	1.06
	0.253	1.07	1.04
	0.317	1.14	1.04
	0.380	1.14	1.09
	0.444	1.12	1.27
	0.507	1.14	1.02
	0.570	1.12	---
$^{+}GTG^{-}$	0.00	1.00	1.00
	0.190	---	1.12
	0.221	---	0.83
	0.253	1.33	1.07
	0.317	1.33	1.17
	0.380	1.29	1.01
	0.444	1.21	1.14
	0.507	1.13	1.08
	0.570	---	---
$^{2+}LT^{-}$	0.00	1.00	1.00
	0.190	---	1.27
	0.221	---	1.22
	0.253	1.32	1.28
	0.317	1.32	1.23
	0.380	1.47	1.27
	0.444	1.47	1.25
	0.507	1.47	1.28
	0.570	1.47	---
$^{+}TG^{-}$	0.00	1.00	1.00
	0.190	---	1.16
	0.221	---	1.07
	0.253	1.36	1.22
	0.317	1.30	1.05
	0.380	1.30	1.05
	0.444	1.24	1.06
	0.507	1.22	1.07
	0.570	1.27	---

TABLE 12 (Cont.)

Peptide	μ	F_T^o / F_T (Trial 1)	F_T^o / F_T (Trial 2)
$^+LT^-$	0.00	1.00	---
	0.190	1.16	---
	0.221	1.11	---
	0.253	1.27	---
	0.317	1.11	---
	0.380	1.10	---
	0.444	1.16	---
	0.507	1.11	---
GT^-	0.00	1.00	---
	0.190	1.12	---
	0.221	1.10	---
	0.253	1.21	---
	0.317	1.08	---
	0.380	1.10	---
	0.444	1.10	---
	0.507	1.10	---

(1) There is evidence of consistent changes in the Stern-Volmer ratio as a function of ionic strength. Some peptides show a general increase in F_T^o/F_T as increases. Others show a general decrease in F_T^o/F_T as μ increases.

(2) A few data points in the F_T^o/F_T vs. μ plot for each peptide do not follow the general trend for the peptide. In general, this erratic behavior is more prevalent in ionic strength experiments with cesium quencher (compare Table 11 to Table 12).

(3) There is not a large degree of reproducibility of results due to the observed erratic behavior.

Table 13 presents values for the percentage change in F_T^o/F_T for each trial as well as the average percent change for each peptide. The % change is given by expression (15):

$$\% \text{ change} = \frac{F_T^o/F_T \ (\mu = \text{minimum; quencher present}) - F_T^o/F_T \ (\mu = \text{maximum})}{F_T^o/F_T \ (\mu = \text{minimum; quencher present})} \qquad (15)$$

This value does not account for all the points but helps to qualitatively describe the change in F_T^o/F_T as a function of ionic strength. A positive % change indicates a consistent decrease in the Stern-Volmer ratio as ionic strength increases. A negative % change value signifies an increase in F_T^o/F_T as μ increases. The following results are obtained from Table (13):

(1) Three peptides show an increase in F_T^o/F_T as a function of increasing ionic strength ($^+TG^-$, TG^- with iodide ion ar $^{2+}LT^-$ with cesium quencher). The remaining ten peptides have positive % change values.

(2) Five peptides have relatively low absolute values (less than 5%) for the average % change. These are $^+TG^-$ and GTG^- with iodide quencher and GT^-, $^+LT^-$, and GT^- with cesium quencher.

TABLE 13

Percentage Change in F_T^o/F_T for Ionic Strength Experiment on Zwitterion and Anion Forms of Small Peptides

Peptide	Quencher	%Change[a] (Trial 1)	% Change[a] (Trial 2)	% Change-AVG
$^{+}GT^{-}$	I^{-}	8.8	5.1	7.0±0.2
$^{+}GTG^{-}$	I^{-}	7.7	18.4	13.1±5.3
$^{+}PT^{-}$	I^{-}	6.2	9.9	8.1±1.8
$^{+}TG^{-}$	I^{-}	0.0	-2.7	-1.3±1.3
TG^{-}	I^{-}	-12.5	-11.3	-11.9±0.6
$^{+}LT^{-}$	I^{-}	11.8	4.0	7.9±3.9
GTG^{-}	I^{-}	-2.0	-4.3	3.1±0.1
$^{+}GT^{-}$	Cs^{+}	-4.7	5.5	0.4±5.1
$^{+}GTG^{-}$	Cs^{+}	15.0	3.6	9.3±5.7
$^{2+}LT^{-}$	Cs^{+}	-11.4	-0.8	-6.1±5.3
$^{+}TG^{-}$	Cs^{+}	6.6	7.8	7.2±0.6
$^{+}LT^{-}$	Cs^{+}	4.3	---	---
GT	Cs^{+}	1.8	---	---

a. % Change =

$$\frac{F_T^o/F_T \ (\mu = \text{minimum; quencher present}) - F_T^o/F_T \ (\mu = \text{maximum}) \times 100}{F_T^o/F_T \ (\mu = \text{minimum; quencher present})}$$

(3) Five peptides have moderately low values (between 5% and 9%) for the average % change. These are $^{+}GT^{-}$, $^{+}PT^{-}$, and $^{+}LT^{-}$ with iodide quencher and $^{2+}LT^{-}$ and $^{+}TG^{-}$ with cesium quencher.

(4) Three peptides have relatively high absolute values (greater than 9%) for the average % change. These are $^{+}GTG^{-}$ and TG^{-} with iodide quencher and $^{+}GTG^{-}$ with cesium quencher. No peptide has an average percent change greater than 15%.

Table 14 summarizes the results of computer calculations on six tryptophan-containing peptides. The number of starting conformations was determined through the use of SETVAR which combines single residue minima. The number of low energy peptide minimized conformations is determined by counting the number of conformations whose energy is within 3.0 Kcal of the lowest energy conformation for a given peptide. Those conformations with hydrogen bonds and/or indole contacts follow the criteria outlined earlier. Table 14 reveals the following information:

(1) There is no change in the number of low energy conformations when uncharged tryptophan becomes a zwitterion.

(2) Although $^{+}TGG^{-}$ has a much greater number of starting conformations than $^{+}TG^{-}$, it has an almost equal number of low energy minimized conformations. Thus the addition of a second glycine does not drastically increase energy stabilization.

(3) There is some dependence of peptide energy stabilization upon the position of the glycine residue in tryptophan-containing dipeptides. It is seen that there are more low energy conformations when glycine is the N-terminal end of the dipeptide than when it is in the C-terminal position.

TABLE 14

Results from Computer Analysis of Zwitterion Forms of Six Tryptophan-Containing Peptides

Peptide	# of Conformations Studied	# of Low Energy Minimized Conformations	# of Hydrogen Bonds	% of Hydrogen Bonds[a]	# of Indole Contacts	% of Indole Contacts[b]
$^{+}T^{-}$	30[c]	30	6	20.0	6	18.8
$^{+}TG^{-}$	270	121	27	22.3	26	21.5
$^{+}TGG^{-}$	1089	129	76	58.9	28	21.7
$^{+}GT^{-}$	270	176	50	28.0	89	50.6
$^{+}PT^{-}$	150	48	11	22.9	16	33.3
$^{2+}LT^{-}$[d]	390	3	0	0.0	3	100

a. This is the percentage of hydrogen bonds among the low energy conformations.

b. This is the percentage of indole contacts among the low energy conformations.

c. Refers to the low energy single residue minima for uncharged blocked tryptophan.

d. Note: Only a few conformations of $^{2+}LT^{-}$ were completely minimized.

(4) There is some dependence of energy stabilization upon the identity of the N-terminal residue (other than tryptophan) in tryptophan-containing dipeptides. When glycine is in this position the greatest number of low energy conformations result (compare $^{+}$GT^{-}, $^{+}$PT^{-}, and $^{2+}$LT^{-}).

(5) All the residues, excepting $^{+}$TGG^{-} (and $^{2+}$LT^{-}) have the same percentage of hydrogen bonds among the low energy conformations. There appears to be little correlation between the position of tryptophan in the dipeptide and the number of hydrogen bonds produced.

(6) The percentage of hydrogen bonds among the low energy conformations increases markedly upon the addition of a second glycine residue to the $^{+}$TG^{-} dipeptide.

(7) There is some dependence of the percentage of low energy conformations which fit the given criteria for indole contacts on the position of the tryptophan residue in the peptides. This percentage varies insignificantly when tryptophan is on the N-terminal end of the peptide. The percentage increases sharply when tryptophan is on the C-terminal end of the peptide.

(8) The addition of a second glycine residue to $^{+}$TG^{-} has no effect upon the percentage of low energy conformations which have indole contacts.

Table 15 presents a comparison of the Zimmerman letter code types (and number of types) for the low energy conformations of single residues to those present when these residues are bound in tryptophan-containing peptides. The letter codes for the peptides listed in the last column of Table 15 are a compilation of the results displayed graphically in Figures 3 through 8. The following trends are evident in Table 15:

TABLE 15

Comparison of Conformational Letter Codes[a]
for Single Residue Minima and Peptide Minima

Peptide	Residue in Peptide	Letter Code Regions for Single Residue Minima	# of Regions for Single Residue	Letter Code Regions for Peptide Minima	# of Regions for Peptide Minima
$^{+}T^{-}$	Trp	A,C,D,E,F,G,A*[b]	7	A,C,D,E,F,G,H,A*,G*	9
$^{+}TG^{-}$	Trp	A,C,D,E,F,G,A*	7	A,C,D,E,F,G,C*,H*	8
	Gly	A,C,D,E,F,A*,C*,D*,F*	9	A,C,D,F,A*,C*,D*,E*,F*	9
$^{+}TGG^{-}$	Trp	A,C,D,E,F,G,A*	7	C,D,E,F,G	5
	Gly_1	A,C,D,E,F,A*,C*,D*,F*	9	A,C,D,A*,C*,D*	6
	Gly_2	A,C,D,E,F,A*,C*,D*,F*	9	A,C,D,F,A*,C*,D*,E*,F*	9
$^{+}GT^{-}$	Gly	A,C,D,E,F,A*,C*,D*,F*	9	A,C,D,F,A*,C*,D*,E*,F*	9
	Trp	A,C,D,E,F,G,A*	7	A,C,D,E,F,G	6
$^{+}PT^{-}$	Pro	A,C,F	3	F	1
	Trp	A,C,D,E,F,G,A*	7	A,C,D,E,F	6
$^{2+}LT^{-}$	Lys	A,C,D,E,F,G,A*	7	F	1
	Trp	A,C,D,E,F,G,A*	7	F	1

a. Developed by Zimmerman, refer to reference 4.

b. Refers to uncharged tryptophan single residue minima.

(1) There is an increase in the number of types of low energy conformations when uncharged tryptophan is converted into its zwitterion form.

(2) There is a consistent decrease in the number of conformational types for tryptophan when it is in the C-terminal position of three dipeptides (see $^{+}GT^{-}$, $^{+}PT^{-}$, $^{2+}LT^{-}$).

(3) There is no change in the number of conformational types of glycine when it is in the C-terminal position of the peptides studied (see $^{+}TG^{-}$, $^{+}TGG^{-}$).

(4) There is a decrease (from 9 to 6) in the number of conformational types of glycine when it is located in the middle of the tripeptide, $^{+}TGG^{-}$.

(5) There is the addition of an E* conformational type for glycine when it is on either the C-terminal or N-terminal end of peptides (see $^{+}TGG^{-}$, $^{+}GT^{-}$, and $^{+}TG^{-}$).

(6) The number of conformational types for tryptophan is decreased when it is located in the tripeptide, $^{+}TGG^{-}$.

Figures 3 through 8, $\phi - \psi$ conformational letter code maps of low energy conformations provide additional information about the distribution of conformational types when the individual residues studied are found in different peptides. The following observations are made:

(1) Figure 3, $^{+}T^{-}$: The majority of conformations are of the unstarred type.

(2) Figure 4, $^{+}TG^{-}$: The majority of tryptophan conformations are unstarred. Glycine has conformations well-distributed throughout the $\phi - \psi$ map.

(3) Figure 5, $^{+}TGG^{-}$: Tryptophan has no starred conformations. In general, both glycine residues are distributed in the same letter code regions (except E* and F* regions).

FIGURE 3

Conformational Letter Code Map for $^{+}T^{-}$

X-Trp

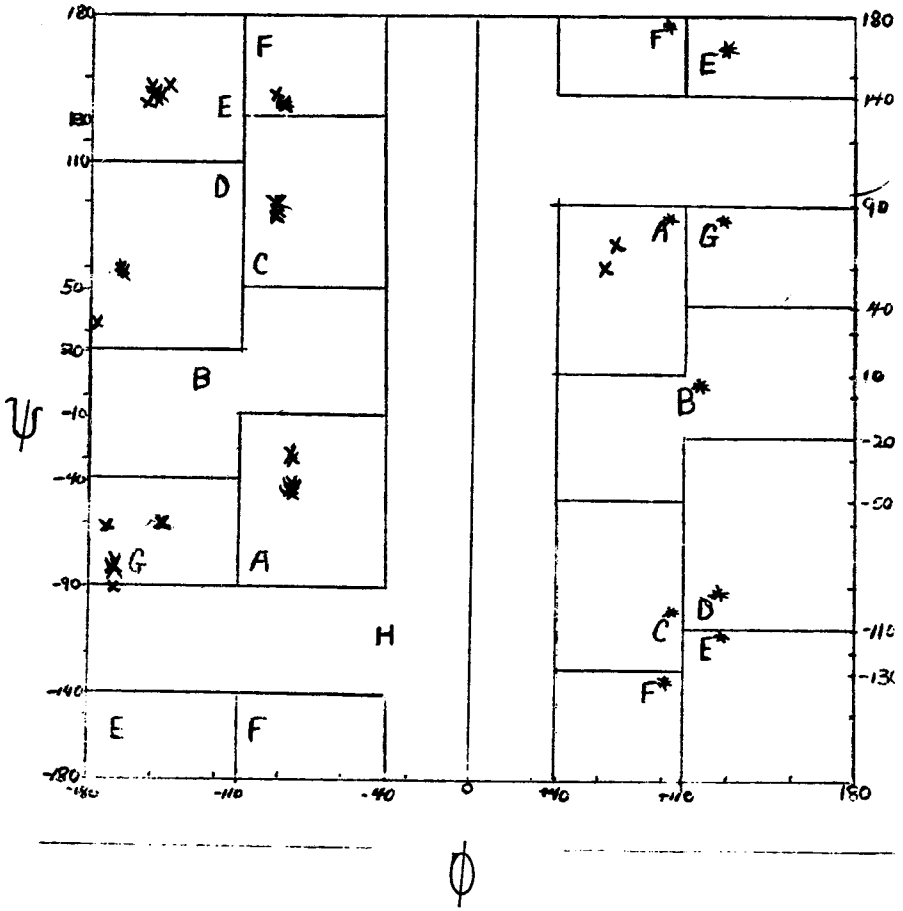
F
E
D
C
B
A
G
H
E
F
F*
E*
A*
G*
B*
C*
D*
E*
F*
ψ
φ
180
140
90
40
10
-20
-50
-110
-130
-180
-140
-110
-40
0
40
110
140
180

FIGURE 4

Conformational Letter Code Map for $^{+}TG^{-}$

X - Trp

O - Gly

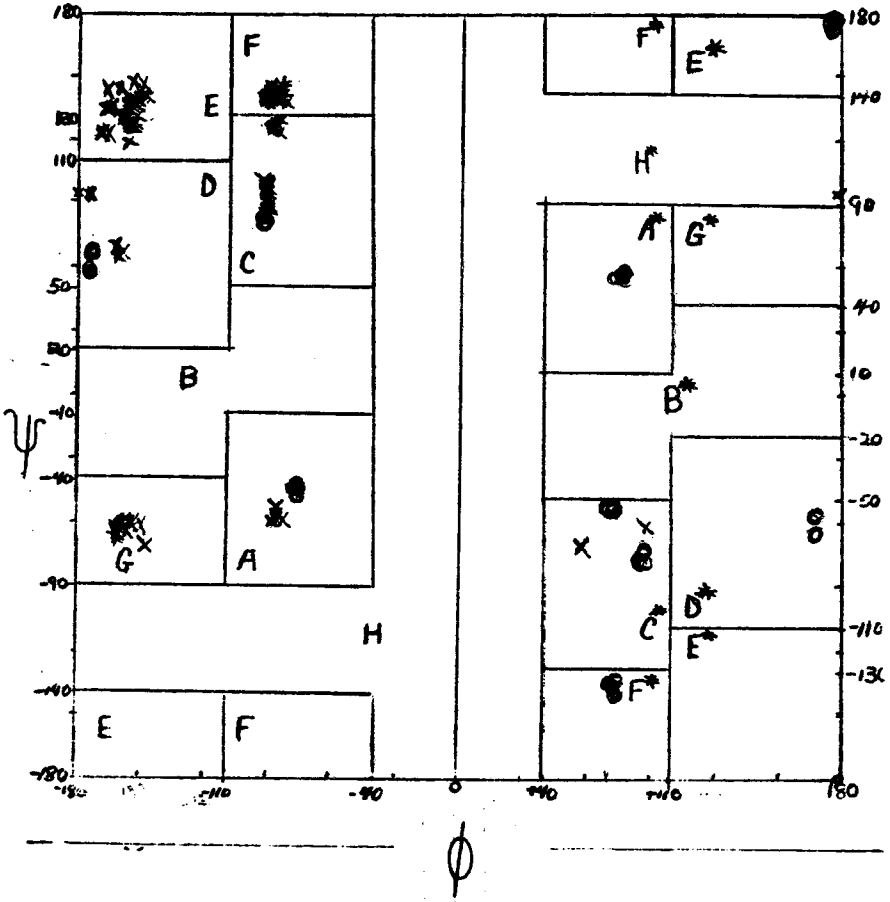
180
110
50
-10
-90
-140
-180
-110
-90
0
90
110
180
40
10
-20
-50
-110
-130
ψ
φ
A
B
C
D
E
F
G
H
A*
B*
C*
D*
E*
F*
G*
H*

FIGURE 5

Conformational Letter Code Map for $^{+}TGG^{-}$

X - Trp

0 - Gly_1

□ - Gly_2

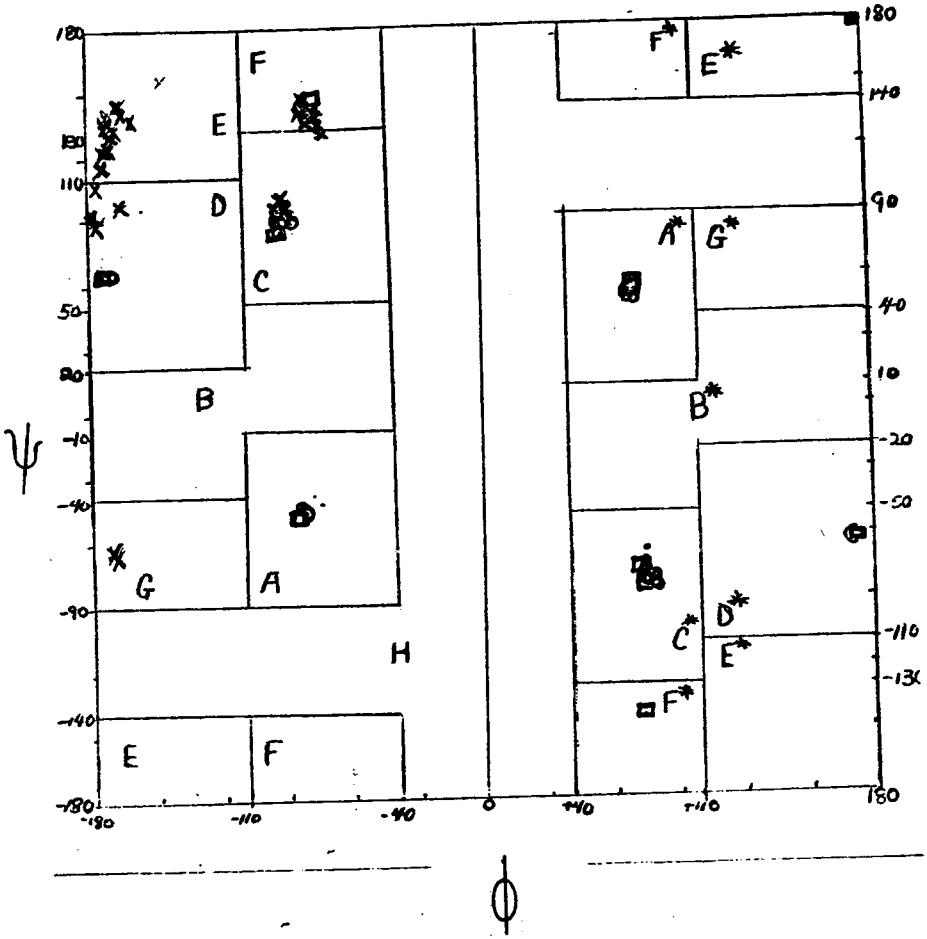
180
110
90
50
10
-10
-40
-90
-140
-180
-180
-110
-40
0
40
110
180
F
E
D
C
B
A
G
H
F*
E*
A*
G*
B*
C*
D*
E*
F*

FIGURE 6

Conformational Letter Code Map for $^{+}GT^{-}$

X - Gly

O - Trp

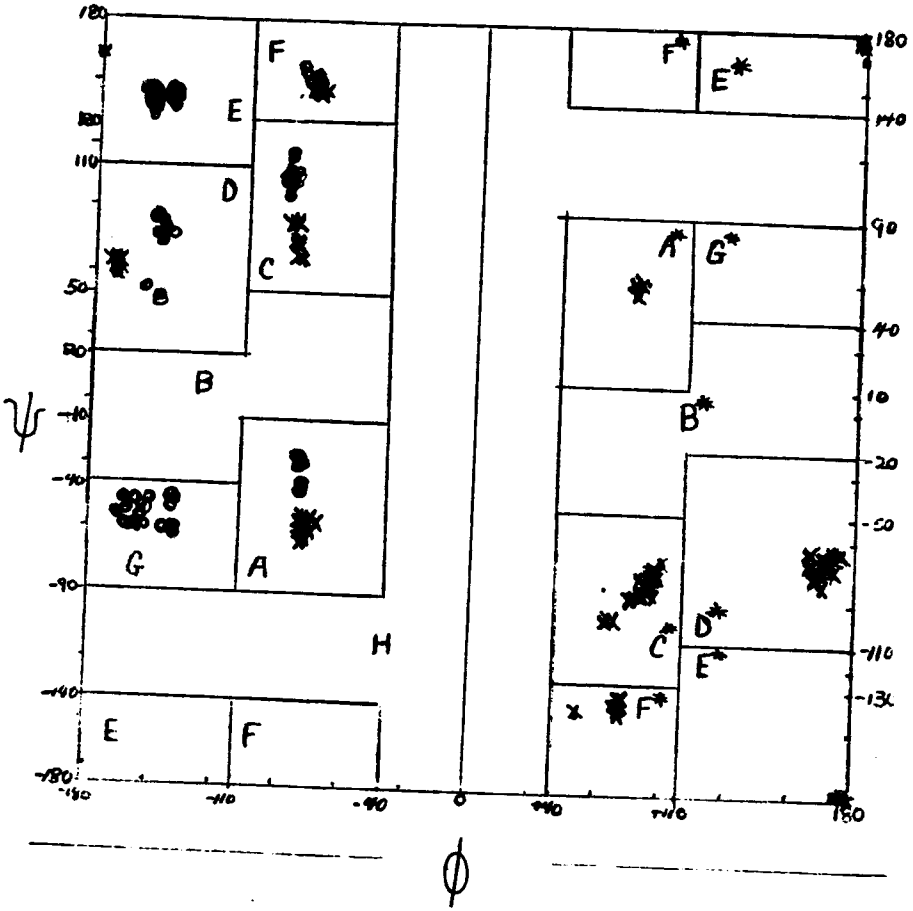
ψ
ϕ
A
B
C
D
E
F
G
H
A*
B*
C*
D*
E*
F*
G*
180
110
90
50
10
-10
-50
-90
-110
-130
-180

FIGURE 7

Conformational Letter Code Map for $^{+}PT^{-}$

X - Pro

0 - Trp

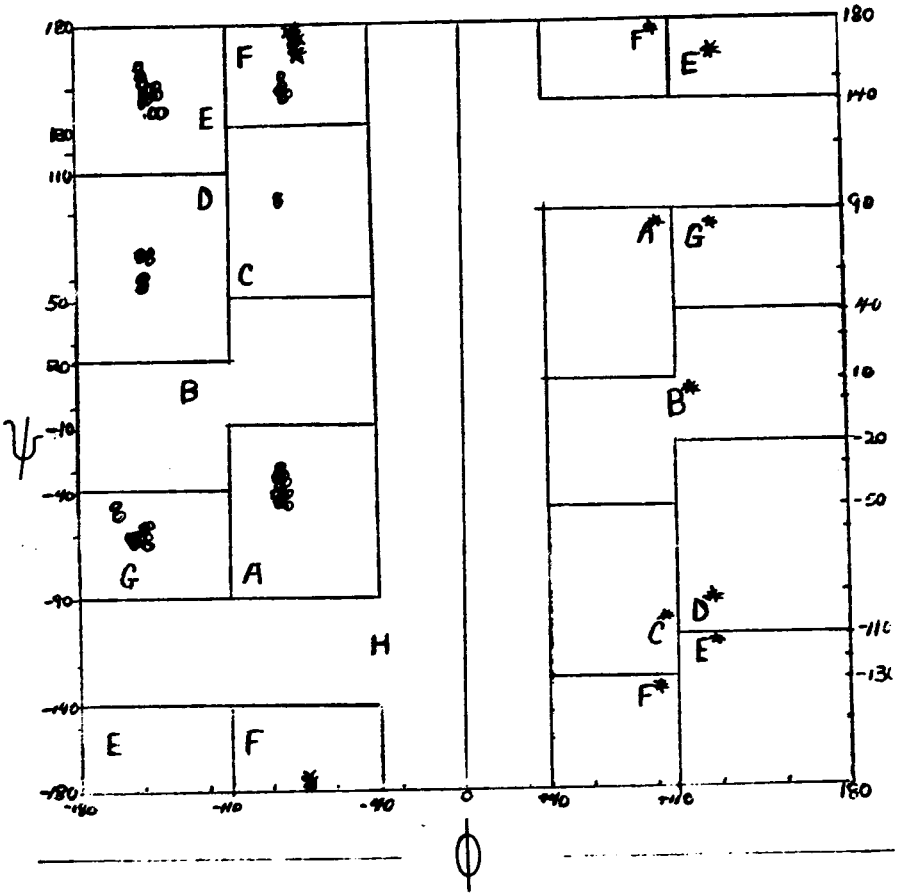
180
140
90
40
10
-20
-50
-110
-130
160
F
E
D
C
B
A
G
H
F*
E*
A*
G*
B*
C*
D*
E*
F*

FIGURE 8

Conformational Letter Code Map for $^{2+}LT^{-}$

X - Lys

O - Trp

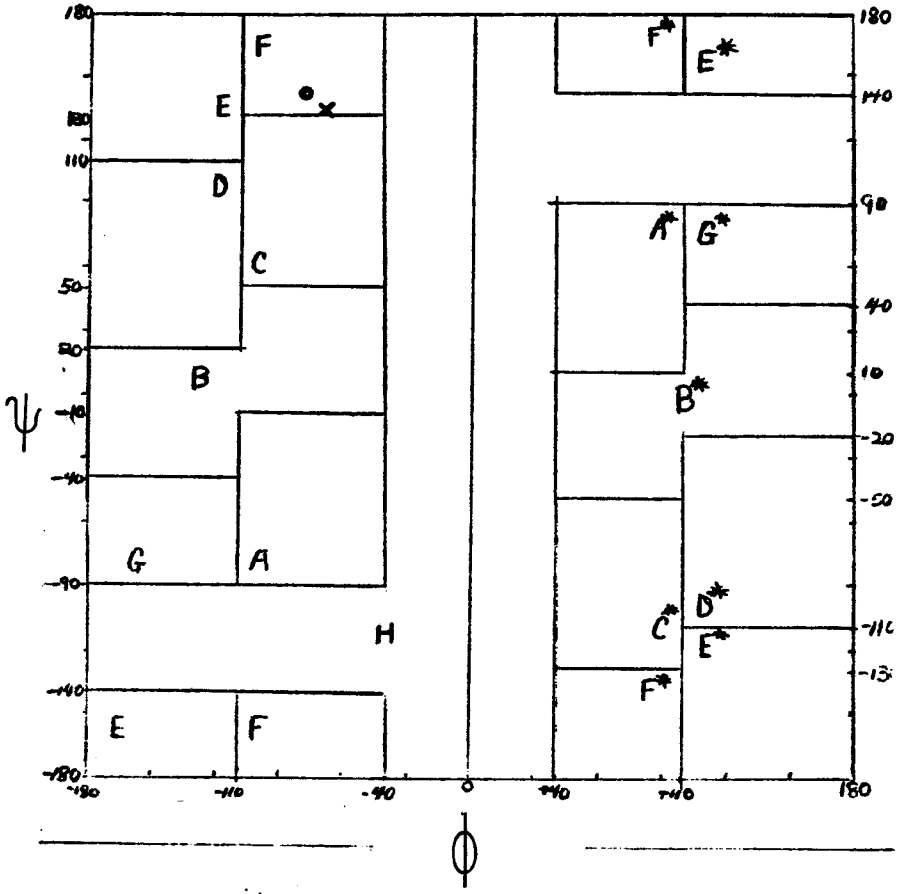
180
110
50
-10
-90
-140
-180
-110
-90
0
90
110
140
180
F
E
D
C
B
G
A
H
F*
E*
A*
G*
B*
C*
D*
E*
F*
ψ
φ

(4) Figure 6, $^{+}GT^{-}$: Tryptophan has no starred conformations. The majority of the tryptophan conformations are in the E region. Glycine is well distributed throughout both the starred and unstarred regions.

(5) Figure 7, $^{+}PT^{-}$: Neither residue in the dipeptide is found in the starred regions of the map. Proline is restricted to the F region. Tryptophan is well distributed throughout the left side of the $\phi - \psi$ map.

(6) Figure 8, $^{2+}LT^{-}$: Too few conformations were actually minimized to reveal much information about $^{2+}LT^{-}$.

Figures 9 through 14 show the structural formula of the peptides studied via computer. Next to each atom is the atom number assigned to it by the computer programs described earlier. Atom numbers facilitate discussions about hydrogen bonding and indole contact interactions.

Figures 15 through 20 present additional information about the six peptides studied via computer. Each figure lists the variable backbone and side chain dihedral angles for each low energy conformation. Next to each set of angles is the energy (designated ENG) for that conformation. The column(s) lists the $\phi - \psi$ conformational letter code for each residue in the peptide. The last two columns show the atom numbers of those atoms in each conformation which undergo hydrogen bonding and/or fulfill the indole contact distance criteria.

Figure 15 presents data on the tryptophan zwitterion. The following information is obtained:

(1) There is only one type of hydrogen bond. This occurs between the amino proton and either partially negatively charged oxygen in the

FIGURE 9

Structure and Atom Numbers for $^{+}T^{-}$

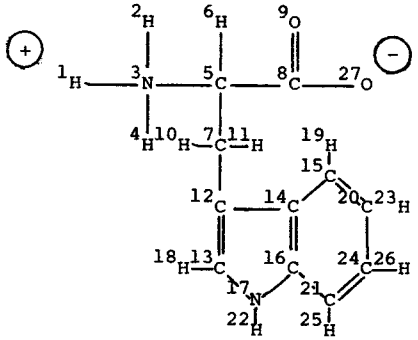
2H
6H
9O
+
1H
3N
5C
8C
27O
−
4H
10H
7C
11H
19H
15C
12C
14C
20C
23H
18H
13C
16C
24C
26H
17N
21C
22H
25H

FIGURE 10

Structure and Atom Number for $^{+}TG^{-}$

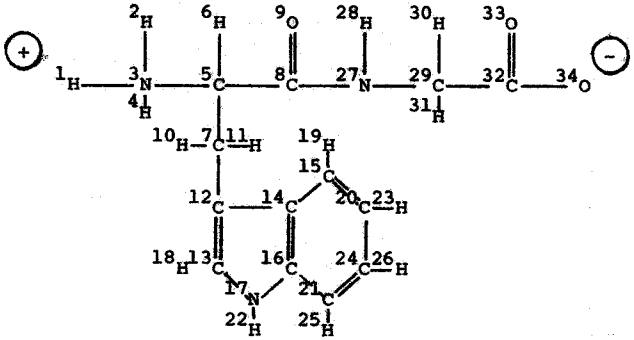

FIGURE 11

Structure and Atom Numbers for $^{+}TGG^{-}$

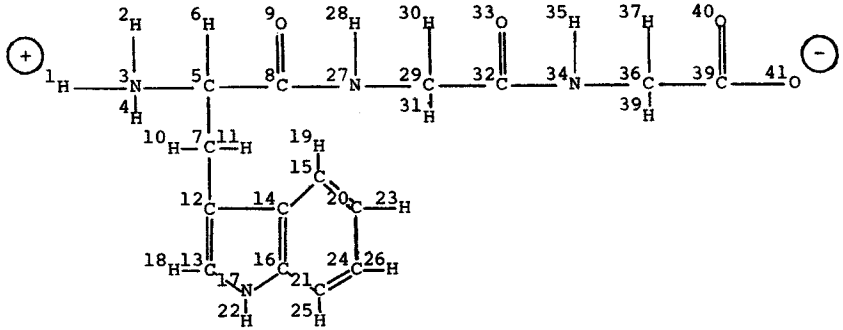

FIGURE 12

Structure and Atom Numbers for $^{+}GT^{-}$

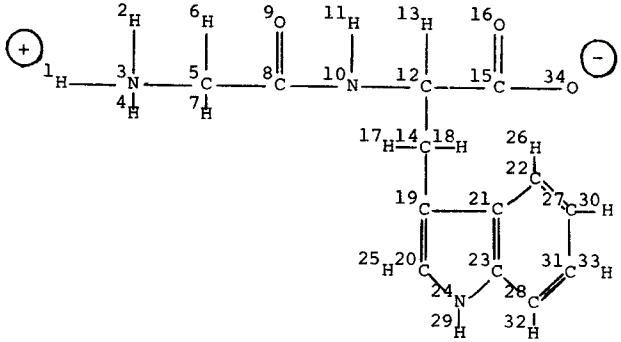

FIGURE 13

Structure and Atom Numbers for $^{+}PT^{-}$

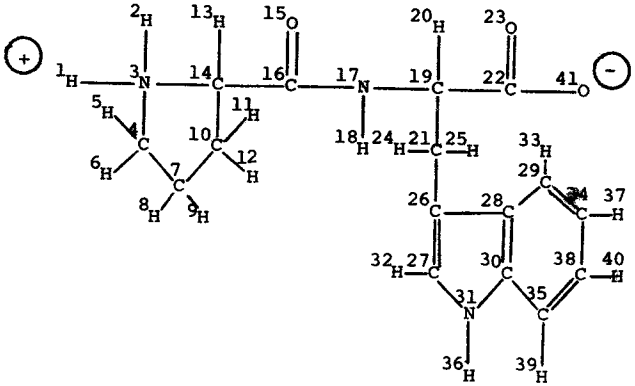

FIGURE 14

Structure and Atom Numbers for $^{2+}LT^{-}$

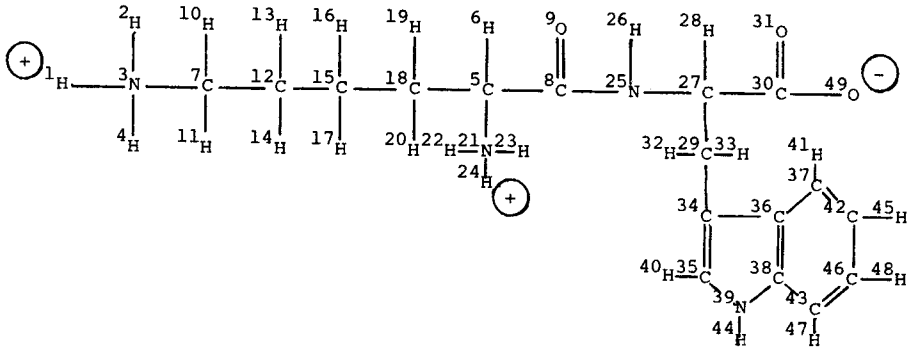

FIGURE 15

Conformational and Energy Data for $^{+}T^{-}$

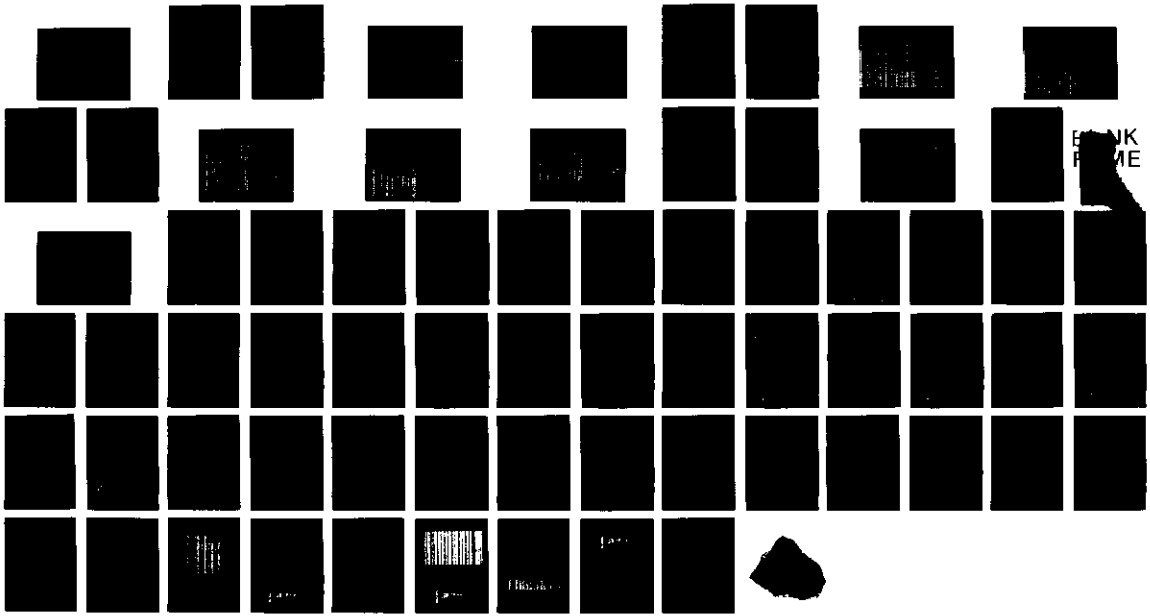

	ϕ_T	ψ_T	χ_T^1	χ_T^2	ENG	$\phi_T - \psi_T$	HYDROGEN-ATOM #'S	INDOLE CONTACT ATOM #'S
100	-73.507	-56.085	65.658	-92.000	-.73656E+01	A	4 - 9	14-27
200	-72.443	139.959	67.901	-92.000	-.71973E+01	F	4 - 9	14-9
300	-77.000	135.000	-179.000	90.000	-.71062E+01	F	4 - 9	
400	-75.000	-47.000	179.000	83.000	-.70505E+01	A		
500	-77.969	-34.051	63.976	83.000	-.66940E+01	A	4 - 27	
600	-69.046	145.000	64.000	81.000	-.66487E+01	F	4 - 9	
700	-75.000	-49.000	179.000	-103.000	-.64752E+01	A		
800	-153.322	143.927	180.000	93.000	-.64498E+01	E		
900	-175.506	-82.024	180.213	74.000	-.61737E+01	E		
1000	-77.000	-48.000	-60.000	105.000	-.60007E+01	A		
1100	-77.000	-48.000	-60.000	-76.000	-.59454E+01	A		
1200	-162.400	139.970	59.730	83.000	-.59115E+01	E		
1300	-162.400	139.970	59.730	83.000	-.59115E+01			
1400	-162.400	139.970	59.730	83.000	-.59115E+01			
1500	-153.022	145.947	-179.004	-105.000	-.58627E+01	E		
1600	-155.023	150.948	60.000	-88.000	-.58094E+01	E		
1700	-174.559	-83.137	180.118	-104.000	-.58085E+01	G		
1800	-144.000	149.000	-60.000	105.000	-.57759E+01	E		
1900	-171.461	59.245	-60.196	105.000	-.55757E+01	D	4 - 9	
2000	-172.332	61.100	-60.378	-87.000	-.53207E+01	D		
2100	56.000	63.000	-174.000	69.000	-.53121E+01	A*		14-9
2200	-172.741	-94.332	-60.134	-86.000	-.52982E+01	H		
2300	-178.685	36.331	58.759	86.000	-.52472E+01	D		
2400	-174.070	-68.922	59.600	-81.300	-.52191E+01	G		14-27
2500	-84.000	89.000	-179.000	73.000	-.51715E+01	C		14-9
2600	-146.024	-51.049	-65.983	105.000	-.50105E+01	G		
2700	57.000	56.000	-54.000	-75.000	-.49710E+01	A*		
2800	-145.103	42.042	59.974	-72.300	-.48908E+01	G*		14-9
2900	-85.000	89.000	-179.000	-105.000	-.48397E+01	C		
3000	-144.019	147.946	-60.937	-87.000	-.48301E+01	E		
3100	-86.000	81.000	-60.000	104.000	-.40920E+01	C		
3200	-86.000	82.000	-60.000	-78.000	-.40607E+01	C		

ATOM # KEY

a. 4-9 = Amino H to Carboxyl O
b. 4-27 = Amino H to Carboxyl O
c. 14-27 = Indole C to Carboxyl O
d. 14-9 = Indole C to Carboxyl O

carbonate group (both oxygens are identical due to resonance effects).

(2) There is no correlation between the occurrence of a hydrogen bond and the conformational type of the tryptophan zwitterion.

Figure 16 presents data on $^{+}TG^{-}$. The following trends are noted:

(1) There are two types of hydrogen bonds. One is an intraresidue hydrogen bond between the tryptophan amino proton and the tryptophan carbonyl oxygen. The other is an intraresidue hydrogen bond between the glycine amino proton and the glycine carboxyl oxygen.

(2) One low energy conformation of $^{+}TG^{-}$ has both types of hydrogen bonding taking place simultaneously. This occurs only when tryptophan is in the F conformation and glycine is in the E* conformation.

(3) The tryptophan intraresidue hydrogen bonding takes place only when tryptophan is in the F conformation. The occurrence of this bond is independent of the glycine residue conformational letter code.

(4) The majority of the glycine intraresidue hydrogen bonding occurs when glycine is in the E* conformation. This bonding is independent of the tryptophan conformation.

(5) There are six types of indole contacts present in the low energy conformations of $^{+}TC^{-}$. A description of each is seen in Figure 16. One type is a tryptophan intraresidue bond. The other five are interresidue indole contacts.

(6) The majority of indole contacts are of the tryptophan intraresidue type with tryptophan in either the F, E or C* conformation. The contacts occur independently of the glycine conformation.

(7) The interresidue indole contacts occur independently of the glycine conformation.

FIGURE 16

Conformational and Energy Data for $^{+}TG^{-}$

	ϕ_T	ψ_T	χ_T^1	χ_T^2	ϕ_G	ψ_G	ENG	$\phi_T-\psi_T$	$\phi_G-\psi_G$	HYDROGEN-ATOM #'S	INDOLE CONTACT ATOM #'S
100	-77.000	135.000	-179.000	90.000	75.000	-140.000	.48494E+00	F	F*		
200	-77.000	135.000	-179.000	90.000	73.000	180.000	.53455E+00	F	E*	28-33	
300	-77.000	135.000	-179.000	90.000	72.000	53.000	.69322E+00	F	A*		
400	-75.772	139.791	67.959	-92.000	73.000	180.000	.67594E+00	F	E*	28-33	14-9
500	-75.423	137.315	65.321	-92.000	74.886	-140.287	.68845E+00	F	E*		14-9
600	-153.000	144.000	180.000	89.000	180.000	180.000	.78090E+00	F	A*	28-33	
700	-75.493	137.380	65.588	-92.000	71.699	-52.736	.81637E+00	F	A*		14-9
800	-159.495	129.916	180.000	89.000	73.633	-140.954	.84417E+00	F	F		
900	-77.000	135.000	-179.000	90.000	83.000	-76.000	.90610E+00	F	C*		
1000	-159.361	150.746	180.000	89.000	71.654	52.041	.99102E+00	F	A*		
1100	-77.000	135.000	-179.000	90.000	173.000	-62.000	.10766E+01	F	C*		
1200	-77.000	135.000	-179.000	90.000	-173.000	-62.000	.10853E+01	F	D		
1300	-75.496	137.376	65.584	-92.000	82.898	-76.176	.11087E+01	F	C*		14-9
1400	-159.000	144.000	180.000	89.000	-173.000	-62.000	.11827E+01	F	D*		
1500	-75.745	126.011	-179.725	90.000	-72.608	-53.008	.12143E+01	F	D		14-34
1600	-76.000	140.000	68.000	-92.000	-173.000	62.000	.12232E+01	F	D		14-9
1700	-75.992	139.961	67.959	-92.000	173.000	-61.995	.12247E+01	F	D*		14-9
1800	-162.543	-64.594	174.630	74.000	179.588	177.648	.12492E+01	F	E*	28-33	
1900	-180.124	94.221	-179.874	-105.000	73.253	-141.910	.12516E+01	F	F*		
2000	-153.024	143.948	180.000	89.000	82.999	-76.004	.13189E+01	F	A*		
2100	-153.000	144.000	180.000	89.000	173.000	-62.000	.13723E+01	F	D*		
2200	-153.000	146.000	-179.000	-105.000	180.000	180.000	.14139E+01	F	F*	28-33	
2300	-79.989	144.950	63.976	81.000	74.999	-140.007	.14153E+01	F	F*		
2400	-162.460	124.212	180.000	89.000	-72.021	-52.846	.14485E+01	F	A		14-34
2500	-80.000	145.000	64.000	81.000	180.000	180.000	.14596E+01	F	E*	28-33;4-9	
2600	-79.988	144.950	63.976	81.000	71.993	52.993	.15209E+01	F	A*	28-33	
2700	-180.157	94.243	-179.874	-105.000	72.239	51.067	.15486E+01	H*	A*		
2800	-167.987	124.937	60.009	-88.000	74.250	-142.818	.15557E+01	F	F*		14-9
2900	-75.175	120.545	-179.957	90.000	-74.964	140.046	.16434E+01	F	E*		14-33;16-33
3000	-168.000	124.956	60.000	-88.000	71.238	50.080	.17251E+01	F	E*		14-9
3100	-74.939	127.803	60.468	-92.000	-72.025	-52.891	.17251E+01	A*	A		14-9
3200	-84.000	89.000	-179.000	73.000	75.000	-140.000	.17495E+01	F	C*		
3300	-166.218	134.984	59.965	85.000	74.527	-143.049	.17549E+01	F	F*		
3400	-79.989	144.949	63.976	81.000	82.999	-76.005	.17898E+01	F	E*	4-9	
3500	-173.316	89.614	-59.993	-87.000	73.588	-141.524	.18433E+01	F	E*		
3600	-153.027	150.950	60.000	-88.000	180.001	180.011	.18706E+01	E	A*	28-33	
3700	-166.222	135.007	59.964	83.000	71.517	49.83	.18865E+01	A*	A		
3800	-165.756	117.652	180.000	89.000	-74.969	140.306	.19164E+01	F	F		14-33
3900	-162.969	141.649	59.793	83.000	180.202	182.970	.19838E+01	F	E*	28-33	
4000	-80.000	145.000	64.000	81.000	173.000	-62.000	.20021E+01	D*	A*	4-9	
4100	-73.982	125.986	60.353	-92.000	-74.983	140.214	.20182E+01	F	F		
4200	-153.000	146.000	-179.000	-105.000	-173.000	62.000	.20232E+01	F	D		
4300	-153.024	145.948	-179.005	-105.000	82.999	-76.004	.20290E+01	C*	C*		
4400	-84.000	89.000	-179.000	73.000	72.000	53.000	.20357E+01	F	A*		
4500	-164.466	145.120	174.746	74.000	-173.468	59.577	.20449E+01	D	D		
4600	-153.000	146.000	-179.000	-105.000	173.000	-62.000	.20725E+01	D*	C*		14-9
4700	-164.334	131.473	60.000	-88.000	82.663	-77.000	.20786E+01	C*	F		
4800	-85.000	89.000	-179.000	105.000	75.000	-140.000	.21296E+01	F	F		
4900	-80.000	145.000	64.000	81.000	-173.000	62.000	.21397E+01	F	D	4-9	
5000	-80.000	145.000	64.000	81.000	-75.000	140.000	.21432E+01	F	F	4-9	
5100	-84.000	89.000	-179.000	73.000	180.000	180.000	.21511E+01	E*	A*	28-33	
5200	-80.000	145.000	64.000	81.000	-73.000	-53.000	.21580E+01	A	A*	4-9	
5300	-173.350	89.634	-59.993	-87.000	70.579	51.461	.21603E+01	A*	A*		
5400	-164.632	158.182	59.877	83.000	82.629	-78.075	.22019E+01	E	C*		
5500	-81.455	-61.603	179.743	83.000	179.192	173.965	.22216E+01	F*	F*	28-33	
5600	56.000	63.000	-174.000	69.000	180.000	180.000	.22842E+01	A	E*	28-33	14-9
5700	-144.000	149.000	-60.000	105.000	180.000	180.000	.22994E+01	C*	F*	28-33	
5800	-163.211	134.862	60.000	-88.000	173.050	-59.563	.23031E+01	F	D*		
5900	-160.033	-63.897	174.869	-104.000	179.740	178.541	.23086E+01	F	F*	28-33	

ATOM # KEY

a. 4-9 = T-Amino H to T-Carbonyl O
b. 28-33 = G-Amino H to G-Carboxyl O
c. 14-9 = T-Indole C to T-Carbonyl O
d. 14-34 = T-Indole C to G-Carboxyl O
e. 14-33 = T-Indole C to G-Carboxyl O
f. 16-33 = T-Indole C to G-Carboxyl O
g. 17-34 = T-Indole N to G-Carboxyl O
h. 17-33 = T-Indole N to G-Carboxyl O

	ϕ_T	ψ_T	χ_T^1	χ_T^2	ϕ_G	ψ_G	ENG	$\phi_T-\psi_T$	$\phi_G-\psi_G$	HYGBOND-ATOM #'s	INDOLE CONTACT ATOM #'s
6000	-159.5[illegible]	-52.2[illegible]	173.8[illegible]	74.0[illegible]	172.607	-63.1[illegible]	.23345E+01	G	D*		
6100	-155.027	150.951	60.000	-88.000	-172.999	62.011	.23590E+01	E	D		
6200	-153.000	146.000	-179.000	-105.000	-72.000	-53.000	.23749E+01	E	A		17-34
6300	-163.496	-65.149	174.804	74.000	-75.412	142.289	.24121E+01	G	F		
6400	-85.000	89.000	-179.000	-105.000	72.000	53.000	.24257E+01	C	C*		
6500	-85.000	89.000	-179.000	-105.000	180.000	180.000	.24426E+01	C	F*	28-33	
6600	-144.021	148.947	-60.000	105.000	74.999	-140.005	.24431E+01	E	F*		
6700	-163.331	124.971	60.000	-88.000	-72.008	-52.356	.24506E+01	E	C*		14-9
6800	-168.335	124.981	60.000	-88.000	-74.949	140.907	.24698E+01	E	F		14-9
6900	-162.978	141.600	59.798	83.000	173.126	-59.280	.24843E+01	E	D*		
7000	-80.000	145.000	64.000	81.000	-83.000	76.000	.25105E+01	F	C		
7100	-84.000	89.000	-179.000	73.000	83.000	-76.000	.25282E+01	C	C*		
7200	-144.021	148.947	-60.000	105.000	71.999	52.995	.25453E+01	E	A*		
7300	-162.477	124.222	180.000	69.000	-83.098	76.054	.25465E+01	E	C		
7400	-153.025	145.948	-179.005	-105.000	-75.000	140.002	.25495E+01	E	F		17-33
7500	-153.000	146.000	-179.000	-105.000	-83.000	76.000	.25642E+01	E	C		
7600	-152.249	67.051	-60.476	105.000	180.003	180.001	.25825E+01	D	F*	28-33	
7700	55.000	63.000	-174.000	69.000	75.000	-140.000	.25900E+01	C*	F*		14-9
7800	-84.000	89.000	-179.000	73.000	173.000	-62.000	.26057E+01	A	D*		
7900	-147.002	72.161	-60.687	105.000	74.889	-139.919	.26198E+01	G	F*		
8000	-75.991	154.944	-179.007	99.000	-83.000	76.000	.26512E+01	F	C		
8100	-159.653	147.829	59.114	83.000	-74.939	140.506	.26630E+01	E	F		
8200	-163.093	141.668	59.797	83.000	-172.777	64.947	.26872E+01	E	D		
8300	-155.029	153.952	58.011	83.000	-71.999	-52.996	.27173E+01	F	A		
8400	-163.469	-66.891	175.661	-104.000	-75.514	142.715	.27436E+01	G	F		
8500	-166.057	-65.618	174.941	74.000	-72.458	-50.360	.27436E+01	G	A		
8600	-144.021	148.947	-60.000	105.000	82.999	-76.004	.27593E+01	E	C*		
8700	-81.532	-61.754	179.748	83.000	-173.768	56.399	.28377E+01	A	D		
8800	55.000	63.000	-174.000	69.000	173.000	-62.000	.28549E+01	C*	D*		14-9
8900	-161.960	-65.643	175.357	-104.000	-173.422	59.820	.28816E+01	G	D		
9000	-165.047	131.535	60.000	-88.000	-83.084	76.681	.28991E+01	E	C		
9100	-85.000	89.000	-179.000	-105.000	173.000	-62.000	.29083E+01	C	D*		14-9
9200	-144.000	149.000	-60.000	105.000	173.000	-62.000	.29124E+01	E	D*		
9300	-85.000	89.000	-179.000	-105.000	83.000	-76.000	.29235E+01	C	C*		
9400	56.000	63.000	-174.000	69.000	72.000	53.000	.29297E+01	C*	A*		14-9
9500	-83.458	-65.219	179.746	-103.000	178.939	172.754	.29354E+01	A	E*	28-33	
9600	-74.087	127.786	60.481	-92.000	-83.091	76.007	.29410E+01	C	C		14-9
9700	-157.430	65.534	-60.685	-87.000	180.005	180.002	.29529E+01	G	E*		
9800	-147.004	72.163	-60.687	105.000	71.692	53.093	.29971E+01	G	A*		
9900	-154.513	67.877	-60.863	-87.000	74.766	-139.828	.30328E+01	G	F*		
10000	-144.000	149.000	-60.000	105.000	-173.000	62.000	.30332E+01	E	D		
10100	-156.029	153.952	58.011	83.000	-83.000	76.005	.30353E+01	E	C*		
10200	-86.000	82.000	-60.000	-78.000	75.000	-140.000	.30385E+01	C*	F*		
10300	-164.328	-67.609	175.839	-104.000	-72.586	-49.785	.30673E+01	G	A		
10400	-151.544	67.637	-60.497	105.000	172.975	-61.965	.30721E+01	D	D*		
10500	-86.000	81.000	-60.000	104.000	75.000	-140.000	.30864E+01	C	F*		
10600	-84.000	89.000	-179.000	73.000	-173.000	62.000	.31054E+01	C	D		
10700	-83.682	-65.657	179.760	-103.000	-75.809	146.205	.32076E+01	A	F		
10800	-86.000	81.000	-60.000	104.000	180.000	180.000	.32518E+01	C	E*	28-33	
10900	-146.034	-61.042	-65.990	105.000	179.997	179.984	.32585E+01	G	E*	28-33	
11000	-83.578	-65.411	179.751	-103.000	-174.026	55.273	.33048E+01	A	D		
11100	-86.000	82.000	-60.000	-78.000	180.000	180.000	.33291E+01	C	E*	28-33	
11200	-86.000	82.000	-60.000	-78.000	72.000	53.000	.33593E+01	C	A*		
11300	-144.020	147.947	-60.997	-87.000	180.000	180.006	.33797E+01	E	E*	28-33	
11400	-161.883	-65.564	175.338	-104.000	172.578	-64.506	.33920E+01	G	D*		
11500	-164.147	-65.693	174.964	74.000	-83.466	78.207	.34034E+01	G	C		
11600	-85.000	89.000	-179.000	-105.000	-173.000	62.000	.34054E+01	C	D		
11700	-154.618	67.882	-60.863	-87.000	71.773	53.196	.34079E+01	G	A*		
11800	-86.000	81.000	-60.000	104.000	72.000	53.000	.34113E+01	C	A*		
11900	-80.818	-60.534	179.725	83.000	172.278	-67.757	.34217E+01	A	D*		
12000	-82.882	-64.012	179.791	83.000	-75.680	145.966	.34499E+01	A	F		
12100	-157.428	65.532	-60.687	-87.000	172.963	-61.948	.34526E+01	G	D*		

The majority take place when tryptophan is in the E region.

Figure 17 presents data on $^{+}TGG^{-}$. The following observations are made:

(1) There exist three distinct types of hydrogen bonding in the low energy conformations of $^{+}TGG^{-}$. One is an intraresidue bond between the tryptophan amino proton and the tryptophan carbonyl oxygen. Another is an interresidue hydrogen bond between the second glycine (hereafter referred to as G_2) amino proton and the tryptophan carbonyl oxygen. The third is an intraresidue bond between the G_2 amino proton and the G_2 carboxyl oxygen. The first glycine residue in the peptide (referred to as G_1) undergoes no hydrogen bonding. The majority of the hydrogen bonds are of the tryptophan-G_2 interresidue variety.

(2) Ten low energy conformations have tryptophan intraresidue and tryptophan-G_2 interresidue hydrogen bonding simultaneously. Two low energy conformations have all three bond types occurring at once. These are generally not the lowest energy conformations.

(3) The tryptophan intraresidue hydrogen bond can occur only when tryptophan is in the F conformation. This hydrogen bonding is independent of the conformations of both G_1 and G_2.

(4) The majority of the tryptophan-G_2 interresidue hydrogen bonds occur when G_1 is in the C* conformation. This phenomenon is independent of the conformation of both tryptophan and G_2.

(5) The majority of E* conformations for G_2 results in either tryptophan-G_2 interresidue hydrogen bonding or G_2 intraresidue bonding. There is some selective dependence upon the conformation of G_1 (see note 6 below).

(6) The majority of the simultaneous hydrogen bonding described above occurs when G_1 is in the A* conformation with G_2 in the E* conformation or when G_1 is in the C* conformation with G_2 in the E* conformation.

FIGURE 17

Conformational and Energy Data for $^{+}TGG^{-}$

	ϕ_T	ψ_T	χ_T^1	χ_T^2	ϕ_{G_1}	ψ_{G_1}	ϕ_{G_2}	ψ_{G_2}	ENG	$\phi_T\psi_T$	$\phi_{G_1}\psi_{G_1}$	$\phi_{G_2}\psi_{G_2}$	HYGBOND ATOM #'s	INDOLE CONTACT ATOM-#'S
100	-75.567	127.704	-179.639	90.000	82.762	-76.520	-75.240	139.901	.22985E+01	L	C*	F	35-9	
200	-164.913	117.275	180.000	89.000	82.322	-77.770	-75.685	139.715	.23237E+01	E	C*	F	35-9	
300	-74.262	131.137	62.140	-92.000	82.679	-76.746	-75.222	139.907	.25067E+01	F	C*	F	35-9	
400	-179.036	93.661	-179.880	-105.000	81.386	-78.922	-76.589	139.376	.25524E+01	D	C*	F	35-9	14-9
500	-76.990	134.944	-179.007	90.000	71.997	52.998	75.001	-140.000	.27083E+01	F	A*	F*		
600	-76.988	134.945	-179.007	90.000	82.998	-76.005	-72.002	-53.001	.27564E+01	F	C*	A	35-9	
700	-164.913	117.273	180.000	89.000	82.347	-77.769	-72.677	-53.222	.28009E+01	E	C*	A	35-9	
800	-159.085	130.694	180.000	89.000	71.652	52.040	75.001	-140.000	.28473E+01	E	A*	F*		
900	-74.263	131.137	62.139	-92.000	82.687	-76.746	-72.220	-53.072	.29085E+01	F	C*	A	35-9	14-9
1000	-171.088	118.313	60.000	-88.000	81.939	-78.479	-75.493	139.806	.29126E+01	E	C*	F	35-9	14-9
1100	-84.003	89.000	-179.000	73.000	83.000	-76.000	-75.000	140.000	.29176E+01	C	C*	F	35-9	
1200	-77.000	135.000	-179.000	90.000	83.000	-76.000	-173.000	62.000	.30174E+01	F	C*	D	35-9	
1300	-179.037	93.657	-179.880	-105.000	81.445	-78.916	-73.568	-53.478	.30193E+01	D	C*	A	35-9	
1400	-75.486	137.334	65.556	-92.000	71.896	52.733	75.001	-140.000	.30306E+01	F	C*	F*		14-9
1500	-167.004	95.182	-60.000	105.000	81.886	-78.445	-76.126	139.549	.30974E+01	D	C*	F	35-9	
1600	-76.990	134.944	-179.007	90.000	71.997	52.998	72.001	53.000	.31586E+01	F	C*	C*		
1700	-153.702	142.379	180.000	89.000	-172.993	62.185	172.991	-61.964	.31712E+01	E	D	D*		16-41;17-41
1800	-75.496	137.376	65.584	-92.000	82.898	-76.176	-173.000	62.000	.32286E+01	F	C*	D	35-9	14-9
1900	-85.000	89.000	-179.000	-105.000	83.000	-76.000	-75.000	140.000	.33163E+01	C	C*	F	35-9	
2000	-76.692	131.349	60.288	81.000	82.621	-77.484	-75.412	139.822	.33445E+01	F	C*	F	35-9	
2100	-170.558	124.894	59.996	83.000	82.110	-79.226	-75.482	139.801	.33498E+01	E	C*	F	35-9	
2200	-159.085	130.694	180.000	89.000	71.652	52.040	72.001	53.000	.33554E+01	E	A*	A*		
2300	-153.347	143.396	180.000	89.000	82.998	-76.007	-172.999	61.999	.33637E+01	E	C*	D	35-9	
2400	-171.088	118.312	60.000	-88.000	81.957	-78.477	-72.486	-53.148	.33787E+01	E	C*	A	35-9	14-9
2500	-76.989	134.944	-179.007	90.000	71.998	52.995	172.999	-61.999	.34210E+01	F	A*	D*		
2600	-84.000	89.000	-179.000	73.000	83.000	-76.000	-72.000	-53.000	.34211E+01	C	C*	A	35-9	
2700	-75.486	137.334	65.555	-92.000	71.896	52.733	72.001	53.000	.34756E+01	F	A*	A		14-9
2800	-167.003	95.180	-60.000	105.000	81.927	-78.442	-73.112	-53.348	.35794E+01	D	C*	A	35-9	
2900	-76.652	133.273	-179.196	90.000	-172.993	62.111	179.964	180.004	.36090E+01	F	D*	E*	35-9	16-40
3000	-77.000	135.000	-179.000	90.000	72.000	53.000	180.000	180.000	.36111E+01	F	A*	E*	35-9	
3100	-77.000	135.000	-179.000	90.000	83.000	-76.000	180.000	180.000	.36247E+01	F	C*	E*	35-9; 35-40	
3200	-180.157	94.243	-179.874	-105.000	70.239	51.067	173.000	-62.000	.36307E+01	D	A*	D*		
3300	-76.988	134.945	-179.007	90.000	82.998	-76.004	-83.002	75.999	.36414E+01	F	C*	C	35-9	
3400	-74.933	134.384	63.695	-92.000	71.797	52.439	172.929	-61.962	.36539E+01	F	A*	D*		14-9
3500	-77.000	135.000	-179.000	90.000	-173.000	62.000	173.000	-62.000	.36695E+01	F	D	D*		
3600	-168.003	124.956	60.000	-88.000	71.238	50.080	75.000	-140.000	.36942E+01	E	A*	F*		14-9
3700	-77.537	134.844	60.945	81.000	82.737	-77.150	-72.302	-53.104	.37199E+01	F	C*	A	35-9	
3800	-159.085	130.694	180.000	89.000	71.653	52.038	172.999	-62.000	.37331E+01	E	A*	D*		
3900	-169.078	128.232	59.977	83.000	82.261	-78.968	-72.354	-53.115	.37628E+01	E	C*	A	35-8	
4000	-78.490	138.273	61.628	81.000	71.689	52.380	75.128	-139.946	.37720E+01	F	A*	F*		
4100	-74.877	134.387	63.687	-92.000	82.804	-76.456	-83.094	75.925	.38138E+01	F	C*	C	35-9	14-9
4200	-85.000	89.000	-179.000	-105.000	83.000	-76.000	-72.000	-53.000	.38198E+01	C	C*	A	35-9	
4300	-75.496	137.376	65.584	-92.000	82.898	-76.176	180.000	180.000	.38330E+01	F	C*	E*	35-9; 35-40	14-9
4400	-161.865	123.927	180.000	89.000	82.558	-77.375	-83.448	75.643	.38446E+01	E	C*	C	35-9	
4500	-75.486	137.334	65.555	-92.000	71.898	52.731	179.999	180.000	.38540E+01	F	A*	E*	35-9	14-9
4600	-154.069	141.542	180.000	89.000	-173.004	62.257	-173.027	62.018	.38697E+01	E	D	D		
4700	-79.989	144.949	63.976	81.000	82.999	-76.005	-173.000	62.000	.38744E+01	F	C*	C	35-9; 4-9	
4800	-166.246	134.955	59.964	83.000	71.514	49.829	75.001	-140.000	.39397E+01	E	A*	F*		
4900	-153.024	143.948	180.000	89.000	82.999	-76.004	180.000	180.000	.39590E+01				35-9; 35-40	
5000	-159.085	130.694	180.000	89.000	71.653	52.038	179.999	180.000	.39794E+01	E	A*	E*	35-40	
5100	-180.157	94.243	-179.874	-105.000	70.239	51.067	180.000	180.000	.40159E+01	D	A*	E*	35-40	
5200	-172.361	90.066	-60.000	105.000	70.760	50.562	172.103	-61.573	.40732E+01	D	A*	D*		
5300	-180.157	94.243	-179.874	-105.000	70.239	51.067	75.000	-140.000	.40847E+01	D	A*	F		
5400	-153.047	145.896	-179.010	-105.000	82.998	-76.008	-172.999	61.999	.40866E+01	E	C*	D	35-9	
5500	-179.049	93.657	-179.879	-105.000	81.536	-78.780	-84.409	74.974	.41147E+01	D	C*	C	35-9	
5600	-171.374	118.265	60.000	-88.000	70.970	49.808	172.820	-61.915	.41523E+01	E	A*	D*		14-9
5700	-77.000	135.000	-179.000	90.000	-173.000	62.000	-173.000	62.000	.41934E+01	F	D	D		
5800	-161.007	108.516	-60.000	105.000	70.699	51.862	75.461	-139.821	.41984E+01	D	A*	F		
5900	-168.000	124.956	60.000	-88.000	71.238	50.080	72.000	53.000	.42065E+01	E	A*	A*		14-9
6000	-78.490	138.272	61.628	81.000	71.695	52.388	72.133	53.043	.42110E+01	F	A*	A*		
6100	-80.000	145.000	64.000	81.000	-83.000	76.000	180.000	180.000	.42472E+01	F	C	E*	35-9; 35-40; 4-9	17-40
6200	-164.147	-65.693	174.964	74.000	-83.466	78.207	75.000	-140.000	.42526E+01	G	C	F	35-9	

ATOM # KEY

a. 4-9 = T-Amino H to T-Carbonyl O

b. 35-9 = G_2-Amino H to T-Carbonyl O

c. 35-40 = G_2-Amino H to G_2-Carboxyl O

d. 14-9 = T-Indole C to T-Carbonyl O

e. 16-40 = T-Indole C to G_2-Carboxyl O

f. 16-41 = T-Indole C to G_2-Carboxyl O

g. 17-40 = T-Indole N to G_2-Carboxyl O

h. 17-41 = T-Indole N to G_2-Carboxyl O

	ϕ_T	ψ_T	χ_T^1	χ_T^2	ϕ_{G_2}	ϕ_{G_1}	ϕ_{G_2}	ψ_{G_2}	ENG	$\phi_T\psi_T$	$\phi_{G_1}\psi_{G_1}$	$\phi_{G_2}\psi_{G_2}$	HYGBOND ATOM #'s	INDOLE CONTACT ATOM #'s
6300	-84.000	89.000	-179.000	73.000	72.000	53.000	75.000	-140.000	.42731E+01	C	A*	F		
6400	-173.350	89.634	-59.993	-87.000	70.579	51.461	173.000	-62.000	.42820E+01	D	A*	D*		
6500	-77.000	135.000	-179.000	90.000	72.000	53.000	83.000	-76.000	.42940E+01	F	A*	C*		
6600	-84.000	89.000	-179.000	73.000	72.000	53.000	173.000	-62.000	.43430E+01	C	A*	D*		
6700	-164.834	131.473	60.000	-88.000	82.463	-77.700	-173.000	62.000	.43452E+01	E	C*	D	35-9	14-9
6800	-78.284	137.892	61.529	81.000	71.815	52.068	172.857	-61.913	.43751E+01	F	A*	D*		
6900	-153.000	146.000	-179.000	-105.000	-173.000	62.000	-173.000	62.000	.43862E+01	E	D*	D		
7000	-79.989	144.949	63.976	81.000	82.999	-76.005	180.000	180.000	.44063E+01	F	C*	E	35-9;35-40;4-9	
7100	-166.246	134.955	59.964	83.000	71.514	49.829	72.001	53.000	.44232E+01	E	A*	A*		
7200	-155.983	139.295	-179.492	-105.000	-172.975	62.717	179.889	180.020	.44323E+01	E	D*	E*	35-40	16-40;17-40
7300	-164.642	138.182	59.877	83.000	82.629	-78.075	-173.000	62.000	.44333E+01	G	C*	D	35-40	
7400	-77.000	135.000	-179.000	90.000	83.000	-76.000	173.000	-62.000	.44394E+01	F	C*	D*	35-40	
7500	-169.564	127.560	59.989	83.000	71.227	49.228	172.811	-61.892	.44648E+01	G	A*	E*		
7600	-169.495	121.603	60.000	-88.000	82.109	-78.269	-83.323	75.764	.44666E+01	F	C*	C	35-9	
7700	-80.000	145.000	64.000	81.000	-83.000	76.000	-173.000	62.000	.45019E+01	F	C	D	35-9;4-9	17-40
7800	-168.025	124.905	60.000	-88.000	71.236	50.078	179.999	180.000	.45615E+01	E	A*	E*	35-40	14-9
7900	-79.977	144.900	63.953	81.000	71.998	52.985	179.999	180.000	.45803E+01	F	A*	E*	35-40;4-9	
8000	-78.327	138.336	61.602	81.000	82.848	-76.801	-83.178	75.848	.45993E+01	F	C*	C	35-9	
8100	-180.157	94.243	-179.874	-105.000	70.239	51.067	72.000	53.000	.46014E+01	D	A*	A*		
8200	-75.486	137.334	65.555	-92.000	71.897	52.733	83.001	-75.999	.46026E+01	F	A*	C*		
8300	-77.000	135.000	-179.000	90.000	72.000	53.000	-173.000	62.000	.46237E+01	F	A*	D		14-9
8400	-75.496	137.376	65.584	-92.000	82.898	-76.176	173.000	-62.000	.46295E+01	F	C*	D*	35-9	14-9
8500	-84.000	89.000	-179.000	73.000	83.000	-76.000	-83.000	76.000	.46376E+01	C	C*	C	35-9	
8600	-159.061	130.746	180.000	89.000	71.654	52.041	83.000	-76.000	.46483E+01	E	A*	C*		
8700	-173.396	89.597	-59.993	-87.000	70.578	51.461	179.999	180.000	.46645E+01	D	A*	E*	35-40	
8800	-156.056	153.903	58.022	83.000	-83.000	76.010	179.998	180.000	.46648E+01	E	C*	E*	35-9;35-40	
8900	-153.024	145.948	-179.005	-105.000	82.999	-76.004	180.000	180.000	.46818E+01	E	C*	E*	35-9;35-40	
9000	-172.164	89.969	-60.000	105.000	81.810	-78.422	-84.186	75.160	.46986E+01	D	C*	C	35-9	
9100	-84.000	89.000	-179.000	73.000	72.000	53.000	180.000	180.000	.47046E+01	C	A*	E*	35-9	
9200	-85.000	89.000	-179.000	-105.000	72.000	53.000	173.000	-62.000	.47102E+01	C	A*	D*		
9300	-153.000	144.000	180.000	89.000	-173.000	62.000	75.000	-140.000	.47167E+01	E	D	F*		
9400	-85.000	89.000	-179.000	-105.000	72.000	53.000	75.000	-140.000	.47193E+01	E	A*	F*		
9500	-164.147	-65.693	174.964	74.000	-83.466	78.207	72.000	53.000	.47287E+01	G	C	A*	35-40	
9600	-77.000	135.000	-179.000	90.000	173.000	-62.000	180.000	180.000	.47400E+01	F	D*	E*	35-40	
9700	-153.000	146.000	-179.000	-105.000	-83.000	76.000	173.000	-62.000	.47464E+01	E	C	D*	35-9	
9800	-161.011	108.516	-60.000	105.000	70.726	51.899	72.486	53.139	.47473E+01	D	A*	A*		
9900	-173.350	89.634	-59.993	-87.000	70.579	51.461	75.000	-140.000	.47569E+01	D	A*	F*		
0000	-166.245	134.955	59.964	83.000	71.515	49.826	179.999	180.000	.47851E+01	E	A*	E*	35-40	
0100	-167.979	130.737	59.963	83.000	82.375	-78.754	-83.237	75.808	.47935E+01	E	C*	C	35-9	
0200	-153.047	143.896	180.000	89.000	82.998	-76.007	173.001	-62.000	.47957E+01	E	C*	D*	35-9	
0300	-84.000	89.000	-179.000	73.000	72.000	53.000	72.000	53.000	.48375E+01	C	A*	A*		
0400	-75.486	137.334	65.555	-92.000	71.898	52.731	-173.001	62.000	.48639E+01	F	A*	D		14-9
0500	-80.000	145.000	64.000	81.000	-72.000	-53.000	180.000	180.000	.48659E+01	F	A	E*	35-9;4-9	
0600	-153.000	146.000	-179.000	-105.000	-83.000	76.000	180.000	180.000	.48914E+01	E	C	E*	35-9;35-40	
0700	-144.041	148.893	-60.000	105.000	82.998	-76.008	-173.000	61.999	.49114E+01	E	C*	D	35-9	
0800	-153.000	146.000	-179.000	-105.000	-173.000	62.000	75.000	-140.000	.49287E+01	E	D	F*		
0900	-80.000	145.000	64.000	81.000	-72.000	-53.000	-173.000	62.000	.49555E+01	F	A	D	4-9	
1000	-77.000	135.000	-179.000	90.000	-173.000	62.000	75.000	-140.000	.49703E+01	F	D	F		
1100	-153.000	144.000	180.000	89.000	-173.000	62.000	72.000	53.000	.49724E+01	E	D	A*		
1200	-165.834	-67.047	175.319	74.000	-72.624	-49.525	-172.991	61.986	.50121E+01	G	A	D		
1300	-159.085	130.694	180.000	89.000	71.653	52.039	-173.001	62.000	.50160E+01	E	A*	D		
1400	-164.834	131.473	60.000	-88.000	82.463	-77.700	180.000	180.000	.50276E+01	E	A*	E*	35-9;35-40	14-9
1500	-153.000	144.000	180.000	89.000	173.000	-62.000	180.000	180.000	.50468E+01	E	D*	E*	35-40	
1600	-85.000	89.000	-179.000	-105.000	83.000	-76.000	-83.000	76.000	.50475E+01	C	C*	C	35-9	
1700	-164.642	138.182	59.877	83.000	82.629	-78.075	180.000	180.000	.50662E+01	E	C*	E*	35-9;35-40	
1800	-85.000	89.000	-179.000	-105.000	72.000	53.000	180.000	180.000	.50667E+01	E	A*	E*	35-40	
1900	-156.056	153.903	58.022	83.000	-83.000	76.011	-173.001	62.001	.50973E+01	F	C	D	35-9	
2000	-75.983	139.922	67.919	-92.000	172.999	-61.989	180.001	180.000	.51052E+01	F	D*	E*	35-40	14-9
2100	-76.000	140.000	68.000	-92.000	-173.000	62.000	180.000	180.000	.51512E+01	F	D	E*	35-40	14-9
2200	-166.664	-67.704	175.487	74.000	-72.707	-49.127	180.020	180.000	.51550E+01	E	A	E*	35-40	
2300	-153.000	146.000	-179.000	-105.000	-173.000	62.000	72.000	53.000	.52145E+01	E	D	A*		
2400	-77.000	135.000	-179.000	90.000	173.000	-62.000	-173.000	62.000	.52182E+01	F	D*	D		
2500	-77.000	135.000	-179.000	90.000	-173.000	62.000	72.000	53.000	.52223E+01	F	D	A*		
2600	-79.989	144.949	63.976	81.000	82.999	-76.005	173.000	-62.000	.52224E+01	E	C*	D*		
2700	-166.227	-69.060	176.137	-104.000	-72.774	-48.885	-172.991	61.986	.52526E+01	G	A	D	35-9;4-9	
2800	-173.350	89.634	-59.993	-87.000	70.579	51.461	72.000	53.000	.52769E+01	D	A*	A*		
2900	-85.000	89.000	-179.000	-105.000	72.000	53.000	72.000	53.000	.52849E+01	C	A*	A*		
3000	-153.000	144.000	180.000	89.000	-173.000	62.000	83.000	-76.000	.53137E+01					

(7) The majority of the indole contacts are an intraresidue type between the tryptophan indole carbon (atom #14) and the tryptophan carbonyl oxygen. This contact occurs most often when tryptophan is in either the F or E conformation and G_1 is in either the C* or A* conformation. This contact is independent of the conformation of G_2.

(8) Four other types of indole contacts occur. These take place between one tryptophan indole carbon (atom #16) or the indole nitrogen (atom #17) and either partially negatively charged oxygen in the G_2 carboxylate group. There is no correlation between the conformational letter codes for tryptophan, G_1 or G_2 and the occurrence of these indole contacts.

Figure 18 presents conformational data on $^{+}GT^{-}$. The following results are obtained:

(1) There is only one type of hydrogen bond in the low energy conformations present. This is an intraresidue hydrogen bond between the tryptophan amino proton and the tryptophan carboxyl oxygen. With only two exceptions, this bonding occurs when tryptophan is in the E conformation. It takes place independently of the conformation of glycine.

(2) There are five types of indole contacts (described in the figure). It is seen that there are interresidue contacts between either of the two tryptophan indole carbons (atom #'s 21 and 23) or the indole nitrogen and the glycine carbonyl oxygen. There are two types of intraresidue contacts.

(3) The majority of the interresidue indole contacts occur when tryptophan is in the G conformation. This phenomenon takes place independently of the glycine conformation.

(4) There is no correlation between the conformations of either tryptophan or glycine and the occurrence of the other types of indole contacts.

Figure 19 presents data on the low energy conformations of $^{+}PT^{-}$. The following observations are made:

FIGURE 18

Conformational and Energy Data for $^{+}GT^{-}$

	ϕ_G	ψ_G	ϕ_T	ψ_T	χ_T^1	χ_T^2	ENG	$\phi_G\psi_G$	$\phi_T\psi_T$	HYDROGEN-ATOM #'S	INDOLE CONTACT ATOM #'S
100	171.793	-66.575-155.025	169.742	59.230	-93.332		-.2834dE+01	D*	E	11-16	21-16
200	172.512	-64.101-155.950	153.022	58.221	80.354		-.2924E+01	D*	E	11-16	21-9
300	171.464	-67.569-144.131	145.769	-62.465	-63.010		-.3052E+01	D*	E	11-16	23-9;24-9
400	-72.270	-64.129-154.811	144.226	59.351	-96.589		-.3010E+01	A	E	11-16	21-16
500	-72.469	-63.006-143.933	143.183	-62.623	-80.655		-.3202E+01	A	E	11-16	23-9;24-9
600	171.311	-67.859-144.243	148.529	-61.958	108.399		-.3219dE+01	D*	E	11-16	21-9;23-9;24-9
700	32.980	-76.028-155.001	150.994	59.990	-88.044		-.3221dE+01	C*	E	11-16	
800	83.000	-76.000-156.000	154.000	58.000	83.000		-.3238E+01	C*	E	11-16	21-9
900	83.000	-76.000-156.000	154.000	58.000	83.000		-.3238E+01	A	E	11-16	21-9
1000	-72.696	-65.567-144.309	147.958	-62.401	109.737		-.3317E+01	A	E	11-16	21-9;23-9;24-9
1100	-71.377	-62.998-155.502	149.735	59.459	74.316		-.3162E+01	A	E	11-16	21-9
1200	83.000	-76.000-144.000	148.000	-61.000	-87.000		-.3375dE+01	D*	E	11-16	23-9;24-9
1300	180.000	180.000-144.000	149.000	-61.000	-87.000		-.3395E+01	D*	E	11-16	21-9;24-9
1400	180.001	179.973-154.999	151.031	58.979	-88.034		-.3400E+01	C*	E	11-16	
1500	170.853	-68.695-153.248	143.223	173.441	89.701		-.3408E+01	D*	E	11-16	23-9;24-9
1600	181.608	171.372-145.388	-51.533	-61.490	-89.018		-.3441E+01	C*	E	11-16	21-9
1700	180.301	179.971-155.999	154.053	57.998	82.961		-.3467E+01	C*	E	11-16	
1800	-73.164	-66.334-153.275	142.796	178.385	90.055		-.3475E+01	A	E	11-16	
1900	-173.000	62.000-155.000	151.000	60.000	-88.000		-.3514E+01	A	E	11-16	
2000	-75.000	140.000-144.000	148.000	-61.000	-87.000		-.3522E+01	A	E	11-16	23-9;24-9
2100	83.000	-76.000-144.000	149.000	-61.000	-87.000		-.3552E+01	D*	E	11-16	21-9;23-9;24-9
2200	73.407	-140.079-154.874	152.223	58.423	-91.734		-.3604E+01	C*	E	11-16	
2300	170.912	-68.546-153.229	145.217	-161.092	-104.223		-.3676dE+01	D*	E	11-16	21-34
2400	171.497	-67.407-146.181	-62.148	-65.558	-81.771		-.3696E+01	D*	A	11-16	23-9;24-9
2500	-73.095	-66.065-153.236	144.767	-141.431	-103.890		-.3746E+01	A	E	11-16	21-34
2600	74.980	-140.041-155.998	154.015	57.982	82.952		-.3764E+01	A	E	11-16	21-9
2700	83.000	-76.000-153.000	148.000	180.000	89.000		-.3765E+01	A	E	11-16	
2800	180.000	180.000-144.000	149.000	-60.000	105.000		-.3785E+01	C*	E	11-16	21-9;23-9;24-9
2900	-173.000	62.000-156.000	154.000	58.000	83.000		-.3800E+01	D*	E	11-16	21-9
3000	-75.000	140.000-144.000	149.000	-61.000	-87.000		-.3806E+01	F*	E	11-16	23-9;24-9
3100	-83.000	76.000-153.000	151.000	60.000	-88.000		-.3807E+01	C*	E	11-16	
3200	168.789	-72.875-158.045	140.879	-182.612	92.027		-.3829E+01	D*	I		23-9;24-9
3300	-72.197	-65.087-146.085	-63.665	-62.618	-79.649		-.3841E+01	A	E		21-34
3400	-77.042	-74.663 -78.947	144.933	163.345	92.867		-.3865E+01	A	E		
3500	-75.343	-71.343 -78.609	142.856	-132.726	92.127		-.3953E+01	A	E		21-9;23-9;24-9
3600	171.306	-67.759-146.256	-61.540	-64.720	108.819		-.3887E+01	D*	E	11-16	21-9
3700	-75.000	140.000-156.000	154.000	58.000	83.000		-.3889E+01	F*	E	11-16	
3800	180.000	180.000-153.000	144.005	179.997	89.002		-.3892SE+01	E*	E		21-34
3900	160.824	173.294-162.657	-46.090	58.037	-90.644		-.3908E+01	E*	E		
4000	-79.277	-78.962 -77.411	-36.220	175.958	86.492		-.3911E+01	A	E		21-34
4100	169.612	-71.378 -76.869	-31.307	59.659	-96.321		-.3930ZE+01	D*	A		
4200	-75.000	140.000-155.000	151.000	60.000	-88.000		-.3953dE+01	F*	E	11-16	
4300	82.974	-76.036-146.002	-61.005	-67.001	-85.964		-.3957GE+01	C*	E		23-9
4400	79.977	-79.782 -76.568	-33.582	64.171	-96.970		-.3964E+01	C*	A		21-34
4500	-74.978	139.988-146.001	-61.001	-66.958	-86.006		-.3964E+01	F*	E		21-16
4600	181.642	171.575-145.608	-50.957	-61.566	101.209		-.3981E+01	C*	A		21-9;23-9;24-9
4700	-72.325	-66.071-146.312	-62.226	-62.416	110.089		-.3991E+01	A	E		21-9;23-9;24-9
4800	169.619	-71.357 -76.858	144.683	59.650	-96.369		-.3992E+01	A	A		21-16
4900	171.887	-66.264-163.018	-53.557	54.998	-85.681		-.4036E+01	D*	E		21-34
5000	83.000	-76.000-153.000	145.000	-179.000	-105.000		-.4039E+01	D*	E	11-16	21-16
5100	79.982	-79.777 -76.355	142.411	64.169	-94.983		-.4047E+01	C*	E		21-16
5200	74.968	-140.001-143.997	149.031	-60.033	105.014		-.4047E+01	C*	E	11-16	21-9;23-9;24-9
5300	71.201	-88.604 -76.356	-37.211	174.826	86.149		-.4077E+01	C*	A		
5400	82.972	-76.037 -77.003	135.023	-179.021	90.009		-.4087SE+01	C*	A		
5500	165.412	-78.948 -78.439	-39.377	-64.407	103.653		-.4159SE+01	D*	A		
5600	74.967	-140.001-152.997	144.027	179.966	89.016		-.4163BE+01	D*	A	11-16	23-9
5700	74.965	-140.002-145.997	-63.968	-67.021	-75.977		-.4166AE+01	F*	A		
5800	169.454	-72.480 -78.821	-29.478	57.688	-77.579		-.4170DE+01	D*	A		
5900	-78.459	-78.394 -78.891	-36.271	-64.359	102.077		-.4171TE+01	A	A		
6000	82.973	-76.037-146.002	-61.002	-66.002	105.034		-.4178TE+01	C*	G		21-9;24-9
6100	169.447	-72.364 -30.799	149.455	57.685	75.332		-.4201TE+01	D*	G		
6200	180.007	179.973-152.999	146.015	-179.013	-104.985		-.4233SE+01	E*	F	11-16	

ATOM # KEY

a. 11-16 = T-Amino H to T-Carboxyl O
b. 21-10 = Indole C to T-Amino N
c. 21-16 = Indole C to T-Carboxyl O
d. 21-9 = Indole C to G-Carbonyl O
e. 21-34 = Indole C to T-Carbonyl O
f. 23-9 = Indole C to G-Carbonyl O
g. 24-9 = Indole C to G-Carbonyl O

	ϕ_G	ψ_G	ϕ_T	ψ_T	χ_T^1	χ_T^2	ENG	$\phi_G\psi_G$	$\phi_T\psi_T$	HYGBOND ATOM #'s	INDOLE CONTACT ATOM #'s
6300	171.375	-67.743	-142.194	[illegible]	-63.297	-83.176	.42534E+01	D*	D		23-9;24-9
6400	-72.876	-63.931	-76.905	-37.218	59.568	-93.431	.42801E+01	A	A		21-34
6500	79.735	-33.027	-78.341	-31.634	61.129	79.473	.42999E+01	C*	A		
6600	74.961	-140.000	-76.997	135.042	-179.001	89.998	.43004E+01	F*	F		
6700	-173.000	62.000	-144.000	149.000	-60.000	105.000	.43146E+01	D	E	11-16	21-9;23-9;24-9
6800	-72.128	-63.107	-162.807	-55.157	58.495	-88.281	.43147E+01	A	G		21-34
6900	-75.000	140.000	-144.000	149.000	-60.000	105.000	.43156E+01	F	E	11-16	21-9;23-9;24-9
7000	80.638	-78.985	-80.250	145.723	61.792	78.315	.43179E+01	C*	F		
7100	164.936	-79.193	-76.736	-58.776	175.938	-99.626	.43232E+01	D*	A		
7200	161.409	171.386	-157.679	-50.787	178.270	78.315	.43255E+01	E*	G		
7300	-73.071	-65.550	-80.837	148.702	58.771	77.972	.43356E+01	A	F		
7400	170.263	-69.955	-158.314	-61.396	175.942	73.859	.43357E+01	D*	G		
7500	-72.876	-63.960	-76.892	143.781	59.570	-93.501	.43367E+01	A	E		21-16
7600	165.272	-79.343	-78.249	-38.796	-64.503	-76.510	.43376E+01	D*	A		
7700	80.372	-79.495	-163.169	-53.217	53.036	-86.588	.43357E+01	C*	G		21-34
7800	-79.315	-79.001	-77.414	-36.293	175.997	-99.330	.43392E+01	A	A		
7900	170.990	-68.318	-158.233	-61.085	175.717	73.859	.43402E+01	D*	G		
8000	-73.083	-65.631	-78.862	-37.265	58.850	80.236	.43526E+01	A	A		
8100	-78.571	-78.963	-78.567	-35.966	-64.474	-77.662	.43526E+01	A	A		
8200	170.915	-68.506	-157.234	-62.087	176.170	-104.011	.43572E+01	D*	G		
8300	69.947	-69.750	-78.361	-37.379	-65.652	105.769	.43595E+01	C*	A		
8400	-173.000	62.000	-153.000	144.000	180.000	89.000	.43716E+01	D	E	11-16	
8500	-82.984	75.946	-144.000	149.995	-59.992	104.996	.43817E+01	C	E		21-9;23-9;24-9
8600	70.335	-139.980	-75.582	-31.043	66.383	-93.954	.43907E+01	F*	A		21-34
8700	-79.660	62.269	-153.384	143.080	181.223	85.697	.44001E+01	C	E	11-16	
8800	70.337	-139.985	-75.583	144.942	66.370	-93.984	.44036E+01	F*	F		21-16
8900	-73.060	-66.248	-158.260	-51.767	178.192	74.237	.44048E+01	A	G		
9000	-72.654	-65.331	-142.117	78.685	-63.280	-81.051	.44083E+01	A	D		23-9;24-9
9100	-73.147	-66.593	-157.252	-62.790	178.233	-103.605	.44200E+01	A	G		
9200	74.961	-140.000	-74.996	-45.959	179.006	82.997	.44243E+01	F*	A		
9300	180.004	179.973	-141.997	81.046	-62.007	-87.019	.44417E+01	E*	D		23-9;24-9
9400	74.965	-140.001	-145.997	-60.968	-66.024	105.021	.44534E+01	F*	G		21-9;24-9
9500	170.055	-70.716	-141.495	78.889	-63.459	109.845	.44693E+01	D*	D		21-9;24-9
9600	82.974	-76.037	-142.002	80.997	-62.017	-86.969	.44706E+01	C*	D		23-9;24-9
9700	180.001	179.997	-77.000	135.004	-178.996	89.998	.44802E+01	F*	F		
9800	72.423	-140.140	-162.791	-50.409	50.564	-87.454	.44805E+01	F*	G		21-34
9900	181.489	171.042	-156.712	-51.544	178.288	-99.674	.44928E+01	E*	G		
10000	74.968	-140.001	-152.997	146.027	-179.035	-104.984	.44984E+01	F*	E	11-16	21-34
10100	-75.000	140.000	-153.000	144.000	180.000	89.000	.45083E+01	F	E	11-16	
10200	70.616	-89.058	-76.413	-38.763	174.723	-99.735	.45118E+01	C*	A		
10300	-72.927	-65.922	-141.476	78.655	-63.082	109.107	.45767E+01	A	D		21-9;24-9
10400	180.002	179.995	-74.999	-45.994	179.011	82.996	.45977E+01	E*	A		
10500	180.002	179.995	-74.999	-46.994	179.011	62.996	.45977E+01	E*	A		
10600	-173.000	62.000	-153.000	146.000	-179.000	-105.000	.46186E+01	D	E	11-16	21-34
10700	-79.680	62.231	-153.386	144.989	-176.710	-108.403	.46299E+01	C	E	11-16	21-34
10800	72.000	53.000	-156.000	154.000	58.000	83.000	.46396E+01	A	E	11-16	21-9
10900	82.971	-76.039	-77.003	-47.978	-60.020	-76.000	.46628E+01	C*	A		
11000	83.000	-76.000	-158.000	-60.000	173.000	74.000	.46694E+01	C*	G		
11100	72.000	53.000	-155.000	151.000	60.000	-88.000	.46712E+01	A*	E	11-16	
11200	-80.508	67.132	-145.996	-61.713	-60.461	103.882	.46805E+01	C	G		21-9;23-9;24-9
11300	83.000	-76.000	-157.000	-61.000	174.000	-104.000	.46836E+01	F	D		
11400	-75.000	140.000	-142.000	81.000	-62.000	-87.000	.46939E+01	F	D		23-9;24-9
11500	-74.977	139.966	-146.001	-61.000	-65.961	104.992	.47064E+01	F	G		21-9;24-9
11600	180.000	180.000	-76.000	-36.000	68.000	-92.000	.47158E+01	E*	A		21-34
11700	82.973	-76.038	-141.003	79.001	-61.029	105.027	.47414E+01	C*	D		21-9;23-9;24-9
11800	74.967	-140.002	-141.997	81.032	-62.031	-86.986	.47566E+01	F*	D		23-9;24-9
11900	180.000	180.000	-76.000	140.000	68.000	-92.000	.47591E+01	E*	F		21-16
12000	74.963	-140.001	-76.997	-47.960	-59.999	105.019	.47864E+01	F*	A		
12100	-173.000	62.000	-146.000	-61.000	-66.000	105.000	.47882E+01	D	G		21-9;24-9
12200	-74.981	139.972	-163.001	-52.002	52.044	-80.988	.48144E+01	F	A		21-34
12300	-75.000	140.000	-153.000	146.000	-179.000	-105.000	.48359E+01	F*	E	11-16	21-34
12400	69.046	-139.982	-77.485	-27.758	63.074	80.273	.48386E+01	F	A		
12500	74.963	-140.001	-76.997	-47.961	-59.999	-75.980	.48603E+01	F	A		
12600	74.961	-140.000	-74.996	-48.959	179.006	-103.003	.48907E+01	F	A		
12700	74.963	-140.000	-79.997	145.039	63.992	80.982	.48922E+01	F	F		
12800	74.960	-140.002	-157.997	-59.970	172.974	74.011	.49052E+01	F	G		21-9;23-9;24-9
12900	180.004	179.976	-140.999	79.045	-51.015	104.979	.49064E+01	E*	D		
13000	180.001	179.997	-77.000	-47.996	-59.995	105.001	.49466E+01	E*	A		

	ϕ_G	ψ_G	ϕ_T	ψ_T	χ_T^1	χ_T^2	ENG	$\phi_G\psi_G$	$\phi_T\psi_T$	HYGBOND ATOM #'s	INDOLE CONTACT ATOM #'s
13100	74.961	-140.002	-156.997	-61.971	173.972	-103.988	.4959[illegible]E+01	F	G		21-9;21-10
13200	172.872	-62.537	-148.997	46.351	50.518	87.405	.49628E+01	D*	G		21-34
13300	51.631	-139.379	-41.931	115.946	-131.430	73.165	.49673E+01	F*	G		
13400	-173.000	62.000	-163.000	-52.000	52.000	-81.000	.50015E+01	F	G		
13500	180.001	179.997	-77.000	-47.996	-59.995	-75.998	.50085E+01	E*	A		
13600	-80.903	-80.967	-86.528	103.263	-185.439	78.014	.50452E+01	A	C		
13700	-80.035	64.049	-157.268	-61.719	161.090	-106.476	.50455E+01	C	G		
13800	-173.000	62.000	-157.000	-61.000	174.000	-104.000	.50633E+01	D	G		
13900	-173.000	62.000	-153.000	-60.000	173.000	74.000	.50697E+01	U	G		
14000	-80.889	67.657	-158.184	-60.444	179.356	72.372	.50755E+01	C	G		
14100	180.002	179.995	-74.999	-49.994	179.011	-103.004	.50798E+01	E*	A		
14200	161.492	-83.607	-86.173	102.512	-185.989	78.203	.50952E+01	D*	C		21-9;23-9;24-9
14300	74.968	-140.001	-140.997	79.033	-61.031	105.012	.50962E+01	F*	D		
14400	165.784	-77.866	-85.537	98.189	-184.517	76.623	.51207E+01	D*	C		
14500	180.000	180.000	-80.000	145.000	64.000	81.000	.51679E+01	E*	F		
14600	83.000	-76.000	-149.000	47.000	50.000	88.000	.51778E+01	C*	D		21-9;21-10
14700	-74.979	139.969	-158.001	-60.000	173.043	73.996	.51810E+01	F	G		
14800	49.414	-139.263	-82.632	119.833	-181.739	-104.726	.51965E+01	F*	C		
14900	180.000	180.000	-78.000	-34.000	64.000	83.000	.52249E+01	E*	A		
15000	163.577	-80.808	-86.850	100.226	-185.271	-100.559	.52286E+01	D*	C		21-16
15100	-74.978	139.966	-157.002	-61.000	174.040	-104.005	.52304E+01	F	G		
15200	62.247	-95.295	-87.193	105.665	-188.323	-99.433	.52838E+01	C*	C		
15300	71.887	-37.997	-86.249	97.846	-155.305	-101.528	.53383E+01	C*	C		
15400	163.386	-81.603	-87.679	92.372	-66.005	103.272	.53609E+01	D*	C		
15500	181.331	176.327	-63.467	94.854	-178.022	71.585	.53781E+01	E*	C		
15600	64.129	-94.215	-87.923	95.969	-68.502	106.621	.54054E+01	C*	C		
15700	71.565	-63.485	-87.212	89.992	-66.131	104.966	.54415E+01	C*	C		
15800	164.904	-79.883	-87.182	91.098	-65.582	-77.819	.54519E+01	D*	C		
15900	172.698	-63.175	-153.036	53.842	58.832	-73.276	.54677E+01	D*	D		21-16
16000	66.588	-92.602	-87.543	94.340	-67.911	-75.199	.55265E+01	C*	C		
16100	71.435	-88.684	-87.099	90.603	-66.296	-76.378	.55327E+01	C*	C		
16200	-75.000	140.000	-141.000	79.000	-61.000	105.000	.55456E+01	F	D		21-9;23-9;24-9
16300	72.000	53.000	-144.000	149.000	-60.000	105.000	.55670E+01	A*	E	11-16	21-9;23-9;24-9
16400	72.000	53.000	-153.000	144.000	180.000	89.000	.55711E+01	A*	E	11-16	
16500	74.964	-140.001	-85.997	81.042	-60.007	104.012	.55858E+01	F*	C		
16600	74.964	-140.001	-85.997	82.042	-60.007	-77.967	.55980E+01	F*	C		21-16
16700	180.008	179.974	-34.996	89.047	-178.988	-105.011	.56483E+01	E*	C		23-9;24-9
16800	-173.000	62.000	-144.000	148.000	-61.000	-87.000	.56540E+01	D	E	11-16	21-16
16900	83.000	-76.000	-153.009	54.000	59.000	-72.000	.56586E+01	C*	D		
17000	180.008	179.974	-85.996	82.046	-59.981	-78.006	.56755E+01	E*	C		
17100	-75.000	140.000	-77.009	135.000	-179.000	90.000	.56777E+01	F	F		
17200	180.008	179.975	-85.996	81.046	-59.980	103.992	.56809E+01	E*	C		
17300	180.000	180.000	-149.000	47.000	59.000	88.000	.57497E+01	E*	D		21-9;21-10
17400	-75.000	140.000	-75.000	-47.000	179.000	83.000	.58041E+01	F	A		
17500	72.000	53.000	-153.000	145.000	-179.000	-105.000	.58081E+01	A*	E	11-16	21-34
17600	-82.985	75.947	-141.001	78.997	-60.987	104.993	.58275E+01	C	D		21-9;23-9;24-9

(1) There is only an intraresidue hydrogen bond between the tryptophan amino proton and the tryptophan carboxyl oxygen. This bonding occurs only when $^{+}PT^{-}$ is in the F-E conformation.

(2) There exists two types of indole contacts in the low energy conformation of $^{+}PT^{-}$. There is an interresidue contact between one tryptophan indole carbon (atom #28) and the proline carbonyl oxygen. There is also an intraresidue contact between the same indole carbon and either partially negatively charged oxygen in the tryptophan carboxylate group.

(3) There is, in general, no consistent correlation between the conformational types of either proline or tryptophan and the occurrence of these indole contacts.

Figure 20 outlines the very limited data for $^{2+}LT^{-}$. The results are as follows:

(1) There is no hydrogen bonding in the low energy conformations of $^{2+}LT^{-}$.

(2) There exists one type of indole contact. It is an intraresidue contact between a tryptophan indole carbon (atom #36) and the tryptophan carboxyl oxygen.

FIGURE 19

Conformational and Energy Data For $^{+}PT^{-}$

	ψ_P	ϕ_T	ψ_T	x^1_T	x^2_T	ENG*
100	179.854	-156.794	153.397	58.747	61.449	-.16805E+02
200	179.644	-156.212	153.161	58.236	80.957	-.16755E+02
300	180.039	-155.051	150.636	59.398	-89.262	-.16395E+02
400	179.737	-155.125	150.523	59.286	-89.547	-.16349E+02
500	180.167	-148.131	134.564	-61.735	-90.006	-.16049E+02
600	179.845	-149.186	136.177	-61.855	-78.233	-.15886E+02
700	180.049	-144.047	148.876	-60.833	105.024	-.15897E+02
800	179.787	-144.078	148.876	-60.837	105.017	-.15813E+02
900	180.209	-152.990	143.952	179.349	69.199	-.15482E+02
1000	179.943	-153.013	143.968	179.318	89.184	-.15429E+02
1100	180.122	-78.652	-36.094	61.394	80.572	-.15403E+02
1200	180.132	-78.656	-36.785	61.073	80.005	-.15376E+02
1300	180.074	-80.628	143.050	61.391	78.678	-.15333E+02
1400	179.862	-80.591	142.903	61.375	78.575	-.15296E+02
1500	179.452	-148.133	-67.247	-60.567	-81.322	-.15207E+02
1600	180.188	-146.036	-61.121	-63.916	105.055	-.15266E+02
1700	179.461	-147.620	-64.859	-61.550	-83.213	-.15241E+02
1800	179.933	-146.059	-61.105	-63.876	105.032	-.15212E+02
1900	180.232	-152.978	145.998	-180.171	-104.765	-.15199E+02
2000	179.969	-153.093	146.016	-180.216	-104.781	-.15146E+02
2100	180.386	-76.375	-36.930	63.657	-93.415	-.15126E+02
2200	180.264	-163.627	-52.379	55.150	-82.083	-.15113E+02
2300	180.165	-76.342	-36.964	63.577	-93.418	-.15098E+02
2400	180.040	-163.083	-52.452	55.662	-82.372	-.15097E+02
2500	180.308	-76.369	139.065	63.566	-93.388	-.15020E+02
2600	180.167	-76.338	139.051	63.586	-93.390	-.14991E+02
2700	179.791	-77.545	-49.100	-61.087	-75.290	-.14963E+02
2800	179.472	-77.536	-49.225	-61.079	-75.193	-.14918E+02
2900	179.563	-145.585	70.796	-61.391	-79.210	-.14767E+02
3000	179.436	-144.590	70.690	-61.383	-79.040	-.14754E+02
3100	180.379	-157.985	-60.082	175.669	74.122	-.14643E+02
3200	180.038	-77.273	134.814	-180.269	89.978	-.14614E+02
3300	180.125	-158.002	-60.056	175.723	74.116	-.14590E+02
3400	180.347	-156.976	-61.035	176.176	-103.847	-.14569E+02
3500	179.775	-77.264	134.826	-180.256	89.973	-.14575E+02
3600	179.842	-77.363	-48.318	-61.011	105.029	-.14572E+02
3700	180.080	-156.994	-61.305	176.214	-103.854	-.14535E+02
3800	179.583	-77.360	-48.351	-61.044	105.056	-.14531E+02
3900	180.036	-141.119	78.604	-61.092	102.288	-.14529E+02
4000	179.769	-141.136	78.615	-61.104	105.265	-.14477E+02
4100	180.026	-75.274	-47.168	178.672	82.950	-.14439E+02
4200	179.761	-75.263	-47.174	178.711	82.955	-.14404E+02
4300	179.896	-149.275	45.775	54.049	86.350	-.14012E+02
4400	179.719	-149.330	45.638	54.194	86.241	-.13998E+02
4500	180.002	-75.279	-49.106	178.614	-103.040	-.13984E+02
4600	179.737	-75.270	-49.113	178.651	-103.036	-.13946E+02
4700	179.669	-86.506	80.804	-80.866	-77.174	-.13931E+02
4800	179.500	-86.603	80.357	-80.956	-76.834	-.13867E+02

ϕ_P	ψ_P	ϕ_T	ψ_T	HYDROGEN-ATOM #'S	INDOLE CONTACT ATOM #'S
F	E			18-23	
F	E			18-23	
F	E			18-23	
F	E			18-23	
F	E			18-23	28-15
F	E				28-15
F	E			18-23	28-15
F	E			18-23	28-15
F	E			18-23	
F	A				
F	A				
F	G				
F	G				28-15
F	G				28-15
F	G				28-15
F	G				28-15
F	E			18-23	
F	E			18-23	
F	A				
F	A				
F	A				
F	A				
F	A				
F	A				
F	A				
F	A				
F	A				
F	A				
F	A				
F	A				
F	A	D			28-15
F	A				28-15
F	A				
F	A				
F	A				
F	A				
F	A				
F	A				

ATOM # KEY

a. 18-23 = T-Amino H to T-Carboxyl O
b. 28-15 = Indole C to P-Carbonyl O
c. 28-23 = Indole C to T-Carboxyl O
d. 28-41 = Indole C to T-Carboxyl O

* Add 0.336 Kcal/mole for Proline Internal Energy

FIGURE 20

Conformational and Energy Data For $^{2+}LT^{-}$

ϕ_L	ψ_L	χ^1_L	χ^2_L	χ^3_L	χ^4_L	$\phi_L-\psi_L$	$\phi_T-\psi_T$	HYGBOND ATOM #'s	INDOLE CONTACT ATOM #'s
-66.451	132.383	180.000	180.000	180.821	-60.861				
χ^5_L	ϕ_T	ψ_T	χ^1_T	χ^2_T	ENG				
-55.456	-76.527	139.325	60.335	-93.941	.13815E+02	F	F	NONE	36-31
ϕ_L	ψ_L	χ^1_L	χ^2_L	χ^3_L	χ^4_L				
-66.451	132.383	180.000	180.000	180.821	-60.861				
χ^5_L	ϕ_T	ψ_T	χ^1_T	χ^2_T	ENG				
64.544	-76.527	139.325	60.335	-93.941	.13815E+02	F	F	NONE	36-31
ϕ_L	ψ_L	χ^1_L	χ^2_L	χ^3_L	χ^4_L				
-66.451	132.383	180.000	180.000	180.000	-60.861				
χ^5_L	ϕ_T	ψ_T	χ^1_T	χ^2_T	ENG				
64.544	-76.527	139.325	60.335	-93.941	.13816E+02	F	F	NONE	36-31

ATOM # KEY

a. 36-31 = Indole C to T-Carboxyl O

DISCUSSION

Charge Effects:

Work by Leher showed a 27% decrease in the K_{sv} value and a 19% decrease in k_q for the iodide quenching of positively charged L-tryptophyl ethyl ester with a charge in ionic strength from 0.06 to 0.20. Negatively charged indole 3-acetate (a compound similar to tryptophan) showed only a 6% change in K_{sv} and a 9% change in k_q with the same change in ionic strength. Uncharged indole-containing compounds were unaffected by changes in ionic strength.[12] In light of such information, an investigation of ionic strength effects upon fluorescence was deemed crucial for either verification or correction of earlier obtained Stern-Volmer data.

Our results show that there is less than a 15% overall change in the F_T^o/F_T ratio for all zwitterions and anions studied with a change in μ from 0.130 to 0.438 with iodide quencher and from 0.19 to 0.570 with cesium quencher. Except for three of the peptides studied, $^+GTG^-$, $^+TG^-$ with iodide and $^+GTG^-$ with cesium quencher, the percentage change in F_T^o/F_T did not exceed 9%. Since K_{sv} is equal to the slope of F_T^o/F_T vs. $[Q]$, this slight change in F_T^o/F_T implies that the $'$ values and the subsequently calculated k_q values would not be radically altered as the ionic strength increases through addition of quencher. Our results show therefore that there is less dependency upon ionic strength than that proposed by Leher. Our studies reveal that the results of

most of Stern-Volmer experiments are generally valid.

The Stern-Volmer results obtained for those peptides which show the greatest % change in F_T^o / F_T may be erroneous. It is suggested that further studies of the effect of ionic strength upon fluorescence need be undertaken to more clearly determine the validity of these Stern-Volmer quenching data.

Tables 2 and 4 list two types of quenching constants, k_q and $\langle k_q \rangle$ for each peptide studied. Each type of k_q value was calculated using a different type of lifetime value. The first type of quenching constant is calculated from equation (16):

$$k_q = K_{sv} / \tau \qquad (16)$$

Work by Werner and Forster defined τ as the lifetime of the peptide derived from a single exponential least squares fit where the average RMS value for reproducible data sets was less than or equal to 0.008.[1] The k_q value thus calculated is a quantitative expression of the quenching efficiency of external quenchers providing the peptide actually exhibits single-exponential decay.

The other value for the quenching constant, $\langle k_q \rangle$ is calculated from equation (17):

$$\langle k_q \rangle = K_{sv} / \tau \qquad (17)$$

where τ represents a weighted average lifetime for the peptide. It is given by expression (18):

$$\tau = f_1 \tau_1 + f_2 \tau_2 \qquad (18)$$

where τ_1 and τ_2 are the two lifetime components and f_1, f_2 are the normalized weighting factors assigned to each component. τ_1 and τ_2 were derived, as seen earlier, from a double exponential least squares fit where the average RMS value for the reproducible data sets was less than 0.008 and the RMS value for a single exponential fit was greater than 0.01.[1]

The quantitative nature of this $\langle k_q \rangle$ value is somewhat ambiguous because the average weighted lifetime does not clearly define which lifetime component is large enough to be quenched by external quenchers. In addition, $\langle k_q \rangle$ may represent an average of the k_q value for each lifetime component, but this is not verifiable. $\langle k_q \rangle$ values, although ambiguous, were listed so that one could look for trends due to electrostatic effects (to be discussed later). If these trends do not exist however, it suggests that the $\langle k_q \rangle$ value may not be the average mentioned above. In summary, the actual quenching efficiency when double-exponential fits are used is not well defined.

Indeed, there is some ambiguity in both types of k_q values because there is some arbitrariness involved in choosing the RMS criteria by which one assigns a double or single exponential fit to the lifetime data sets. Clearly, one cannot be absolutely sure which type of k_q value most accurately conveys the quenching efficiency of external quenchers.

Our results lead to the conclusion that the quenching efficiency of iodide ion is dependent upon the location of charge(s) relative to tryptophan in the peptides studied.

It was seen that when tryptophan is the uncharged residue in zwitterionic tripeptides, the k_q value was comparable to those for the reference compounds, NATA and NATE. This suggests that the electrostatic interaction between the indole ring or tryptophan and the iodide ion is the same for these compounds.

The tryptophan zwitterion also has a k_q value comparable to those found for NATA and NATE. Both charges in the zwitterion apparently compensate for one another and affect the quenching by iodide in the same manner as if tryptophan were uncharged.

Our results show that when tryptophan is uncharged in anionic peptides, e.g. TG^-, GTG^- and $GTGG^-$, the quenching efficiency, as measured by both k_q and $\langle k_q \rangle$ is relatively high as compared to the other anions studied. This can be attributed to the small degree of electrostatic repulsion between the negatively charged iodide ion and the site of quenching. This conclusion is substantiated by an observed increase in the single lifetime k_q value as tryptophan is moved farther away from the negatively charged residue in the peptide. Clearly, the electrostatic repulsion is decreased around tryptophan allowing for greater contact between the indole ring and the iodide ion.

This electrostatic effect is further substantiated by the presence of relatively low k_q values (both types) for those zwitterionic and anionic peptides in which the tryptophan

residue contains a negative charge. The quenching efficiency for these peptides is less than that for peptides with uncharged tryptophan because the negative iodide ion is electrostatically repelled away from the quenching site to a greater extent.

When peptidyl tryptophan is positively charged the k_q values are low as compared to the other peptides studied. The positive charge on tryptophan electrostatically attracts the negative iodide ion. This increases the contact between the indole ring and the quencher, thus increasing the quenching efficiency. This charge effect is further substantiated by the rise in k_q as the negatively charged residue is moved away from the positive tryptophan residue. According to our model, as the negative charge is moved away the electrostatic repulsion of the iodide ion around tryptophan is reduced. The ability for iodide to contact tryptophan is increased, leading to an increase in quenching efficiency.

Meyer and Seybold have observed these charge effects over a much more limited range of data.[13] Our conclusions are also supported by results of reference 6.

Our results also reveal that there is no simple relationship between the location of charge relative to tryptophan in both anionic and zwitterionic peptides and the quenching efficiency of positively charged cesium ion. The k_q and $\langle k_q \rangle$ for cesium quenching do not increase or decrease in a regular fashion as would be expected by the electrostatic interaction

model proposed above for iodide ion.

This phenomenon can first be attributed to the fact that the data for cesium quenching are much more limited than that for iodide quenching. This is due to the fact that the measured fluorescence intensities of the zwitterions which were useful in the iodide quenching experiments, now with cesium ion, show only a negligible change after each addition of quencher. Hence, many zwitterions cannot even be used in the cesium quenching experiments.

In addition, the low quenching efficiency seen for cesium ion as compared to iodide ion might be explained as follows:

Cs^+ and I^- are isoelectronic and are therefore about the same size. Thus steric factors are excluded. Instead, this difference in quenching efficiency suggests that the exciplex formed between the indole ring and the quencher is more stable with iodide ion. Apparently, the indole ring acts more as an electron acceptor than as an electron donor. Consequently, the electrophilic cesium ion would be less likely to form a stable exciplex, and would therefore quench rather inefficiently.

Evidence for Double-Exponential Decay:

It is believed that the Stern-Volmer plots can be useful for detecting double-exponential decay. It was seen earlier that the Stern-Volmer constant, K_{sv}, which is the slope of a F_T^o/F_T vs. [Q] plot, is proportional to the fluorescence decay lifetime, τ_f. It was hypothesized that if there exists more than a single exponential decay lifetime component for a pep-

tide, this would be reflected in the K_{sv}, and a non-linear slope would result.

To verify this hypothesis, a Stern-Volmer quenching experiment with cesium quencher was performed on a solution containing two peptides each with a known single exponential decay lifetime. This mixture was created in order to simulate a single peptide which exhibits double exponential decay.

NATA and $^{+}GT^{-}$ were used because their single exponential lifetimes, 2.8 ns and 0.90 ns respectively, vary significantly. The k_q values for each peptide, $4.7 \times 10^9 M^{-1} sec^{-1}$ for NATA and $3.0 \times 10^9 M^{-1} sec^{-1}$, for $^{+}GT^{-}$ are also quite different. A large difference in the lifetime and k_q values was deemed essential because this, it was hoped, would increase the probability that the slope would deviate from linearity. Cesium quencher was used because it was thought that an inefficient quencher might be more likely to expose the existence of double exponential decay.

Our results have shown that the Stern-Volmer plots for the quenching of mixtures with different amounts of each peptide all had linear slopes (see Figures 21-23). This indicates that the lifetime of NATA may indeed be too similar to that of $^{+}GT^{-}$ to produce non-linearity in the Stern-Volmer plot. This implies that under certain circumstances, the Stern-Volmer experiment is not sensitive enough to detect double exponential decay.

Rayner and Szabo have seen that aqueous tryptophan exhibits

FIGURE 21

Stern-Volmer Plot

F_T°/F_T vs $[Cs^+]$

NATA : $^+GT^-$

λ_{ex} = 290 nm

K_{sv} = 1.35

r = .9976

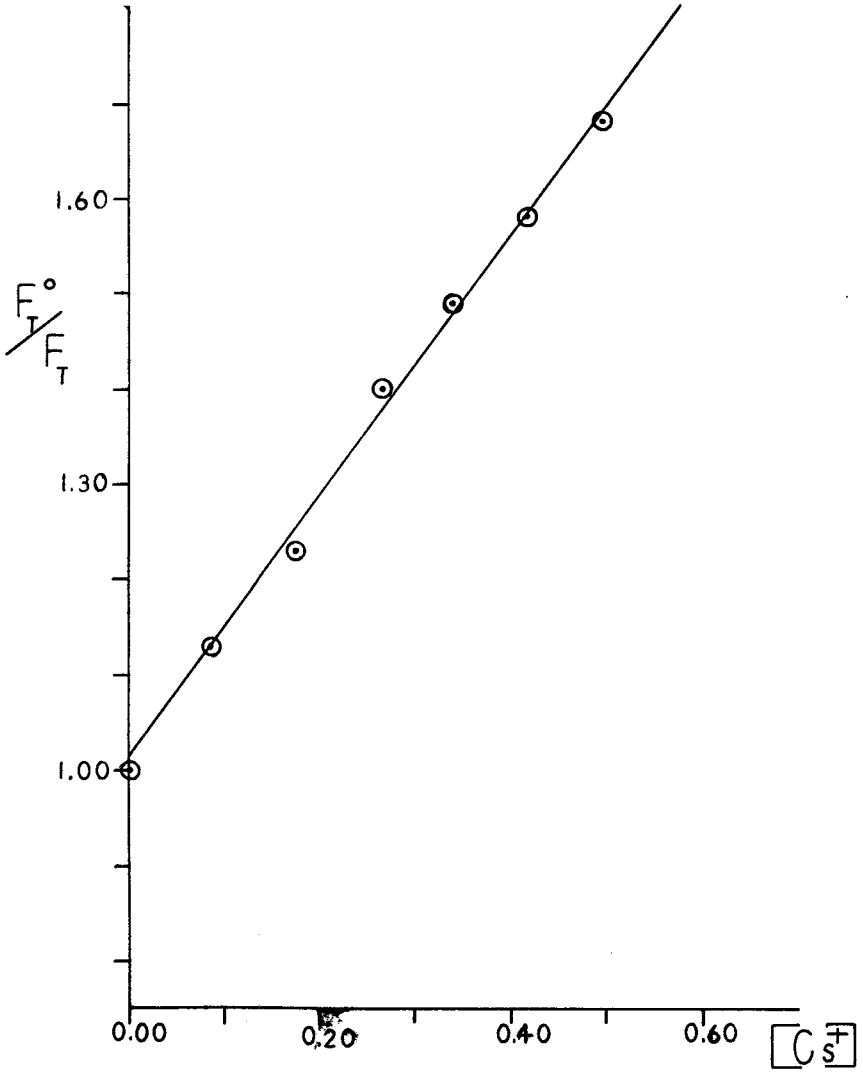
1.60
1.30
1.00
F_T° / F_T
0.00
0.20
0.40
0.60
$[Cs^+]$

FIGURE 22

Stern-Volmer Plot

$F_T°/F_T$ vs $[Cs^+]$

2 NATA : $^+GT^-$

λ_{ex} = 290 nm

K_{sv} = 1.48

r = .9972

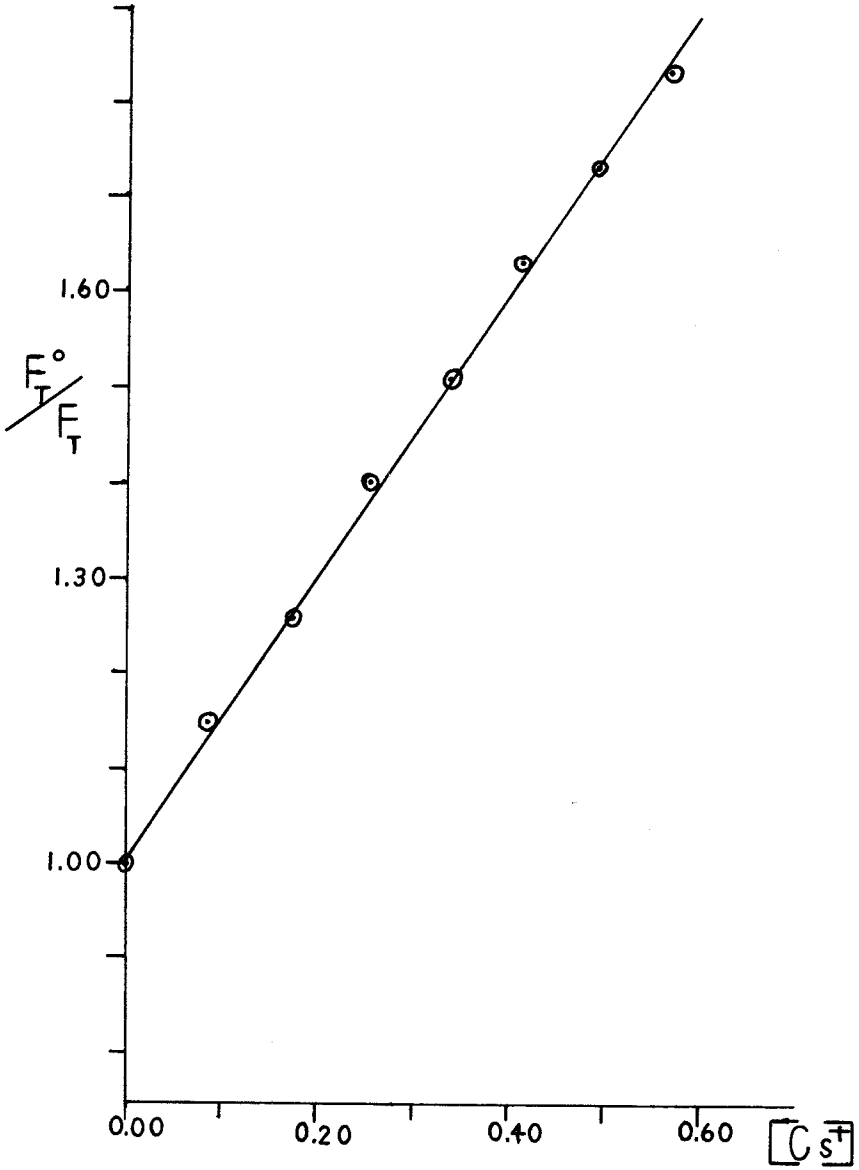
1.60
1.30
1.00
$\frac{F_T^\circ}{F_T}$
0.00
0.20
0.40
0.60
$[Cs^+]$

FIGURE 23

Stern-Volmer Plot

F_T°/F_T vs $[Co^+]$

NATA : 2^+GT^-

λ_{ex} = 290 nm

K_{sv} = 1.1

r = .9962

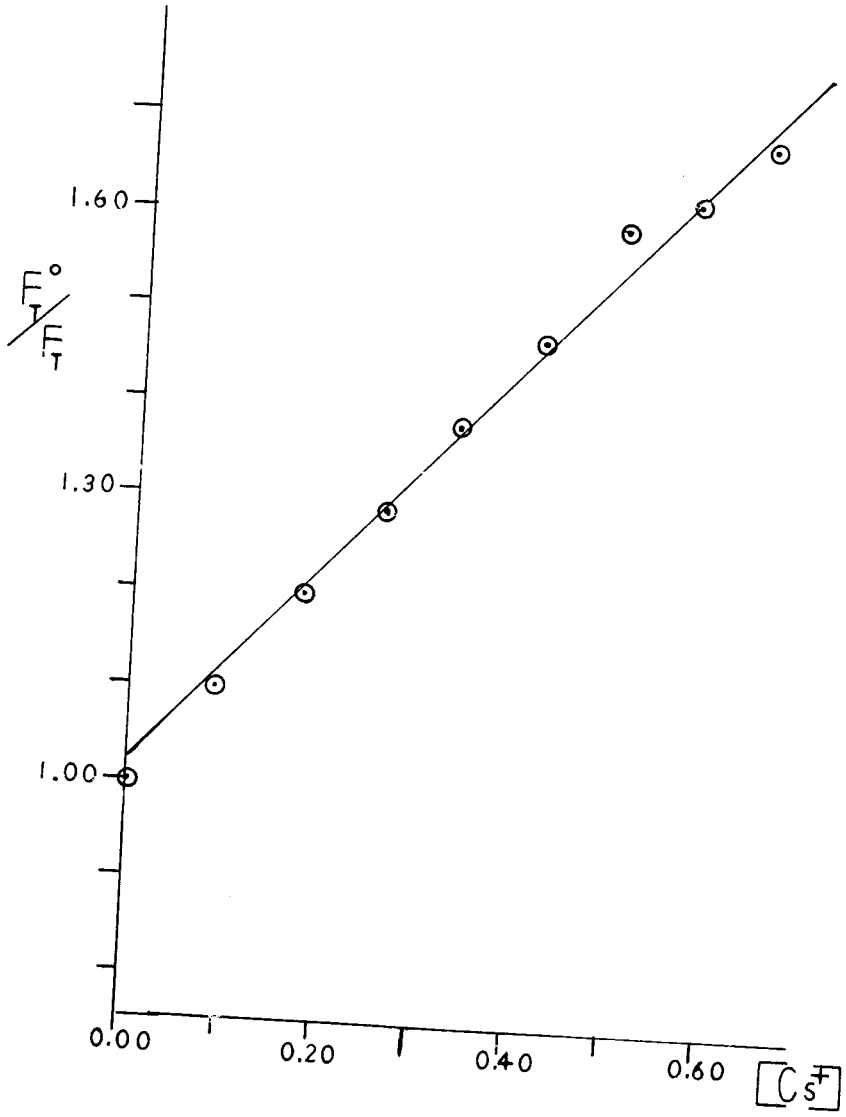
1.60
1.30
1.00
$\frac{F_T^\circ}{F_T}$
0.00
0.20
0.40
0.60
$[Cs^+]$

multi-exponential decay. They found τ_1 to equal 3.13 ns $\pm$ 0.02 ns and τ_2 = 0.51 ns $\pm$ 0.04 ns. They have also seen that the ratio of the pre-exponentials is emission wavelength dependent. This ratio is quite different at 330 nm and 370 nm. The ratio is 7.35 $\pm$ 2.3 at 370 nm and 2.11 $\pm$ 0.44 at 330 nm.[2]

Because of this variation, it was deemed worthwhile to examine Stern-Volmer quenching of tryptophan with cesium ion at each wavelength. Since $K_{sv} = k_q\langle\tau\rangle$ where $\langle\tau\rangle = f_1\tau_1 + f_2\tau_2$, this difference in the ratio of f_1/f_2 should, if two lifetimes do indeed exist, cause K_{sv} to be different at each wavelength.

Our results have shown that the Stern-Volmer plots at each wavelength produced linear slopes. The linear plots seen to reflect the quenching of only a single lifetime. This is to be expected however, because the ratio of f_1/f_2 is large at both wavelengths. The longer lifetime is therefore weighted much more heavily in both cases. Hence, the Stern-Volmer technique is, as stated earlier, not sensitive enough to reflect the quenching of the shorter, least weighted, lifetime at both 330 nm and 370 nm.

In addition, it is seen that the K_{sv} for the linear plots at each wavelength are almost identical. The difference in the values of 0.2 is probably a reflection of statistical and experimental error rather than an indication of a difference in the ratio of pre-exponentials. This result does not prove

nor disprove Rayner and Szabo's assertion that tryptophan exhibits double exponential decay and that the ratio of pre-exponentials is wavelength dependent. Instead, we see that the Stern-Volmer technique is insufficient, in this case, for proving the existence of non-single exponential decay.

Our results showed that $^{2+}LT^{-}$ consistently exhibited non-linear plots for Stern-Volmer quenching experiments with cesium quencher. Leher, who observed consistent deviations from the Stern-Volmer law for large peptides with many tryptophyl side chains, developed a modified Stern-Volmer equation in order to more clearly elucidate the fluorescence properties of such compounds.[12] In these proteins, some fluorescence sites are fully exposed to the solvent and are thus accessible to quencher ions. Other fluorophors are buried and inaccessible to quencher.

If there are n fluorescent side chains with the same K_{sv}, and m accessible fluorophors, then there are m-n inaccessible fluorophors. To account for this, the Stern-Volmer law is modified to produce equation (19):

$$F^{o}/\Delta F = \frac{1}{(\Omega f_a K_{sv})} + 1/f_a \qquad (19)$$

where F^{o} and F are the fluorescence quantum yields in the absence and presence of quencher respectively, $\Delta F = F^{o} - F$ and f_a is the fractional maximum accessible protein fluorescence summed over m accessible fluorescence sites. As in the case of earlier Stern-Volmer work, the relative fluorescence intensities can be substituted for the quantum yield values.

A plot of $F^{o}/\Delta F$ vs. $1/[Q]$ should yield a straight line with a slope of $1/f_a K_{sv}$ and an intercept of $1/f_a$. K_{sv} is therefore given by the intercept divided by the slope. f_a is equal to 1/intercept.

A modified Stern-Volmer plot for the cesium quenching of $^{2+}LT^{-}$ produced a linear slop (see Figure 24). Based on Leher's work, it was believed that this result might be evidence for the existence of two fluorescence 'sites' in $^{2+}LT^{-}$. Theoretical calculations were carried out in order to simulate $^{2+}LT^{-}$ with two fluorescence sites. The fluorescence decay for each site would represent the fluorescence decay for a different lifetime component for $^{2+}LT^{-}$.

Werner and Forster reported double exponential decay for $^{2+}LT^{-}$. They found $\tau_1 = 0.90$ ns with a weighting factor, $f_1 = 0.84$ and $\tau_2 = 3.7$ ns with $f_2 = 0.16$.[1] The fluorescence quantum yield in the absence of quencher for each site is given by ϕ_{f_n}; where n equal the number of the site. Since ϕ_{f_n} is proportional to the decay lifetime, τ_f, its value can be calculated by equation (20):

$$\frac{\phi^{o}_{f_n}}{\tau_{f_n}} = \frac{\phi^{o}_{f_{NATA}}}{\tau_f} \qquad (20)$$

where $\phi^{o}_{f\ NATA}$ and $\tau_{f_{NATA}}$ are the experimentally determined quantum yield and lifetime for our reference compound, NATA. $\phi^{o}_{f_{NATA}} = 0.14$ and $\tau_{f_{NATA}} = 2.8$ ns. ϕ_{f_1} for site 1 is calculated to equal 0.045. $\phi^{o}_{f_2}$ for site 2 equals 0.185. The total quantum yield for the peptide in the absence of quencher, ϕ^{o}_{T} is equal to the weighted sum of the quantum yields for each

FIGURE 24

Modified Stern-Volmer Plot

$^{2+}_{LT^-}$

$F_T°/\Delta F$ vs $[Cs^+]^{-1}$

$K_{sv} = 3.0$

$f_a = 0.59$

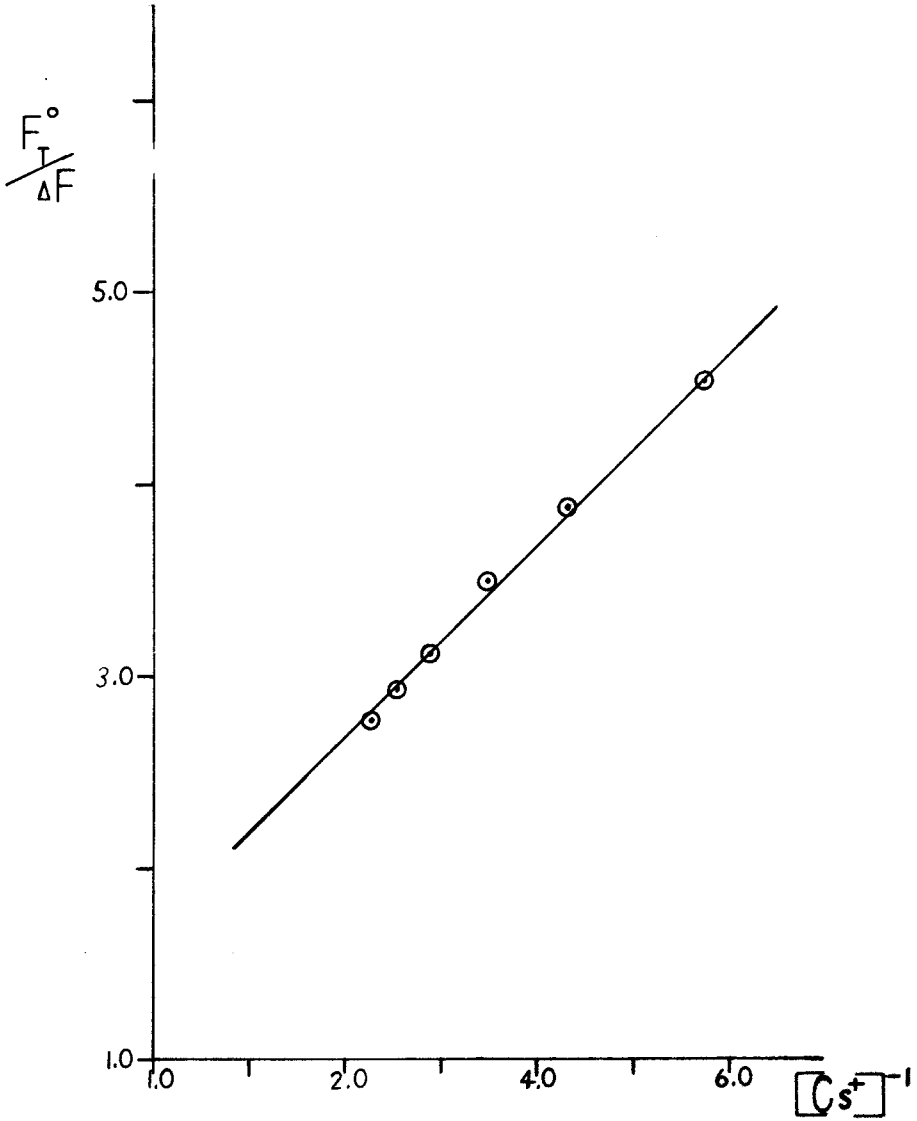
F°I / ΔF
5.0
3.0
1.0
1.0
2.0
4.0
6.0
[Cs+]⁻¹

site: $\phi_T^o = f_1\phi_{f1}^o + f_2\phi_2^o$.

$\phi_{f_n}^o$ is also given by equation (21):

$$\phi_f^o = k_f / k_f + k_i \qquad (21)$$

where k_f is the fluorescence rate constant and k_i is the rate constant for all the other decay pathways in the absence of quencher. Ricci and Nesta have observed that k_f for indole and other tryptophan containing compounds is environment independent and has a constant value of $4.5 \times 10^7 sec^{-1}$.[3] Since ϕ_f for each site is known, k_i can be calculated with equation (21). For site 1, $k_i = 9.6 \times 10^8 sec^{-1}$ and for site 2. $k_i = 2.0 \times 10^8 sec^{-1}$.

In the presence of quencher, the quantum yield for each site ϕ'_{f_n} is given by equation (22):

$$\phi'_{f_n} = k_f \quad (k_f + k_i + k_q [Q]) \qquad (22)$$

where k_q is the second order rate contant for quenching and $[Q]$ is the concentration of quencher. Since k_f and k_i for each site are known, if one assumes a k_q for each site, the quantum yield ϕ'_{f_n} at a given quencher concentration can be calculated. Several values of k_q for each site were assumed. The most useful and realistic values assumed for k_q were as follows: k_q for site 1 = $4.0 \times 10^8 mile^{-1} sec^{-1}$ and k_q for site 2 = $1.0 \times 10^9 mol^{-1} sec^{-1}$.

The total quantum yield for the peptide in the presence of quencher is the weighted sum of the quantum yields for each site, i.e. $\phi'_T = f_1\phi'_1 + f_2\phi'_2$. One can therefore determine

ϕ_T' at any given quencher concentration. The calculated Stern-Volmer equation is:

$$\frac{\phi_T^\circ}{\phi_T'} = 1 + K_{sv} \quad Q$$

A Stern-Volmer plot of ϕ_T° ϕ_T' vs. Q for $^{2+}LT^-$ using the calculated values for the quantum yields is seen in Figure 25. The figure shows clear curvature. Figure 26 shows a comparison of the Stern-Volmer plots for the calculated and experimentally measured values. Good agreement is seen.

Since the calculated Stern-Volmer plot revealed curvature, a modified Stern-Volmer plot using calculated values was constructed in accordance with Leher's work. This is seen in Figure 27. Figure 28 compares the modified Stern-Volmer plot using calculated values with that obtained with measured values. As seen in our results, the values of K_{sv} and f_a from our calculated plot is in very good agreement with those found experimentally.

This correspondence between experimental and calculated results seems to verify the assumption used in the calculations that there are two fluorescence sites for $^{2+}LT^-$. Since we assumed that each 'site' represented the fluorescence decay of a different lifetime component for $^{2+}LT^-$, our results support Werner and Forster's contention that $^{2+}LT^-$ exhibits double exponential decay.

This conclusion is not arrived at without reservation. The longer lifetime component for $^{2+}LT^-$, unlike the tryptophan

Figure 25

Theoretical Ster-Volmer Plot

$^{2+}_{LT^-}$

$\emptyset_T^\circ/\emptyset_T'$ vs $[Cs^+]$

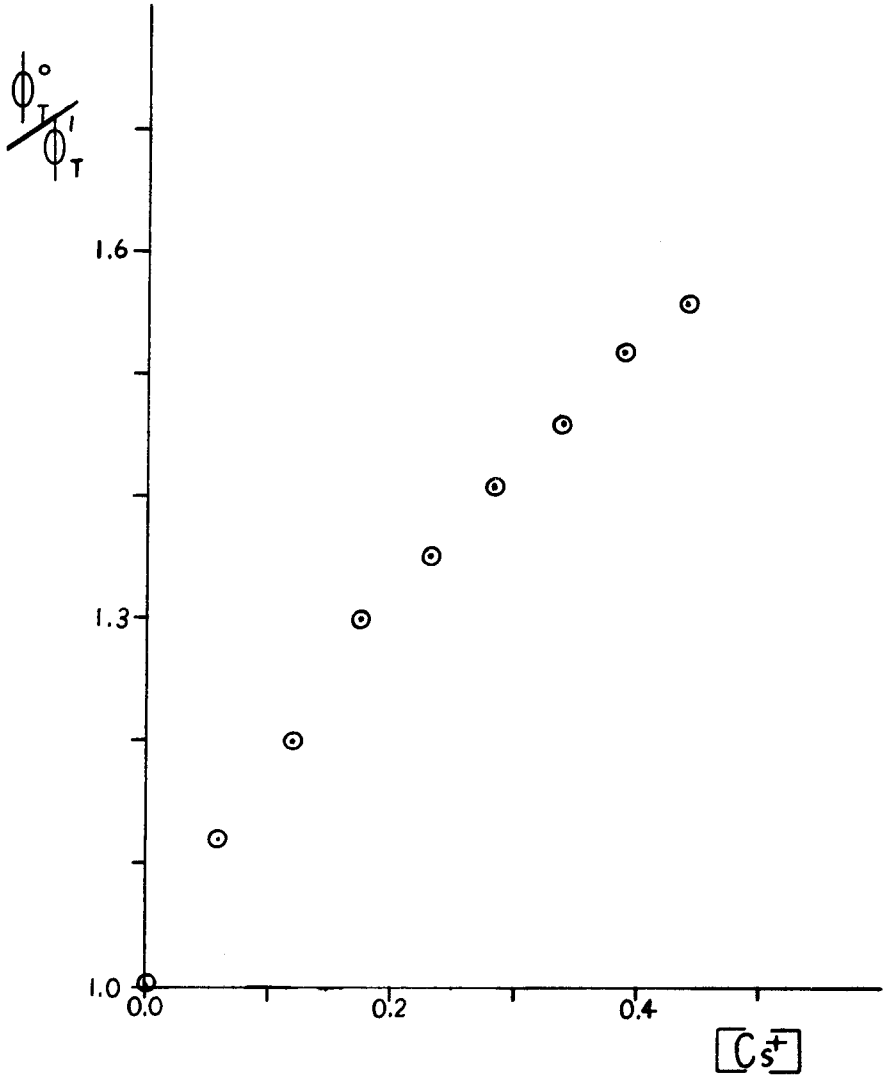
Φ_T° / Φ_T^i
1.6
1.3
1.0
0.0
0.2
0.4
$[Cs^+]$

FIGURE 26

Stern-Volmer Plot

$^{2+}_{LT^-}$

$\phi_T^\circ/\phi_T^{'}$ vs $[Cs^+]$

+ - Experimentally measured values for ϕ_T°/ϕ_T

$\odot$ - Theoretically calculated values ϕ_T°/ϕ_T

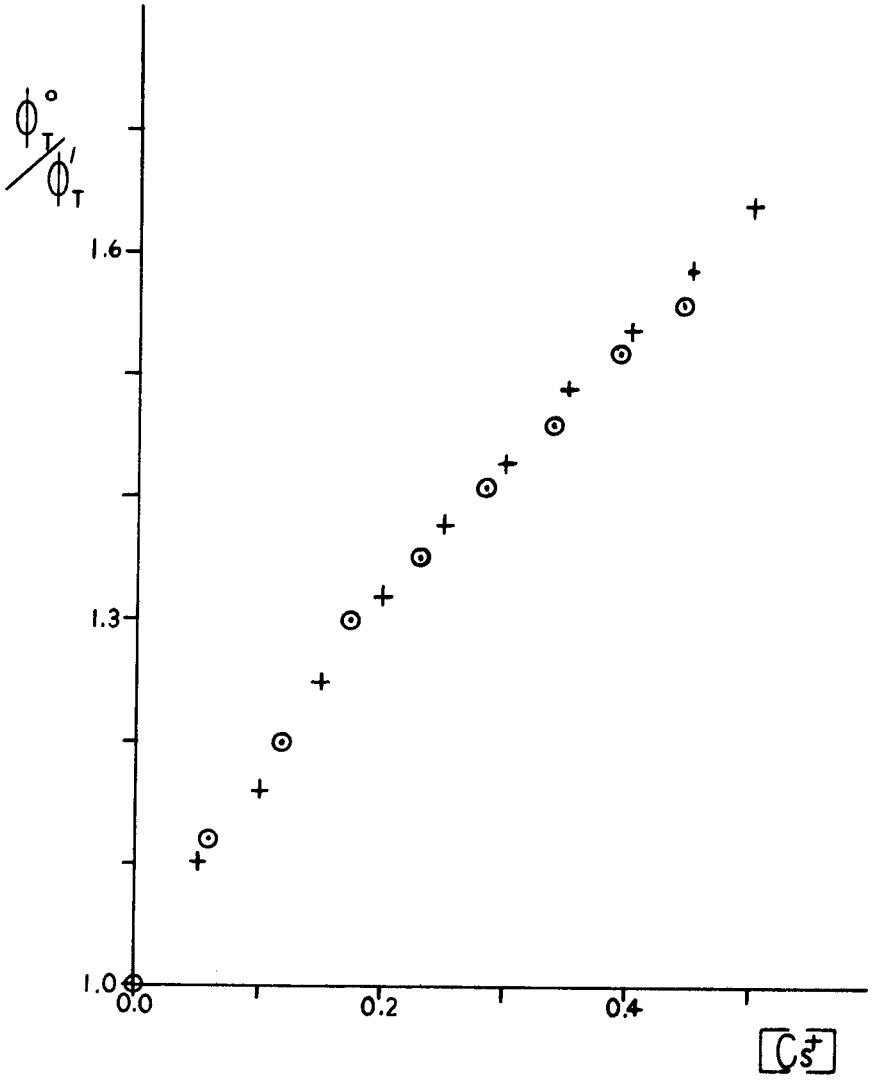
ϕ_T° / ϕ_T'
1.6
1.3
1.0
0.0
0.2
0.4
$[Cs^+]$

FIGURE 27

Theoretical Modified Stern-Volmer Plot

$^{2+}_{LT^-}$

$F°/\Delta F$ vs $[Cs^+]^{-1}$

$K_{sv} = 2.90$

$f_a = 0.65$

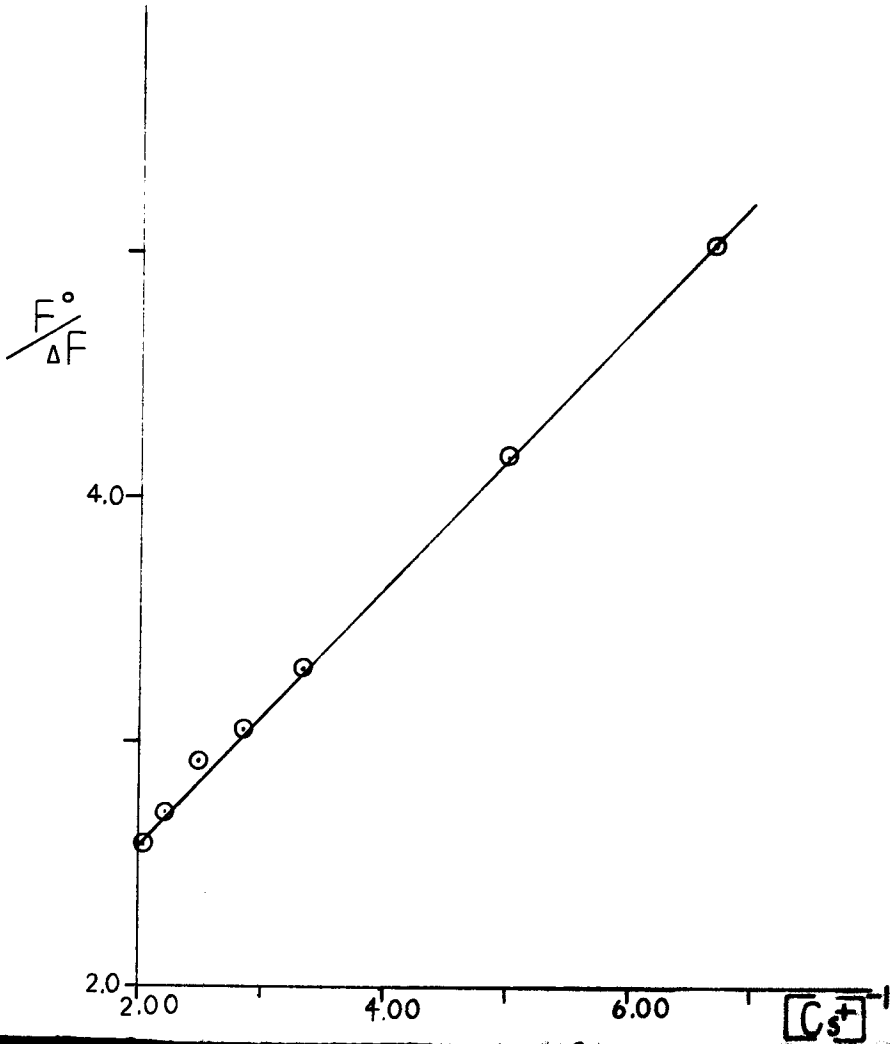
F°/ΔF
4.0
2.0
2.00
4.00
6.00
[Cs+]

FIGURE 28

Theoretical and Experimental Modified Stern-Volmer Plot

$^{2+}_{LT^-}$

$F^\circ/\Delta F$ vs $[Cs^+]^{-1}$

+ - Theoretical values

$\odot$ - Experimentally Measured Values

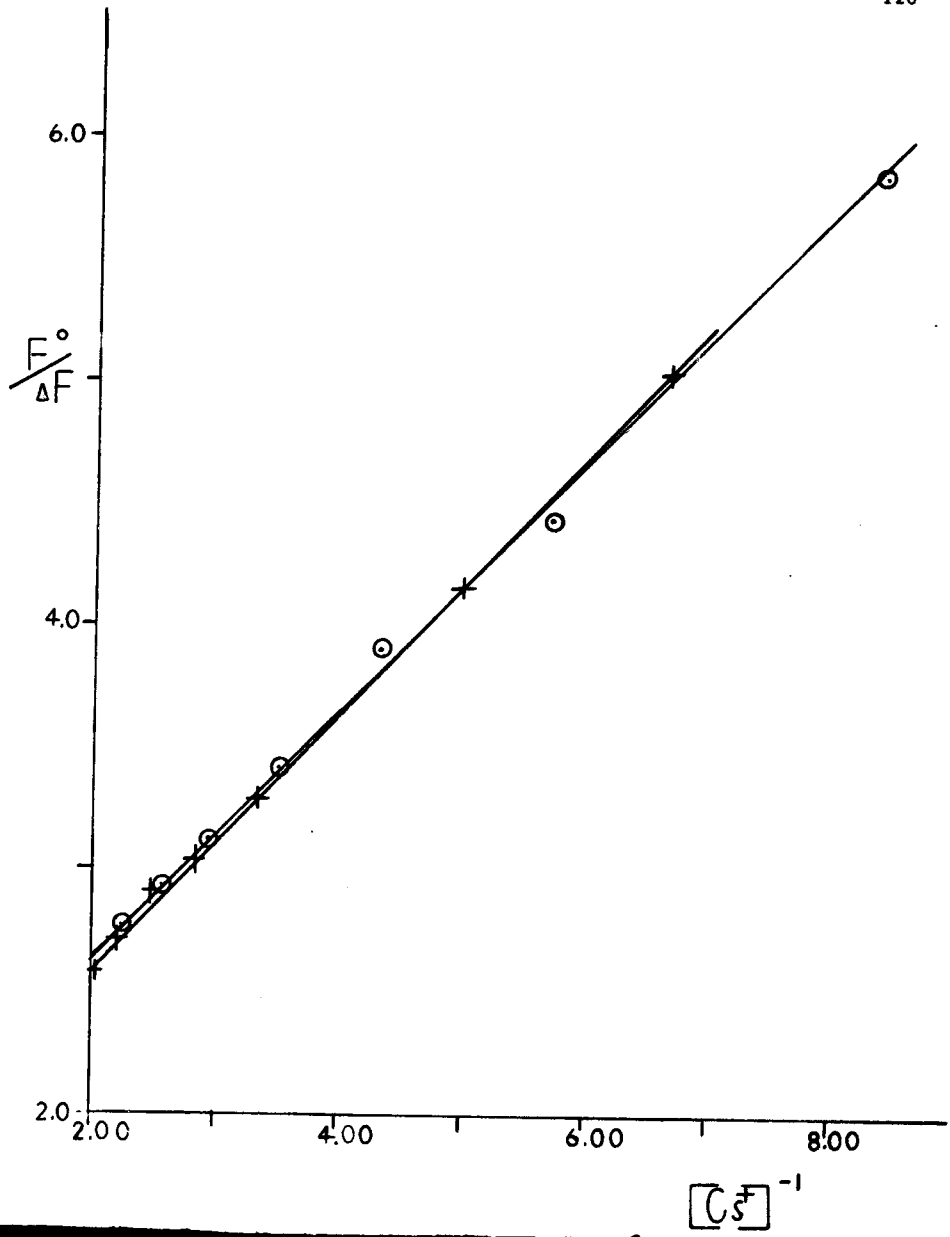
6.0
4.0
2.0
F°/ΔF
2.00
4.00
6.00
8.00
[Cs⁺]⁻¹

results discussed earlier, is not the most heavily weighted component. Instead, the shorter lifetime for $^{2+}LT^{-}$ has the larger weighting factor. This may explain why the Stern-Volmer plot for $^{2+}LT^{-}$ showed curvature and that for tryptophan did not. Under these lifetime conditions, the Stern-Volmer technique is apparently sensitive enough to show evidence for double exponential decay.

This curvature however, may be due to another factor entirely, i.e. ionic strength. Although the % change in F_T^o/F_T is less than 10% for the cesium quenching of $^{2+}LT^{-}$, our experiments were not extensive enough to conclusively eliminate the effect of ionic strength upon Stern-Volmer quenching. It is suggested that further quenching experiments be performed upon $^{2+}LT^{-}$ in which the quencher concentration is vaired but the ionic strength is kept constant throughout.

Conformational effects of addition of one or two glycine residues to the C-terminal end of tryptophan:

Our results have shown that when one glycine is added to the C-terminus of tryptophan ther is, as expected, an increase in the number of low energy conformations. Addition of a second glycine to the same end of the peptide, however, does not radically increase the number of low energy conformations. The second glycine must have only a few conformation which add onto $^{+}TG^{-}$ and still yield peptide energies within 3Kcal of the minimum.

When one glycine is added to the C-terminus of tryptophan, there is almost no change in the percentage of hydrogen bonds

which exist among the low energy conformations. One can conclude from this that the increased number of low energy conformations found for $^{+}TG^{-}$ (as compared to $^{+}T^{-}$) is not due solely to the existence of hyrdrogen bonds. Since there are only intraresidue hydrogen bonds in $^{+}TG^{-}$, hydrogen bonding within each residue does not play a major role in stabilizing the dipeptide. The type of hydrogen bond found in $^{+}T^{-}$ and $^{+}TG^{-}$ is the C_5 ring which is generally a very weak type of hydrogen bond.[4] When another glycine is added to $^{+}TG^{-}$, there is a dramatic rise in the percentage of hydrogen bonds among the low energy conformations. Most of the bonds are interresidue hydrogen bonds between tryptophan and G_2. The conformational freedom attributed to glycine by Zimmerman in reference 5 may allow rotation about the center glycine and bring T closer to G_2. Since most of these hydrogen bonds are stronger than the C_5 hydrogen bonds present in $^{+}T^{-}$ and $^{+}TG^{-}$, they may lower the conformational energy and thus many conformations without this kind of interresidue interaction may have an energy greater than 3Kcal from the minimum.

Our results have shown that the occurrence of hydrogen bonding among the low energy conformations of the tryptophan zwitterion is independent of the many conformational types present. This indicates that there is a high degree of backbone flexibility which allows the close proximity of the amino proton to the carboxyl oxygen. When tryptophan is located in the N-terminal position of glycine-containing di- and tripeptides, however, tryptophan intraresidue C_5 hydrogen bonding can occur only when tryptophan is in the F conformation.

Perhaps steric hindrance with the rest of the residue prohibits this type of hydrogen bond in di- and tripeptides, although the presence of this bond is independent of the conformation of glycine in $^{+}TG^{-}$ and of both glycines in $^{+}TGG^{-}$.

Glycine intraresidue hydrogen bonding for glycine in $^{+}TG^{-}$ and G_2 in $^{+}TGG^{-}$ is favored when it is in the E* conformational region. Although the E* region is not a low energy one for glycine as a single residue,[7] it may be stabilized in these peptides by this weak hydrogen bond. This is indirectly supported by data which show that G_1 in $^{+}TGG^{-}$ undergoes no intraresidue hydrogen binding and the E* conformational region is disallowd for this residue. Apparently, when G_1 is in the center of the tripeptide, its conformational freedom is restricted to such an extent as to prohibit the interaction of the G_1 amino proton and its carbonyl oxygen.

It is seen that $^{+}TG^{-}$ exhibits no interresidue hydrogen bonding. This is unexpected due to the conformational freedom of glycine and its high probability for bend conformations in Gly-X (X denotes another residue) dipeptides.[5] $^{+}TGG^{-}$ however, exhibits interresidue hydrogen bonding between the tryptophan carbonyl oxygen and the G_2 amino proton. Our results show that such bonding is favored when G_1 is in the C* conformation. The occurrence of an interresidue hydrogen bond is generally independent of the conformations of both tryptophan and G_2. This phenomenon suggests that the C* conformation for G_1 may pull the two residues on the ends of the peptide close together. When G_1 and G_2 are in the C*-F conformation, they come close

to satisfying the dihedral angle criteria for a type V bend.[14]

The majority of the indole contacts in all three peptides are tryptophan intraresidue contacts between the indole ring and the tryptophan carbonyl oxygen. This might be attributed to the close proximity of these atoms in the tryptophan zwitterion in general. This observation might also account for the similarity in the percentage of indole contacts found for each peptide.

Our results indicate that interresidue indole contacts between the atoms in the indole ring and the glycine carboxyl oxygen in $^{+}TG^{-}$ can take place. In $^{+}TGG^{-}$, indole contacts between tryptophan and the adjacent glycine residue do not occur; instead only indole contacts between the ring and the G_2 carboxyl oxygens are allowed. The exact reason for this is unclear because its occurrence is independent of the conformations of tryptophan, G_1 and G_2. It seems likely however, that G_1 cannot contact the ring because of its position in the center of the peptide is too restricted. G_2 can make an indole contact because of the propensity of glycine to form bend conformations[5] and the length of the peptide allows G_2 to swing around and contact the ring.

Effect of Position of Glycine in Tryptophan-Containing Dipeptides:

Our results indicate that $^{+}GT^{-}$ has almost 50% more low energy conformations than $^{+}TG^{-}$. This was also observed for some other Gly-X and X-Gly blocked dipeptides such as Gly-Phe (Glycyl-Phenylalanine) and Phe-Gly (52 vs. 39 low energy

conformations), Gly-Tyr (Glycyl-tyrosine) and Tyr-Gly (100 vs. 72 low energy conformations), but not for Gly-X and X-Gly dipeptides where X = Ala (Alanine), Asn (Asparagine), Asp (Aspartic acid), Ser (Serine), Thr (Threonine) and Val (Valine). Since Phe, Tyr, and Trp are all aromatic residues, it is interesting to observe the increase in low energy conformations when glycine occurs at the N-terminal end of the dipeptides. Although $^{+}GT^{-}$ has more low energy conformations than $^{+}TG^{-}$, it has only a lightly greater percentage of hydrogen bonds among these conformations. Both exhibit only weak C_5 type intraresidue hydrogen bonding. This agrees with our earlier results for $^{+}T^{-}$, $^{+}TG^{-}$, $^{+}TGG^{-}$ which indicated that there were no strong correlations between the existence of C_5 hydrogen bonding and the number of low energy conformations found for the peptides.

Tryptophan intraresidue C_5 hydrogen bonding can occur in both $^{+}TG^{-}$ and $^{+}GT^{-}$. In $^{+}TG^{-}$, tryptophan is often in the F conformation while in $^{+}GT^{-}$ it is often in the E conformation. Glycine intraresidue C_5 hydrogen bonding occurs only in $^{+}TG^{-}$. This hydrogen bonding is found to be most favored when glycine is in the E* conformation as previously noted. An explanation of the above may be that the bulky side chain of tryptophan must restrict the conformational freedom of glycine when it precedes tryptophan more than glycine restricts tryptophan when it precedes glycine. Even though the E* conformation is observed for glycine in $^{+}GT^{-}$, no intraresidue hydrogen bonds are formed.

Our results have indicated that interresidue indole contacts exist for both $^{+}TG^{-}$ and $^{+}GT^{-}$. In both cases, the presence of such contacts is independent of the conformation of the glycine residue. In $^{+}TG^{-}$, the contact is most favored when tryptophan is in the E conformation. In $^{+}GT^{-}$, the contact is most favored when tryptophan is in the G conformation. E and G conformations for single residue tryptophan are allowed and are relatively well populated for both $^{+}TG^{-}$ and $^{+}GT^{-}$. The location of glycine in the dipeptide naturally would result in different tryptophan backbone conformations being more favored for an interresidue indole contact.

Tryptophan intraresidue indole contacts exist for both $^{+}GT^{-}$ and $^{+}TG^{-}$. In $^{+}GT^{-}$ there is no correlation between their occurrence and the conformations of either tryptophan and glycine. In $^{+}TG^{-}$, these indole contacts are slightly more favored when tryptophan is in the F, E, or C* region. Their occurence is independent of the glycine conformation. Thus it appears that intraresidue indole contacts do not depend very strongly on backbone conformations of either residue in the dipeptide.

Conformational Effects of Nature of Reside on N-Terminus of Tryptophan-Containing Dipeptides:

Before we begin this discussion, it must be noted that any comparison with the results for $^{2+}LT^{-}$ is impossible. Since only a few low energy backbone minima were reminimized with lysine side chains added, our results for $^{2+}LT^{-}$ are very limited.

In this light, let us compare $^{+}PT^{-}$ with $^{+}GT^{-}$. Our results indicate that $^{+}GT^{-}$ has more than three times as many low energy conformations as $^{+}PT^{-}$. It is also seen that glycine in $^{+}GT^{-}$ has many more allowed conformational types than proline which is restricted to only the F conformation in $^{+}PT^{-}$. Tryptophan, however, has almost the same number and type (excepting conformation G for $^{+}GT^{-}$) of conformational types in both $^{+}GT^{-}$ and $^{+}PT^{-}$. This suggests that the large number of conformations for $^{+}GT^{-}$ is due to the greater flexibility of glycine since proline backbone conformations are severly restricted by the pyrrolidine ring.

Our results have shown that although $^{+}GT^{-}$ has a much greater number of low energy conformations than $^{+}PT^{-}$, it only has a slightly greater percentage of hydrogen bonding among these conformations. All of the hydrogen bonds in both $^{+}GT^{-}$ and $^{+}PT^{-}$ present are weak C_5 intraresidue ones for tryptophan. This again substantiates our early conclusion that there is little correlation between the degree of C_5 hydrogen bonding and the number of low energy conformations. This suggests that hydrogen bonding within the individual residues in the peptide does not play a major role in stabilizing the total peptide.

Of course, since proline has no amino hydrogen it can have no intraresidue hydrogen bonds. The tryptophan intraresidue hydrogen bonding in both $^{+}PT^{-}$ and $^{+}GT^{-}$ is favored when tryptophan is in the E conformation. Zimmerman found

this to be a favored conformation for residues like tryptophan with aromatic rings on the side chains.[5] In $^{+}GT^{-}$, the occurrence of this intraresidue bond is independent of the glycine conformation. In $^{+}PT^{-}$, for all dipeptide conformations, proline is only in the F region. In this light it seems then that the conformations of both proline and glycine have little influence upon the occurrence of tryptophan intraresidue hydrogen bonding.

$^{+}GT^{-}$ has a greater percentage of indole contacts among its low energy conformations than $^{+}PT^{-}$. Most of these indole contacts are interresidue interactions. These data seem to suggest that glycine, in the N-terminus of $^{+}GT^{-}$ has greater conformational freedom than proline in $^{+}PT^{-}$ (which is to be expected because of proline's pyrrolidine ring) allowing for greater contact with the indole ring. The allowed values for ϕ and ψ of proline are clearly restricted, thus prohibiting many proline interresidue indole contacts.

Comparison of Results for $^{+}PT^{-}$ with that of Earlier Workers:

Zimmerman and other workers have carried out conformational studies on N-Acetyl-N-Methylamide Proline-X (blocked, uncharged) dipeptides where X = Ala, Asn, Asp, Gly, Leu, Ser, Val, and Phe.[4] Our results agree fairly well with those of Zimmerman on the following points.

Zimmerman found that proline in the Pro-X dipeptides studied was restricted to the C, F and A conformations because ϕ_P is -75.000 degrees in the pyrrolide ring. Our results show

that proline in $^{+}PT^{-}$ was restricted to the F conformational region. The exclusion of regions C and A suggests that the bulky side chain of tryptophan may restrict the conformational space available to proline more than the other residues studied by Zimmerman.

Zimmerman also found that the X residues in Pro-X dipeptides had the same conformations in the peptide as those of single residue minima.[4] Similarly, tryptophan in $^{+}PT^{-}$ has all the same conformational types as in its single residue minima excepting conformation regions G and A*. Finally, Zimmerman found that in the Pro-Ala dipeptide, alanine showed a propensity for forming C_5 intraresidue hydrogen bonds when it is in the E conformation. The conformations of the peptide in which this occurred were thus CE, FE and AE.[4] Our work has shown that tryptophan undergoes C_5 hydrogen bonding when tryptophan is in the E region. In this regard then tryptophan acts like alanine and other X residues in Zimmerman's proline dipeptides.

Correlation of Experimental and Calculated Results:

Results from ECEPP calculations show that the sum of the electronic charges for all the atoms in the indole ring is +0.03 electronic charge units (E.C.U.). Although the magnitude of this value is quite small, the fact that it is positive may provide an additional explanation for the low quenching efficiency of cesium ion as compared to that for iodide ion. Apparently, the positively charged cesium ion is electrostatically repelled away from the indole ring to a greater extent than

the iodide ion. In fact, the negatively charged iodide ion may be electrostatically attracted to the ring, increasing its quenching efficiency.

As stated earlier, ϕ_R is an expression of the efficiency of fluorescence in the tryptophan residue. A low ϕ_R indicates that a good deal of internal quenching is taking place. This occurs due to the formation of an excited state charge transfer complex (exciplex). The exciplex is formed between the indole ring, which acts as an electron donator, and the electrophilic amide carbonyl oxygen. Werner and Forster claim that any effect which will increase the electrophilic character of the carbonyl oxygen will result in increased quenching and a decrease in ϕ_R.[1]

They have shown that the quantum yield for the zwitterion forms of T and TG are lower than those for the corresponding anions. They suggested that this occurs because protonation of the amino group on tryptophan results in an inductive effect which enhances the electrophilicity of the tryptophan carbonyl oxygen.[1] The likelihood of exciplex formation is thus increased resulting in increased internal quenching. Our experimental results have shown that ϕ_R for $^{+}TGG^{-}$ is lower than that for TGG^{-}. One can conclude that this probably occurs because of the inductive effect model proposed by Werner and Forster.

Our results also reveal that ϕ_R for both the anion and zwitterion forms of TGG is much lower than that for the corresponding forms of TG. Since it has been seen that the wavelength

maximum for the zwitterion forms of both TG and TGG are 10 nm lower than that for the anion forms, it seems clear that there is no difference in the fluorescing environments for the two peptides. Environmental factors are thus ruled out as the cause for this decrease in ϕ_R.

This increased quenching in TGG also does not appear to be due to exciplex formation between the G_1 carbonyl oxygen and the indole ring because the conformational calculations show that no indole contacts between these atoms take place.

The calculations have also shown that both $^{+}TG^{-}$ and $^{+}TGG^{-}$ have almost the same percentage of indole contacts, of which, the majority for both peptides are tryptophan intraresidue contacts. Thus, the reason for the decrease in ϕ_R in $^{+}TGG^{-}$ is unclear.

It is suggested that the presence of two glycine residues in $^{+}TGG^{-}$ may affect the peptide in such a way as to enhance the quality of the tryptophan intraresidue indole contact. Calculations have shown that the majority of hydrogen bonds in $^{+}TGG^{-}$ are between the G_2 amino proton and the tryptophan carbonyl oxygen. Perhaps this bond withdraws electron character away from this carbonyl oxygen resulting in an increase in its electrophilicity. If this is the case, the tryptophan intraresidue indole contact will have a greater quenching efficiency in $^{+}TGG^{-}$ than in $^{+}TG^{-}$.

Werner and Forster have found that the relative quantum yield for $^{+}GT^{-}$ is much lower than that for $^{+}TG^{-}$. ϕ_R for $^{+}GT^{-}$

is 0.30 as opposed to 0.62 for $^{+}TG^{-}$. Space filling molecular models built by Werner and Forster have shown that the amide carbonyl oxygen in GT contacts the indole ring to a greater extent than does the amide carbonyl oxygen in TG. In TG, the amide carbonyl is in contact only with the periphery carbons in the ring. In GT, however, the carbonyl group is able to extend beyond the periphery and come within 2-3Å of the indole nitrogen. Thus GT has greater opportunity to exhibit exciplex formation and therefore will quench more efficiently.[1] The results of the conformational calculations are in good agreement with this model. It is seen that $^{+}GT^{-}$ has indole contacts among 50.6% of its low energy conformations as opposed to only 21.5% for $^{+}TG^{-}$.

Werner and Forster has also shown tha ϕ_R for $^{+}PT^{-}$ and $^{+}GT^{-}$ were the two lowest values for any of the short peptides studied by their group.[1] Conformation calculations suggest that this is due to the more frequent contact of the amide carbonyl oxygen with the indole ring in $^{+}PT^{-}$ and $^{+}GT^{-}$. Our results indicate that $^{+}PT^{-}$ and $^{+}GT^{-}$ have indole contacts among 33.3% and 50.6% respectively of their low energy conformations. These percentage values are higher than the average percentage of indole contacts found for the other peptides studied (excluding $^{2+}LT^{-}$). Again, the calculations are consistent with the exciplex quenching model proposed by Werner and Forster.

Appendix A

Computer Program Input - Output Scheme

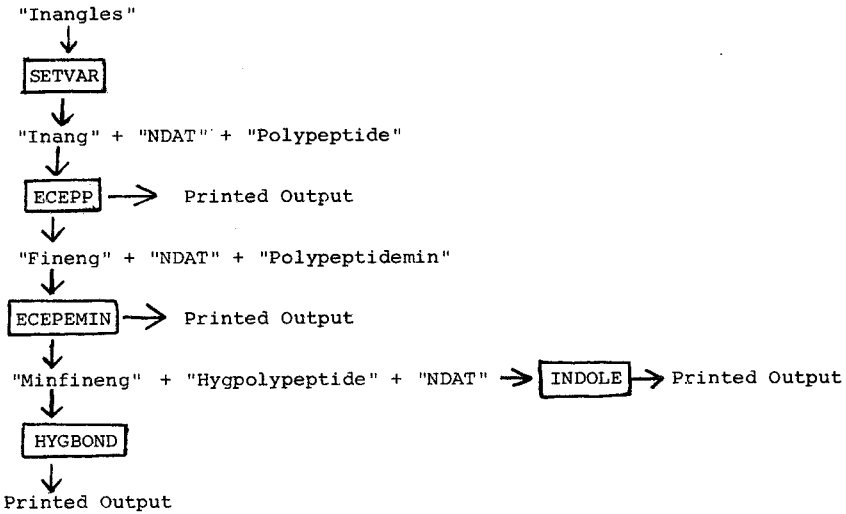

Explanation of Input-Output Scheme:

A. [ ] designates workobjects.

" " designates input and/or output files.

B. Each work object can be run as a "batch" job using the following files:

Runsetvar is used to run the workobject SETVAR.

Runecepp is used to run the workobject ECEPP.

Runecepemin is used to run the workobject ECEPEMIN.

Runhygbond is used to run the workobject HYGBOND.

Runindole is used to run the workobject INDOLE.

C. The following is a description of the input and output files used:

1. "Inangles" is the input file for SETVAR. It contains a listing of the single residue minima dihedral angles for each residue in the polypeptide under examination. The following is a sample of "Inangles" used to generate a list of dihedral angles for a sample polypeptide, Pro-Try (Blocked L-Prolyl-L-tryptophan):

```
INANGLES
100        1       2       5
200      176.000   79.000
300      180.000  159.000
400      180.000  -48.000
500       -5.000  -48.000
600       -4.000  162.000
700        2       4      30
800     -156.000  154.000   58.000   83.000
900     -155.000  151.000   60.000  -88.000
1000    -153.000  144.000  180.000   89.000
1100     -77.000  135.000 -179.000   90.000
1200     -84.000   89.000 -179.000   73.000
1300    -153.000  146.000 -179.000 -105.000
1400    -144.000  148.000  -61.000  -87.000
1500     -85.000   89.000 -179.000 -105.000
1600     -86.000   82.000  -60.000  -78.000
1700     -86.000   81.000  -60.000  104.000
1800    -142.000   81.000  -62.000  -87.000
1900    -144.000  149.000  -60.000  105.000
2000     -76.000  140.000   68.000  -92.000
2100    -141.000   79.000  -61.000  105.000
2200     -80.000  145.000   64.000   81.000
2300     -75.000  -47.000  179.000   83.000
2400     -76.000  -36.000   68.000  -92.000
2500    -149.000   47.000   50.000   88.000
2600     -75.000  -49.000  179.000 -103.000
2700    -157.000  -61.000  174.000 -104.000
2800    -153.000   54.000   59.000  -72.000
2900    -158.000  -60.000  173.000   74.000
3000    -146.000  -61.000  -67.000  -86.000
3100     -77.000  -48.000  -60.000  105.000
3200     -77.000  -48.000  -60.000  -76.000
3300    -146.000  -61.000  -66.000  105.000
3400     -76.000  -34.000   64.000   83.000
3500      57.000   58.000  -54.000  -75.000
3600    -163.000  -52.000   52.000  -81.000
3700      56.000   63.000 -174.000   69.000
```

Line 100: This line specifies the input parameters. The first value represents the number of the residue of interest in the peptide. The second value designates the number of dihedral angles to be varied in the residue. The third value represents the number of set of angles for the specified residue (Format 3I5).

Lines 200-600: These lines show a listing of the sets of single residue minima dihedral angles (Format 8F8.3).

Line 700: This line gives the same information as line 100, only this line specifies the parameters for the next residue in the polypeptide.

Lines 800-END: These lines give similar information as lines 200-600. Here the set of dihedral angles apply to the second residue examined in the peptide.

2. "Inang" is the output file for SETVAR and is one of the input files for ECEPP. It contains a listing of all of the combinations of backbone dihedral angles in the peptide to be examined by ECEPP. In the example above, the first residue has five sets of minimum dihedral angles. The second has 30 sets of minimum dihedral angles. Therefore the total number of minimum dihedral angle combinations for the whole peptide will be 30 x 5 or 150. In the example, each combination will be represented by six dihedral angles. Thus ECEPP will examine 150 different conformations of the sample polypeptide.

3. "NDAT" is an input file which contains information regarding the fixed bond lengths and bond angles in each peptide. Refer to reference 9 for a more detailed explanation of this file.

4. "Polypeptide" specifies the input parameters to be used by ECEPP. It also contains all of the dihedral angles for one starting conformation of the peptide. The following is a sample "polypeptide" file used for the peptide, blocked Pro-Trp:

```
100          4  151    0    6    0
200          1    3    4    2
300    180.000 178.000
400    -75.000  79.000 180.000
500   -156.000 154.000 180.000  58.000  83.000
600    180.000
700    SPEC
710          1    1    2
720          2    1    2
800          3    4    1    2    4    5
900          0
```

Line 100: The first value represents the number of residues in the peptide. The second value designates the number of conformations to be studied by ECEPP. The fourth and fifth numbers control the printed information in the ECEPP output (Format 16I5).

Line 200: These numbers are the list numbers for each residue in the polypeptide. The list numbers are referenced in NDAT (Format 16I5).

Lines 300-600: These are the dihedral angles for the starting conformation of the polypeptide under examination (Format 8F8.3).

Line 700: This line is read by subroutine SPECV in ECEPP. SPEC tells the program that it will vary only those dihedral angles specified in input file "Inang" (Format I4).

Lines 710-900: These tell the program which angles in the particular residue in the polypeptide will be varied. For example, the first value on each line designates the residue whose angles will be varied. The second value on each line designates the number of angles in that residue which are to be varied. The subsequent values on each line designate the number of the angles which will be varied. The dihedral angles are numbered as follows: $\emptyset = 1$; $\psi = 2$; $\omega = 3$, $X_{1 \cdots n} = 4 \cdots 3 + n$. For a more detailed explanation of this input file, refer to pages 11-17 in reference 9.

5. "Fineng" is a summary of the output from ECEPP. It provides a listing of the calculated energies in increasing order. Alongside (on the left) of each energy is a listing of the corresponding dihedral angles which were used to generate this energy. Note that the only angles listed are those which were varied. All the other dihedral angles in the peptide are the same as those designated in the starting conformation listed in the "Polypeptide" file. The following is a sample of some of the 150 conformations studied for the example, Pro-Trp:

```
178.000   79.000  180.000  -86.000   81.000  -60.000  104.000  -.18698E+02
178.000   79.000  180.000 -144.000  149.000  -60.000  105.000  -.18464E+02
178.000   79.000  180.000 -141.000   79.000  -61.000  105.000  -.18377E+02
178.000   79.000  180.000 -146.000  -61.000  -66.000  105.000  -.17984E+02
178.000   79.000  180.000 -155.000  151.000   60.000  -88.000  -.17925E+02
178.000   79.000  180.000  -77.000  -48.000  -60.000  105.000  -.17828E+02
178.000   79.000  180.000  -77.000  135.000 -179.000   90.000  -.17799E+02
178.000   79.000  180.000 -153.000  144.000  180.000   89.000  -.17623E+02
178.000   79.000  180.000  -84.000   89.000 -179.000   73.000  -.17617E+02
178.000   79.000  180.000  -76.000  140.000   68.000  -92.000  -.17558E+02
180.000  159.000  180.000 -144.000  149.000  -60.000  105.000  -.17555E+02
178.000   79.000  180.000  -85.000   89.000 -179.000 -105.000  -.17507E+02
180.000  159.000  180.000 -155.000  151.000   60.000  -88.000  -.17418E+02
180.000  -48.000  180.000  -86.000   81.000  -60.000  104.000  -.17334E+02
178.000   79.000  180.000 -153.000  146.000 -179.000 -105.000  -.17300E+02
178.000   79.000  180.000 -150.000  -60.000  173.000   74.000  -.17237E+02
178.000   79.000  180.000  -76.000  -36.000   68.000  -92.000  -.17228E+02
178.000   79.000  180.000  -77.000  -48.000  -60.000  -76.000  -.17212E+02
180.000  -48.000  180.000  -86.000   82.000  -60.000  -78.000  -.17201E+02
178.000   79.000  180.000 -157.000  -61.000  174.000 -104.000  -.17165E+02
180.000  159.000  180.000 -141.000   79.000  -61.000  105.000  -.17120E+02
180.000  -48.000  180.000  -76.000  -36.000   68.000  -92.000  -.17078E+02
180.000  159.000  180.000  -77.000  135.000 -179.000   90.000  -.17043E+02
178.000   79.000  180.000  -75.000  -47.000  179.000   83.000  -.17021E+02
178.000   79.000  180.000   57.000   50.000  -54.000  -75.000  -.17003E+02
180.000  -48.000  180.000 -153.000  144.000  180.000   89.000  -.16996E+02
180.000  159.000  180.000 -153.000  144.000  180.000   89.000  -.16917E+02
180.000  -48.000  180.000  -77.000  -48.000  -60.000  -76.000  -.16910E+02
180.000  -48.000  180.000  -84.000   89.000 -179.000   73.000  -.16887E+02
180.000  -48.000  180.000 -144.000  149.000  -60.000  105.000  -.16868E+02
180.000  159.000  180.000  -86.000   82.000  -60.000  -78.000  -.16858E+02
```

"Fineng" is then used as an input file ECEPEMIN.

6. "Polypeptidemin" is another input file for ECEPEMIN. It specifies the input parameter used by the minimizer program. It, like file "Polypeptide", provides the dihedral angles for one starting conformation for the peptide. The following is a sample input file for the Pro-Trp example:

```
100          1    6    0
150          4    9
200          1    3    4    2
300    180.000 178.000
400    -75.000  79.000 180.000
500   -156.000 154.000 180.000   58.000   83.000
600    180.000
700    SPEC
710          1    1    2
720          2    2    5    3
800          3    4    1    2    4    5
900          0
950               .001         .001    4    1
```

Line 100: The first number in the sequence represents the number of peptides to be studied. The following two numbers control the information which is printed in the ECEPEMIN output (Format 16I5). Refer to pages 11, 14-16 in reference 9.

Line 150: The first value designates the number of residues in the peptide. The second value designates the number of conformations which will be examined by ECEPEMIN (Format 16I5).

Line 200: These are the list numbers of the residues in the peptide (Format 16I5).

Lines 300-900: These lines perform the exact same function as lines 300-900 in the ECEPP input file, "Polypeptide" (Format 8F8.3).

Line 950: These values are used by subroutine MNOP, which minimizes the energy values and optimizes the geometrics which were first examined in ECEPP. The first value is the step size. The second value is the energy criterion for convergence. The third value designates the maximum number of iterations to be carried out upon the conformation being studied. The fourth value is a print option (Format 2F10.0, 2I5).

7. "Minfineng" is a summary of the output file for ECEPEMIN. Similar to "Fineng", it provides a list of the conformations and their corresponding energies (in increasing order). The following is some of the "Minfineng" file for the Pro-Trp example:

```
178.036  79.007 180.017 -85.991   80.991 -60.014 104.036 -.18690E+02
178.023  79.002 180.007-143.995  148.980 -59.997 105.048 -.18464E+02
178.166  79.030 180.083-140.960   78.878 -60.518 105.320 -.18385E+02
178.109  79.036 180.041-145.950  -61.138 -65.798 105.289 -.17991E+02
178.182  79.013 180.126-154.974  150.914  60.053 -88.317 -.17950E+02
178.047  79.018 180.034 -76.981  -48.031 -60.001 105.072 -.17828E+02
178.059  79.009 180.026 -76.983  134.997-179.046  90.059 -.17798E+02
178.070  79.007 180.036-152.986  143.949 180.026  89.019 -.17623E+02
178.014  79.004 180.063-156.089  154.066  58.000  83.037  .32898E+04
```

8. "Hygpolypeptide" is an input file used by HYGBOND and INDOLE. It specifies the parameters to be used by these programs. It also designates the dihedral angles for one starting conformation for the peptide. The following is a sample used

in the Pro-Trp example:

```
100          4    9    0    6    0
200          1    3    4    2
300    180.000  180.000
400    -75.000   79.000  178.000
500    -86.000   81.000  180.000 -60.000  104.000
600    180.000
700    SPEC
710          1    1    2
720          2    2    2    3
800          3    4    1    2    4    5
900          0
```

Lines 100-900: Each line in this input file provides exactly the same parameter information as the input file for ECEPP. Refer to section C4 in this appendix.

BIBLIOGRAPHY

1. T.C. Werner and Leslie S. Forster, Photochem. Photobiol. 29, 905 (1975).

2. D.M. Rayner and A.G. Szabo, preprint, "Time Resolved Fluorescence of Awueous Tryptophan."

3. Robert W. Ricci and Joseph M. Nesta, J. Phys. Chem. 80, 974 (1976).

4. S. Scott Zimmerman and Harold A. Scheraga, Biopolymers 16, 811 (1977).

5. S. Scott Zimmerman and Harold A. Scheraga, Biopolymers 17, 1871 (1978).

6. K. Marshall, B.S. Thesis, Union College, 1979.

7. S. Scott Zimmerman, Marcia S. Pottle, George Némethy, and Harold A. Scheraga, Macromolecules 10, 1 (1977).

8. F.A. Momany, R.F. McGuire, A.W. Burgess, and H.A. Scheraga, J. Phys. Chem 79, 2361 (1975).

9. A computer program named ECEPP (Empirical Conformational Energy Program for Peptides) was used.[8] The Fortran computer program for ECEPP, its description, and the associated structural energy parameters are available on magnetic tape from the Quantum Chemistry Program Exchange, as program No. QPCE 286. See footnote 60 of ref. 8 for the procedure to obtain the material.

10. J.E. Dennis and H.H.W. Mei, TR 75-246 (1975), Department of Computer Science, Cornell University.

11. Wijaya Altekar, Biopolymers 16, 341 (1977).

12. Sherwin S. Leher, Biochem. 10, 3254 (1971).

13. Martin L. Meyers and Paul G. Seybold, Analytical Chem. 51, 1609 (1979).

14. Peter N. Lewis, Frnak A. Momany, and Harold A. Scheraga, Biochem, Biophys. Acta. 303, 211 (1973).


END